

AD-A076 493

MCDONNELL AIRCRAFT CO ST LOUIS MO

F/6 11/4

EFFECT OF SERVICE ENVIRONMENT ON F-15 BORON/EPOXY STABILATOR.(U)

JUN 79 T V HINKLE

F33615-77-C-3124

UNCLASSIFIED

AFFDL-TR-79-3072

NL

1 OF 2  
AD A  
076493



AFFDL-TR-79-3072

AD A 076493

## **EFFECT OF SERVICE ENVIRONMENT ON F-15 BORON/EPOXY STABILATOR**

**T.V. HINKLE**

**McDonnell Douglas Corporation  
McDonnell Aircraft Company  
P.O. Box 516  
St. Louis, Missouri 63166**

**June 1979**

**Final Technical Report August 1977 - June 1979**

Approved for public release; distribution unlimited.

**AIR FORCE FLIGHT DYNAMICS LABORATORY  
AIR FORCE WRIGHT AERONAUTICAL LABORATORIES  
AIR FORCE SYSTEMS COMMAND  
WRIGHT-PATTERSON AIR FORCE BASE, OHIO 45433**

REPRODUCED BY  
**NATIONAL TECHNICAL  
INFORMATION SERVICE**  
U.S. DEPARTMENT OF COMMERCE  
SPRINGFIELD, VA. 22161

79 13 11 102 138



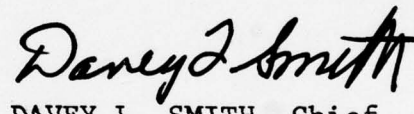
# NOTICE

When Government drawings, specifications, or other data are used for any purpose other than in connection with a definitely related Government procurement operation, the United States Government thereby incurs no responsibility nor any obligation whatsoever; and the fact that the government may have formulated, furnished, or in any way supplied the said drawings, specifications, or other data, is not to be regarded by implication or otherwise as in any manner licensing the holder or any other person or corporation, or conveying any rights or permission to manufacture, use, or sell any patented invention that may in any way be related thereto.


This report has been reviewed by the Information Office (OI) and is releasable to the National Technical Information Service (NTIS). At NTIS, it will be available to the general public, including foreign nations.

This technical report has been reviewed and is approved for publication.

  
CARL L. RUPELT  
Project Engineer

  
DAVEY L. SMITH, Chief  
Structural Integrity Branch

FOR THE COMMANDER

  
RALPH L. KUSTER, JR., Col. USAF  
Chief, Structural Mechanics Division

If your address has changed, if you wish to be removed from our mailing list, or if the addressee is no longer employed by your organization please notify, AFFDL/FBE, W-PAFB, OH 45433 to help us maintain a current mailing list.

Copies of this report should not be returned unless return is required by security considerations, contractual obligations, or notice on a specific document.

# NOTICE

THIS DOCUMENT HAS BEEN REPRODUCED FROM THE BEST COPY FURNISHED US BY THE SPONSORING AGENCY. ALTHOUGH IT IS RECOGNIZED THAT CERTAIN PORTIONS ARE ILLEGIBLE, IT IS BEING RELEASED IN THE INTEREST OF MAKING AVAILABLE AS MUCH INFORMATION AS POSSIBLE.

CLASSIFIED  
ON OF THIS PAGE (When Data Entered)

REPORT DOCUMENTATION PAGE

READ INSTRUCTIONS  
BEFORE COMPLETING FORM

1. REPORT NUMBER AFFDL-TR-79-3072	2. GOVT ACCESSION NO.	3. RECIPIENT'S CATALOG NUMBER
4. TITLE (and Subtitle) EFFECT OF SERVICE ENVIRONMENT ON F-15 BORON/EPOXY STABILATOR		5. TYPE OF REPORT & PERIOD COVERED Final Report August 1977 - June 1979
7. AUTHOR(s) T. V. Hinkle		6. PERFORMING ORG. REPORT NUMBER
9. PERFORMING ORGANIZATION NAME AND ADDRESS McDonnell Aircraft Company P.O. Box 516 St. Louis, Missouri 63166		8. CONTRACT OR GRANT NUMBER(s) F33615-77-C-3124
11. CONTROLLING OFFICE NAME AND ADDRESS Air Force Flight Dynamics Laboratory (FBE) Wright-Patterson Air Force Base, Ohio 45433		10. PROGRAM ELEMENT, PROJECT, TASK AREA & WORK UNIT NUMBER 2401-01-16
14. MONITORING AGENCY NAME & ADDRESS (if different from Controlling Office)		12. REPORT DATE June 1979
		13. NUMBER OF PAGES 126
		15. SECURITY CLASS. (of this report) Unclassified
		15a. DECLASSIFICATION/DOWNGRADING SCHEDULE
16. DISTRIBUTION STATEMENT (of this Report) Approved for public release; distribution unlimited.		
17. DISTRIBUTION STATEMENT (of abstract entered in Block 20, if different from Report)		
18. SUPPLEMENTARY NOTES		
19. KEY WORDS (Continue on reverse side if necessary and identify by block number) Advanced Composites      Full-Scale Static Tests Boron/Epoxy Structures      Moisture Content Predictions Environmental Effects		
20. ABSTRACT (Continue on reverse side if necessary and identify by block number) → The objective of this program was to conduct a series of tests for evaluating the effects of service environment on the strength of the boron/epoxy skins which are an integral part of the F-15 horizontal stabilator. Full scale static tests were conducted on two stabilators, and test results were compared with the capability of the F-15 stabilator demonstrated in previous testing. Moisture contents at various locations in the composite skins were predicted by evaluating the environmental histories of both →		

UNCLASSIFIED

SECURITY CLASSIFICATION OF THIS PAGE(When Data Entered)

20. (Continued)

test articles. Predicted contents were corroborated by moisture contents measured at conclusion of the static tests. F-15 deployments were projected for a 25-year service life, and moisture contents of stabilator composite skins were calculated for each projected deployment. Structural element tests were conducted under the maximum temperature and absorbed moisture conditions expected in service. Physical and chemical characteristics of the test article skins were evaluated relative to baseline boron/epoxy characteristics.

UNCLASSIFIED

SECURITY CLASSIFICATION OF THIS PAGE(When Data Entered)



## FOREWORD

This report was prepared by the McDonnell Aircraft Company (MCAIR), St Louis, Missouri, for the Structural Integrity Branch, Structural Mechanics Division, Air Force Flight Dynamics Laboratory, Wright-Patterson Air Force Base, Ohio, under Contract F33615-77-C-3124, "Effects of Service Environment on F-15 Boron/Epoxy Stabilator". This contract was administered by C. L. Rupert, Project Engineer, AFFDL/FBE.

The Structural Research Department of the McDonnell Aircraft Company had the responsibility for the performance of this program. The program manager for MCAIR was R. A. Garrett. The principal investigator for MCAIR and author of this report was T. V. Hinkle. Other MCAIR personnel contributing to this program and their technologies are:

- o J. W. Harvey and B. J. Colvin - Structural Analysis Consultants from the F-15 Project.
- o B. A. Dike - Operations Analysis
- o R. J. Janitch - Thermodynamic Analysis
- o T. S. Jones - Nondestructive Evaluation
- o T. A. Sewell - Materials Evaluation
- o J. F. Siller - Structures Laboratory
- o W. D. Tims - Materials Laboratory

This report covers work accomplished during the period from August 1977 through June 1979.

This report was released by the author in June 1979 for publication.



# TABLE OF CONTENTS

SECTION		PAGE
I	INTRODUCTION AND SUMMARY . . . . .	1
II	NONDESTRUCTIVE EVALUATIONS . . . . .	3
	1. STABILATOR PRIOR USAGE . . . . .	3
	2. STRUCTURAL DESCRIPTION . . . . .	3
	3. INSPECTION METHODS . . . . .	6
	4. NONDESTRUCTIVE EVALUATION OF EAGLE 14 STABILATORS . . . . .	7
	5. NONDESTRUCTIVE EVALUATION OF THE PDV STABILATOR . . . . .	15
III	STABILATOR TEST PROGRAM . . . . .	22
	1. LOADS USED FOR F-15A STABILATOR DESIGN AND DESIGN VERIFICATION TESTING . . . . .	22
	2. TEST LOADS USED IN THIS PROGRAM . . . . .	22
	3. STATIC TESTS OF STABILATORS . . . . .	26
	4. CORRELATION OF TEST DATA . . . . .	38
IV	MOISTURE CONTENTS OF TEST ARTICLE SKINS . . . . .	40
	1. ENVIRONMENTAL HISTORIES . . . . .	40
	2. COMPOSITE SKIN THERMAL MODELS . . . . .	43
	3. MOISTURE DIFFUSION PROPERTIES . . . . .	48
	4. PROCEDURES FOR CALCULATING MOISTURE CONTENTS . . . . .	55
	5. MOISTURE HISTORIES . . . . .	59
	6. CORRELATION OF MEASURED AND PREDICTED MOISTURE CONTENTS . . . . .	65
V	SKIN MOISTURE PROFILES FOR PROJECTED F-15 DEPLOYMENTS . . . . .	67
	1. F-15 DEPLOYMENT PROJECTIONS . . . . .	67
	2. MOISTURE-TIME PROFILES . . . . .	69
VI	ELEMENT TEST PROGRAM . . . . .	75
	1. SPECIMEN DEFINITION . . . . .	75
	2. RESULTS OF STRUCTURAL ELEMENT TESTS . . . . .	75
	3. EVALUATION OF PHYSICAL AND CHEMICAL CHARACTERISTICS . . . . .	85
VII	CONCLUSIONS . . . . .	92

Preceding page blank

# TABLE OF CONTENTS (Continued)

APPENDIX	PAGE
A EAGLE 14 ENVIRONMENTAL HISTORY . . . . .	93
B PDV ENVIRONMENTAL HISTORY . . . . .	100
C BASE WEATHER DATA FOR PROJECTED F-15 DEPLOYMENTS . . . . .	105
D RESULTS OF STRUCTURAL ELEMENT TESTS . . . . .	121
REFERENCES. . . . .	126

# LIST OF ILLUSTRATIONS

FIGURE		PAGE
1	Usage History of Eagle 14 and PDV Stabilators . .	4
2	F-15 Stabilator Structure . . . . .	5
3	Torque Box from Eagle 14 Stabilator . . . . .	8
4	Ultrasonic Inspection Record for Left-Hand Eagle 14 Torque Box . . . . .	9
5	Ultrasonic Inspection Record for Right-Hand Eagle 14 Torque Box . . . . .	12
6	Ultrasonic Inspection Record for PDV Torque Box .	16
7	Blown Core Areas in PDV Torque Box . . . . .	19
8	Disbonds in PDV Root Splice Found Using Ultrasonics . . . . .	20
9	PDV Stabilator Repairs . . . . .	21
10	Stabilator Loading System . . . . .	23
11	Comparison of Design and Test Loads . . . . .	24
12	Strain Gage Locations for Data Analysis . . . . .	25
13	Stabilator Static Test Setup . . . . .	26
14	Eagle 14 Stabilator at 150% DLL . . . . .	27
15	Tension Skin of Eagle 14 Stabilator After Static Test . . . . .	29
16	Fracture in Root Splice of Eagle 14 Tension Skin . . . . .	30
17	Disbonds, Fractures and Delaminations in the Failed Eagle 14 Skin . . . . .	31
18	Disbonds of Eagle 14 Root Splice . . . . .	32
19	Strains in PDV Torque Box and Trailing Edge Structure . . . . .	33
20	Tension Skin of PDV Stabilator After Static Test . . . . .	35

# LIST OF ILLUSTRATIONS (Continued)

FIGURE		PAGE
21	Fracture in Root Splice of PDV Tension Skin . . .	36
22	Disbonds, Fractures and Delaminations in the Failed PDV Skin . . . . .	37
23	Stabilator and Box Beam Test Results . . . . .	39
24	Data for Thermodynamic Models of Torque Box . . .	44
25	Moisture Absorption in 4-Ply Boron/Epoxy Coupons.	49
26	Equilibrium Moisture Contents for Stabilator Composite Skins . . . . .	51
27	Diffusivity for Stabilator Composite Skins . . .	52
28	Program and Literature Diffusivity Data for Unpainted AVCO 5505 Boron/Epoxy . . . . .	53
29	Range of Effective Diffusivities for Painted and Unpainted Boron/Epoxy . . . . .	54
30	Surface Cracks After Exposures to Severe Laboratory Environments . . . . .	56
31	Upper and Lower Bounds on Predicted Skin Temper- atures for the Eagle 14 Environmental History . .	57
32	Upper and Lower Bounds on Predicted Surface Air Humidities for the Eagle 14 Environmental History . . . . .	58
33	Predicted Moisture-Time Profile and Measured Value for 14-Ply Eagle 14 Skins . . . . .	60
34	Predicted Moisture-Time Profile and Measured Value for 24-Ply Eagle 14 Skins . . . . .	61
35	Predicted Moisture-Time Profile and Measured Value for 38-Ply Eagle 14 Skins . . . . .	62
36	Predicted Moisture-Time Profile and Measured Value for 14-Ply PDV Skins . . . . .	63
37	Predicted Moisture-Time Profile and Measured Value for 24-Ply PDV Skins . . . . .	64
38	Predicted Moisture-Time Profile and Measured Value for 38-Ply PDV Skins . . . . .	65

# LIST OF ILLUSTRATIONS (Concluded)

FIGURE		PAGE
39	Distribution of Peak Moisture Contents Predicted for F-15 Deployments . . . . .	70
40	Moisture-Time Profile in 14-Ply Skins Predicted for a Median-Case Deployment . . . . .	71
41	Moisture-Time Profile in 14-Ply Skins Predicted for a Worst-Case Deployment . . . . .	73
42	Moisture-Time Profile in 44-Ply Skins Predicted for a Worst-Case Deployment . . . . .	74
43	Specimen Layout on the Eagle 14 Tension Skin . .	76
44	Specimen Layout on the Eagle 14 Compression Skin.	77
45	Specimen Layout on the PDV Tension Skin . . . . .	77
46	Specimen Layout on the PDV Compression Skin . . .	78
47	Eagle 14 Moisture Contents at Conclusion of Static Test . . . . .	80
48	Maximum Moisture Contents Calculated for Use in Element Tests . . . . .	80
49	Tensile Strength of Bonded Root Splice . . . . .	82
50	Compressive Strength of Boron/Epoxy Skins . . . .	85
51	Pyrograms Identifying Full Range of Pyrolysis Products. . . . .	89
52	Pyrogram Identifying Light Gaseous Products . . .	90



# LIST OF TABLES

TABLE		PAGE
1	Nondestructive Evaluations Performed on Eagle 14 and PDV Stabilators . . . . .	7
2	Eagle 14 Test Data . . . . .	28
3	PDV Test Data . . . . .	34
4	Test Data Correlation . . . . .	38
5	Peak Strain Comparisons . . . . .	38
6	Eagle 14 Stabilator History . . . . .	41
7	PDV Stabilator History . . . . .	42
8	Emissivity and Solar Absorptivity Used for Stabilator and Runway Surfaces . . . . .	46
9	Overall Conductance and Radiation View Factors .	46
10	Laboratory Environments Used for Determining Moisture Diffusion Properties . . . . .	48
11	Moisture Contents Predicted in Individual Upper and Lower Skins and Measured Values . . . . .	66
12	Bases Used for F-15 Deployment Projections . . .	68
13	Projected 25-Year F-15 Deployments . . . . .	68
14	Configuration of Stabilator Composite Skin. . . .	79
15	Results of Bonded Joint Tests . . . . .	81
16	Shear Modulus Measured in Rail Shear Tests . . .	83
17	Results of Compression Tests . . . . .	84
18	Results of Flatwise Tension Tests . . . . .	86
19	Physical Properties . . . . .	87
20	Full Range of Pyrolysis Products . . . . .	90
21	Light Gaseous Pyrolysis Products . . . . .	91

## SECTION I

### INTRODUCTION AND SUMMARY

Laboratory tests of epoxy matrix composite specimens have repeatedly demonstrated that certain structural properties are degraded by absorbed moisture. These strength reductions may be reversible or irreversible depending on whether the absorbed moisture, in conjunction with thermal and mechanical loadings, damages the epoxy matrix. There is, however, a lack of data on the combined effects of moisture absorbed from actual service environments and mechanical loads. These data are needed for evaluation of the future highly-loaded composite structures which must withstand temperature and humidity extremes over their mission life.

In this program, the effects of exposure to realistic environments and structural loads were evaluated using the F-15 horizontal stabilator as a typical composite structure. This stabilator incorporates boron/epoxy skins in the main torque box assembly. Effects of the extremes of USAF service environments were evaluated by subsequent static testing of a stabilator which previously was part of the F-15 climatic test program. Effects of service life spectrum fatigue loadings and laboratory environments were examined using a stabilator which sustained static and spectrum fatigue loads in F-15 design verification testing and a subsequent long-term storage period.

This program was conducted in three phases:

- Phase I - Nondestructive Evaluations
- Phase II - Moisture Contents of Composite Skins
- Phase III - Full-Scale Static Tests and Element Tests

Phase I consisted of nondestructive evaluation of the candidate stabilators for this program following their previous usage. One of the two stabilators from the F-15 climatic test airplane was selected as a test article following these evaluations. Inspection results were compared with original production records to detect any damage resulting from the interim service and storage exposures. The stabilator used originally for F-15 design verification testing was also nondestructively examined. Repairs needed before use as a static test article were also accomplished in this phase.

Phase II consisted of analytically predicting moisture contents of the stabilator composite skins for a variety of different F-15 deployments. These analyses required development of thermodynamic models of various locations in the composite skins and

experimental determination of moisture diffusion properties of the boron/epoxy skin material. Moisture content histories were also calculated for each of the test articles and predicted moisture contents were compared with values measured at the conclusion of the static tests to verify the predictive methodology. This predictive methodology was used in conjunction with projected F-15 deployments to determine the maximum expected moisture contents.

Phase III consisted of full-scale tests of the two F-15 stabilators followed by element tests of specimens removed from both failed articles. Both stabilators were loaded statically to failure and the results compared to earlier design verification test results. Composite skins were ultrasonically inspected to locate undamaged areas from which additional coupons could be machined. Coupons were used for evaluation of physical, chemical and structural properties of the boron/epoxy skins and for measuring moisture contents. Structural testing of these coupons was conducted after conditioning them to preselected moisture contents, including maximum expected moisture levels.

## SECTION II

### NONDESTRUCTIVE EVALUATIONS

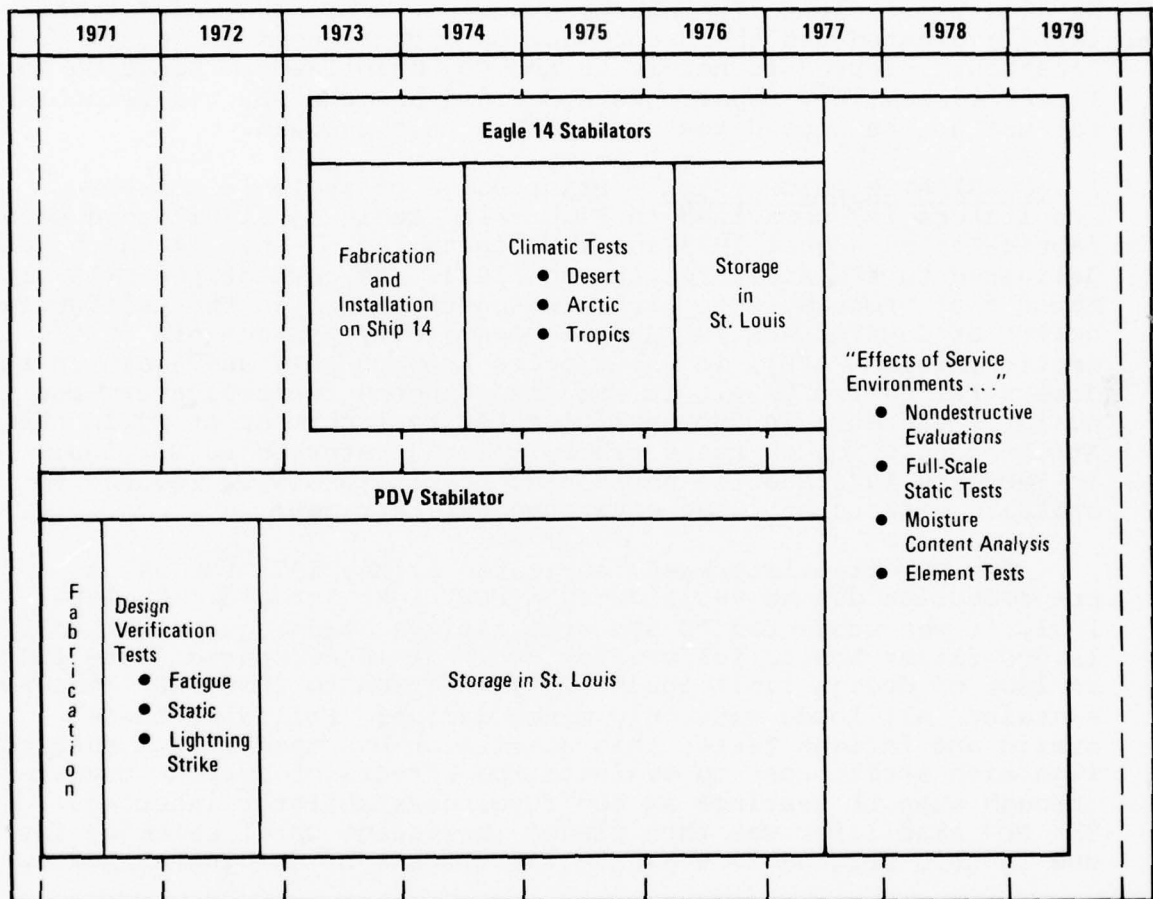
A total of three stabilators were nondestructively evaluated in this program. Two were from the F-15 climatic test airplane, McDonnell serial number 14, and are referred to in this report as Eagle 14 stabilators. One of the Eagle 14 stabilators was selected as a test article following these evaluations. The third stabilator evaluated was the preproduction article used for design verification, referred to herein as the PDV stabilator. Based on this latter evaluation, repairs were defined and the PDV was refurbished for use as the second test article in this program.

1. STABILATOR PRIOR USAGE - Prior usage of Eagle 14 and PDV stabilators is summarized in Figure 1. Eagle 14 stabilators were fabricated by August 1973 and then installed on Ship 14 which was delivered to the Air Force in June 1974. As part of the F-15 climatic test program, this airplane was stationed in the California desert at Edwards AFB but saw temporary duty assignments in the arctic (Eielson AFB), in the tropics (Howard AB), and again in the desert (El Centro NAS). It was also exposed to temperature and humidity extremes in the environmental test chamber at Eglin AFB. At the conclusion of these tests, Ship 14 returned to St. Louis in February 1976 and the horizontal stabilators were removed to evaluate effects of these environmental extremes.

The PDV stabilator was fabricated by May 1971 for use as a preproduction design verification (PDV) test article. In late 1971, it was subjected to spectrum fatigue loads equivalent to 16,000 flight hours, followed by two individual static tests first to 150% of design limit loads (DLL) and then to 200% DLL. The PDV sustained all loads with only minor damage. Following these static and fatigue tests, this stabilator was used in a simulated lightning strike test to evaluate the effects of current transfer through support bearings at the fuselage/stabilator interface. The PDV stabilator was then placed in storage until selected for use in this program to evaluate the effects of loading extremes.

2. STRUCTURAL DESCRIPTION - The F-15A horizontal stabilators are entirely moveable and may be actuated differentially, for roll control, or collectively for longitudinal trim and pitch control. Stabilator surfaces are symmetrical airfoil sections with no camber, a 50° leading edge sweep, and an aspect ratio of 2.05. Due to the midplane symmetry, the same stabilator can be installed on either side of the F-15.





GP79-0344-3

Figure 1. Usage History of Eagle 14 and PDV Stabilators



Eagle 14 stabilators are representative of production articles in that a "snag" was incorporated in the inboard leading edge structure. The PDV stabilator was a preproduction article and had no "snag". The stabilators were otherwise structurally identical and are shown in Figure 2.

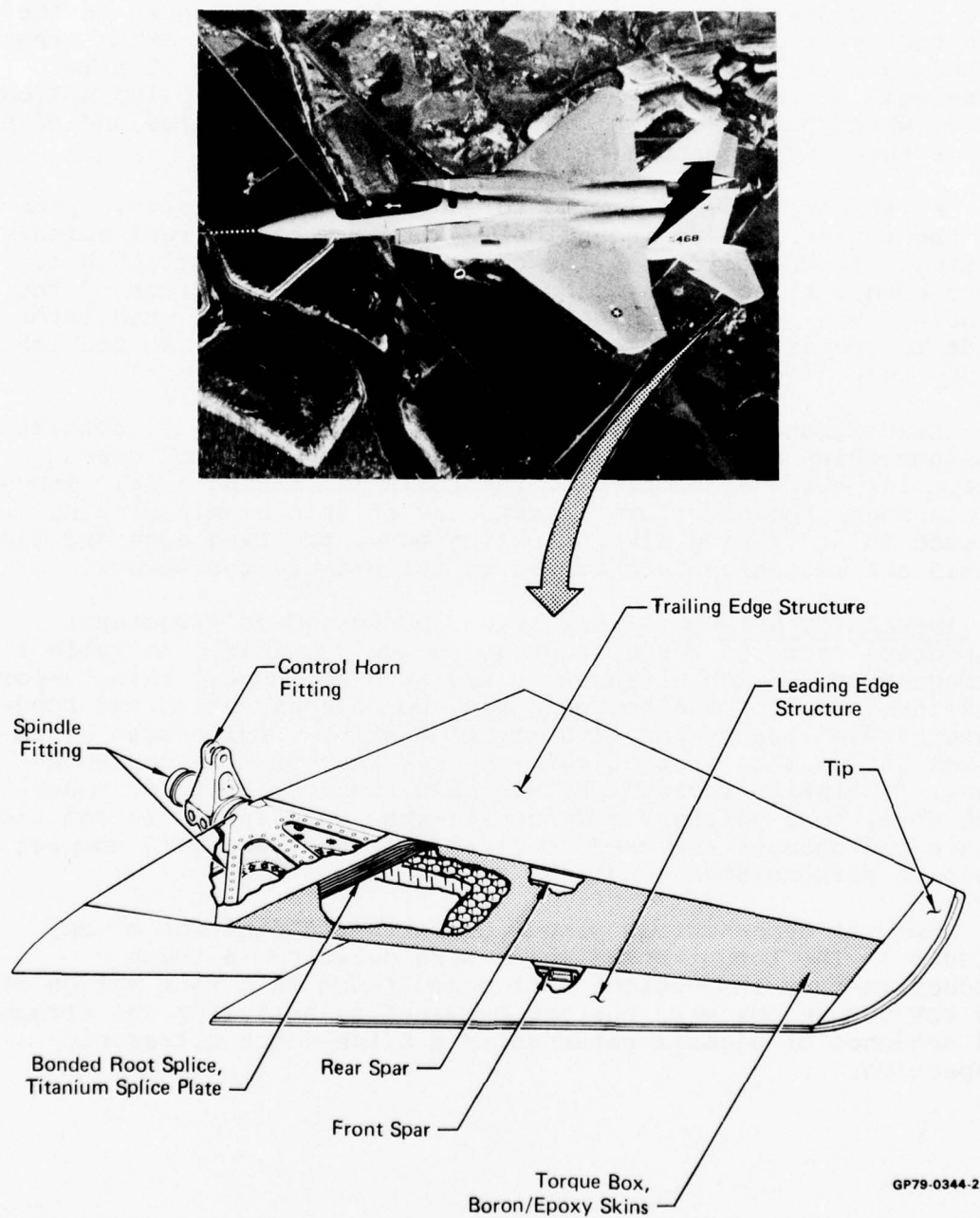


**Figure 2. F-15 Stabilator Structure**

The primary torque box is a bonded assembly of boron/epoxy skins, aluminum full-depth honeycomb core, and titanium spars, ribs and "picture-frame" splice plates. Skins for the Eagle 14 and PDV stabilators were fabricated from AVCO 5505 boron/epoxy prepreg. Each was cured and post-cured and, in the same operation, bonded to the titanium splice plate using FM400 adhesive. In a second operation, upper and lower skins were bonded to the honeycomb core again using FM400. These boron/epoxy skins range in thickness from 44 plies (.23-inch) at the root to 12 plies (.06-inch) at the tip. Each skin is bonded to a step-lap splice plate, which has five machined steps in the root splice and either two or three steps on the remaining three sides.

At the inboard end of the torque box, splice plates, spars and the torque rib are mechanically attached to a forged spindle fitting. In the aircraft, the control actuator is attached to a drive horn fitting which is bolted to the barrel section of the spindle. The spindle and horn fittings transfer all stabilator loads to the aircraft fuselage or, for this program, to the laboratory test fixture.

Leading and trailing edge panels and the tip panel consist of aluminum skins bonded to full-depth aluminum honeycomb cores except for the snagged area of the Eagle 14 leading edge. Inboard of the snag, the structure is composed of thin aluminum skins riveted to stiffening ribs. Leading edge, trailing edge and tip panels are mechanically attached to the primary torque box.

3. INSPECTION METHODS - Inspections performed on structural components from the three stabilators are summarized in Table 1. Through-transmission ultrasonics was used to inspect skin-to-core bondlines and, for the torque boxes, boron/epoxy skins and bondlines between boron/epoxy and titanium skins. Pulse-echo ultrasonics was used to inspect skin-to-spar and core-to-spar bondlines. In-motion radiography was used for inspection of honeycomb core, core splices, and core-to-spar bondlines. In addition, static radiography was used to clarify thicker and more complex areas of core-to-spar bondlines in the torque box.

Special emphasis was placed on further definition of any defects in the torque boxes which were detected in these production-type inspections. Disbonds found in a root splice of the PDV torque box were further examined by analyzing the strength and sequence of signals returned in a pitch-catch ultrasonic inspection.

**TABLE 1. NONDESTRUCTIVE EVALUATIONS PERFORMED ON EAGLE 14  
AND PDV STABILATORS**

Inspection Method	Eagle 14 Left				PDV					Eagle 14 Right
	Torque Box	Leading Edge	Trailing Edge	Tip	Torque Box	Leading Edge	Trailing Edge	Tip	Spindle	Torque Box
Automated Through-Transmission Ultrasonic C-Scan	Yes	Yes	Yes	Yes	Yes	Yes	Yes	Yes		Yes
Pulse-Echo Ringing Ultrasonic A-Scan	Yes	Yes	Yes	Yes	Yes	Yes	Yes	Yes		Yes
Pitch-Catch Ultrasonic A-Scan, Signal Analysis					Yes					
In-Motion Radiography	Yes	Yes	Yes	Yes	Yes	Yes	Yes	Yes		Yes
Stationary Radiography	Yes				Yes					Yes
Dye Penetrant									Yes	
Visual	Yes	Yes	Yes	Yes	Yes	Yes	Yes	Yes	Yes	Yes

GP79-0344-4

4. NONDESTRUCTIVE EVALUATION OF EAGLE 14 STABILATORS - The stabilators were disassembled and both torque boxes, Figure 3, were ultrasonically and radiographically inspected. Results of the through-transmission ultrasonic inspection are shown in Figures 4 and 5. Squirter-coupled automated techniques were used. Sound attenuation greater than 55 dB is printed as black areas on the C-scan record; attenuation of less than 20 dB is represented by white areas. Attenuation between these two values is represented by various shades of gray obtained by the progressive darkening of a 4 x 4 dot matrix until solid black at 55 dB. The significant darkening of the C-scan records along the thinnest step of the root splice fitting is a response characteristic of all torque box inspections and does not represent flawed areas. This darkening results from destructive interference between the sound beam being transmitted through the structure and a standing wave created by the unique relationship of step thickness to input sound wavelength.

The original production inspection records were also reviewed for evidence of flaws in the torque boxes. Static radiography and through-transmission ultrasonics had been used for these inspections. The sensitivity of C-scan records was compatible with that obtained in this program, although the ultrasonic equipment and the printout format for the C-scans differed from those currently used.

No defects were found from the current inspection records or from the original production records. Consequently, the left-hand stabilator from Ship 14 was selected for testing in this program on the basis of compatibility with the test setup designed for the PDV stabilator.

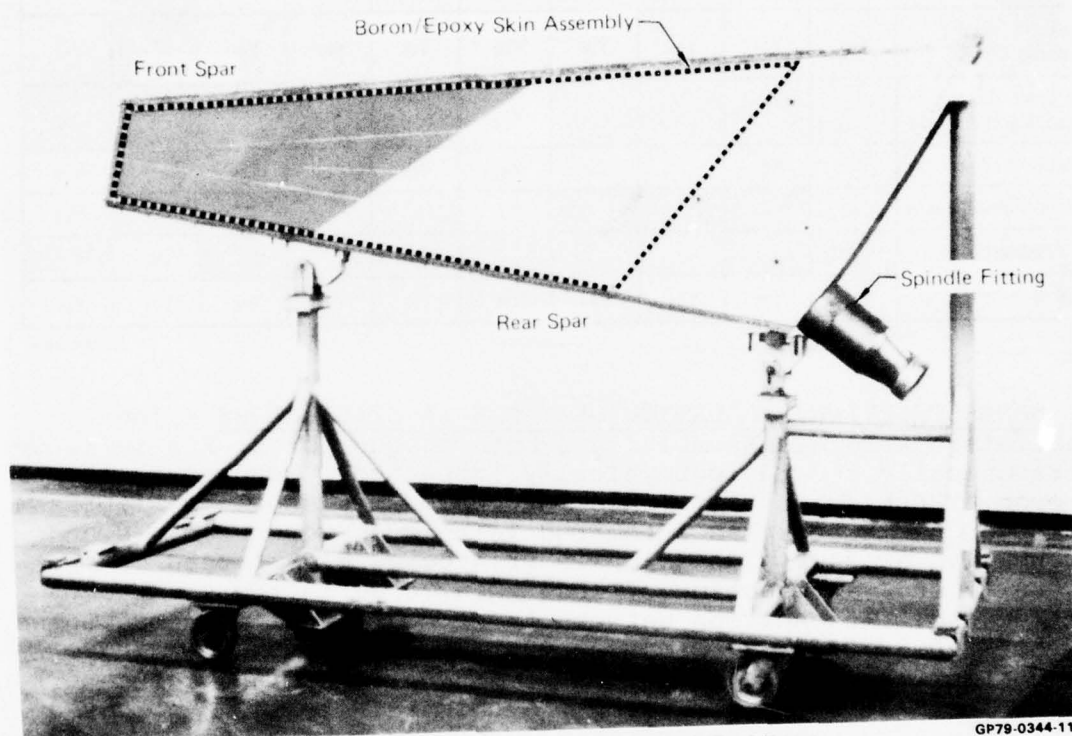
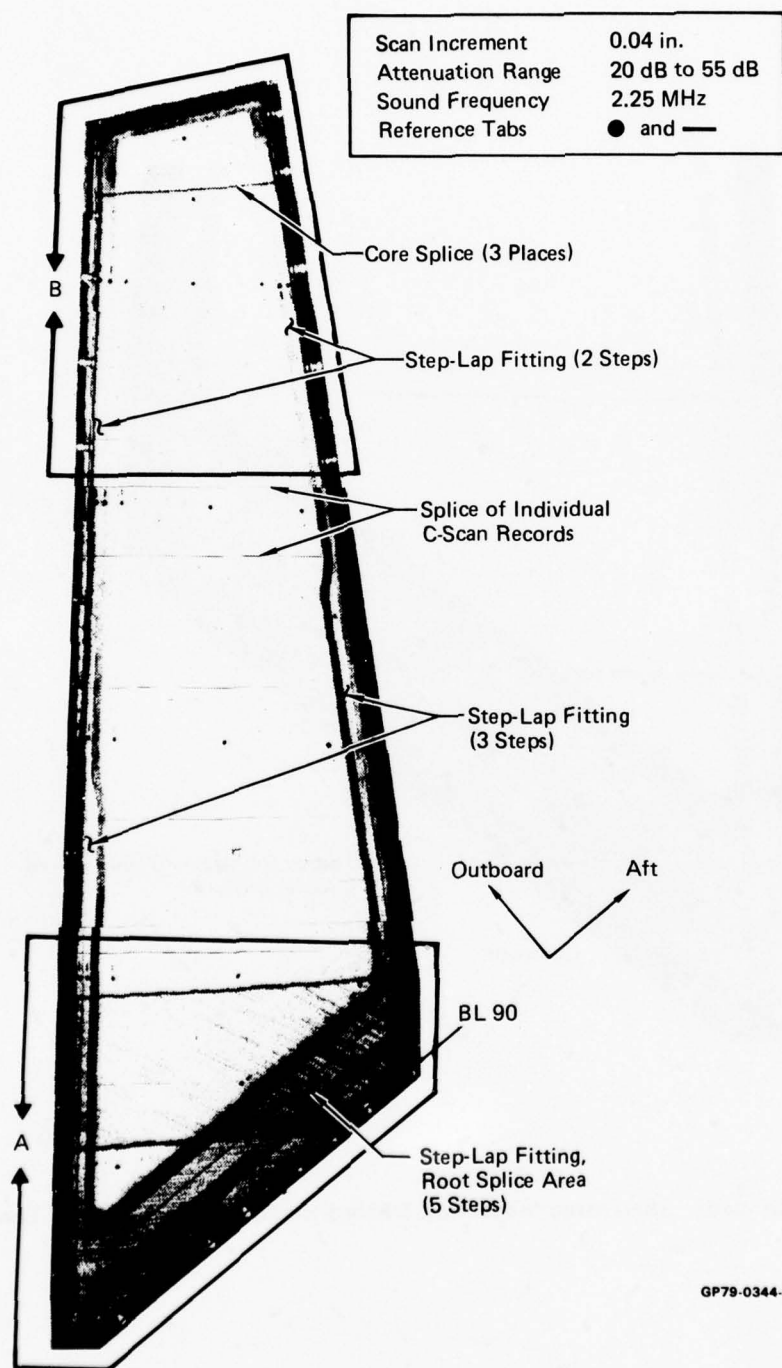


Figure 3. Torque Box from Eagle 14 Stabilator

GP79-0344-11

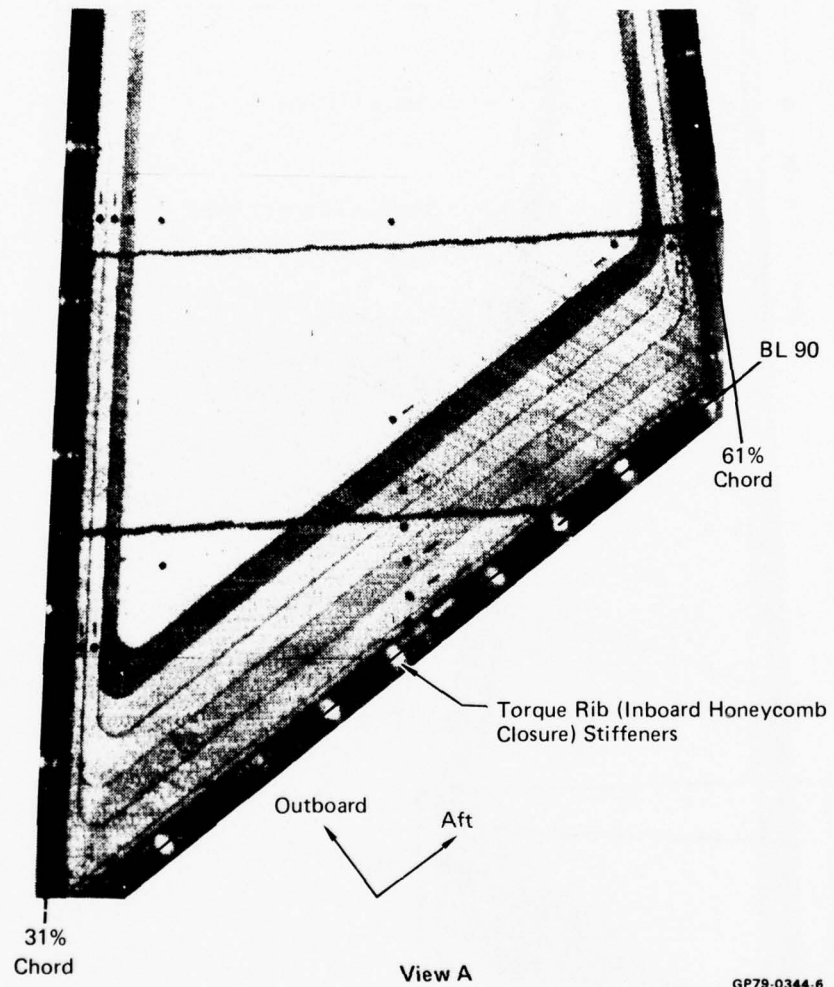




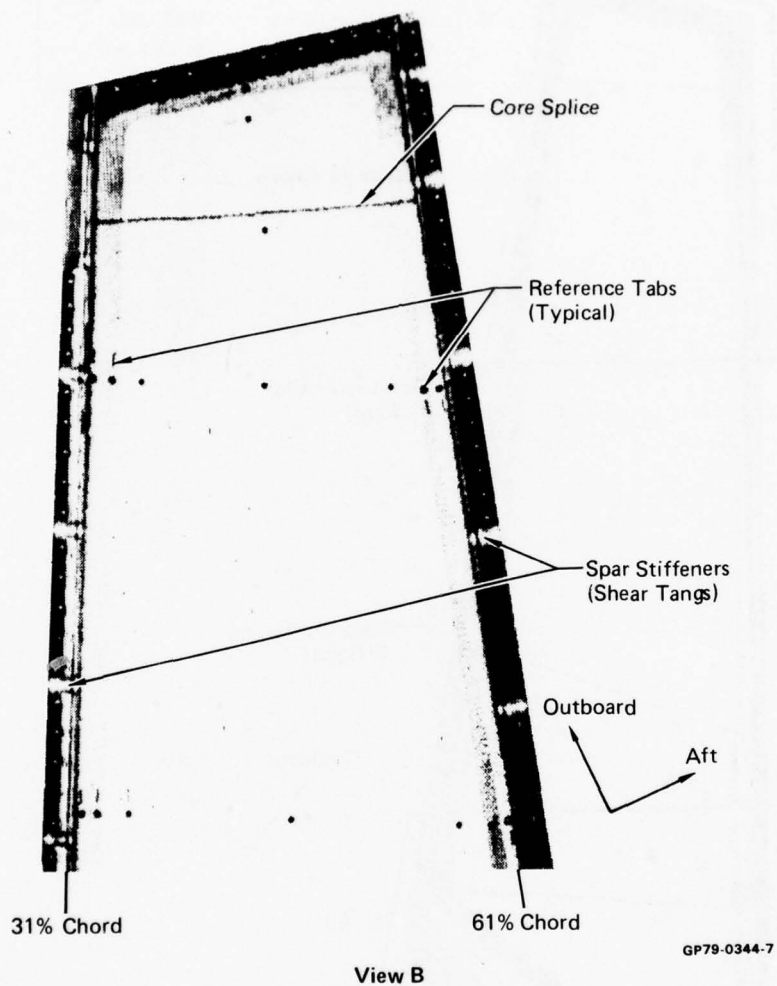
GP79-0344-5

Figure 4. Ultrasonic Inspection Record for Left-Hand Eagle 14 Torque Box

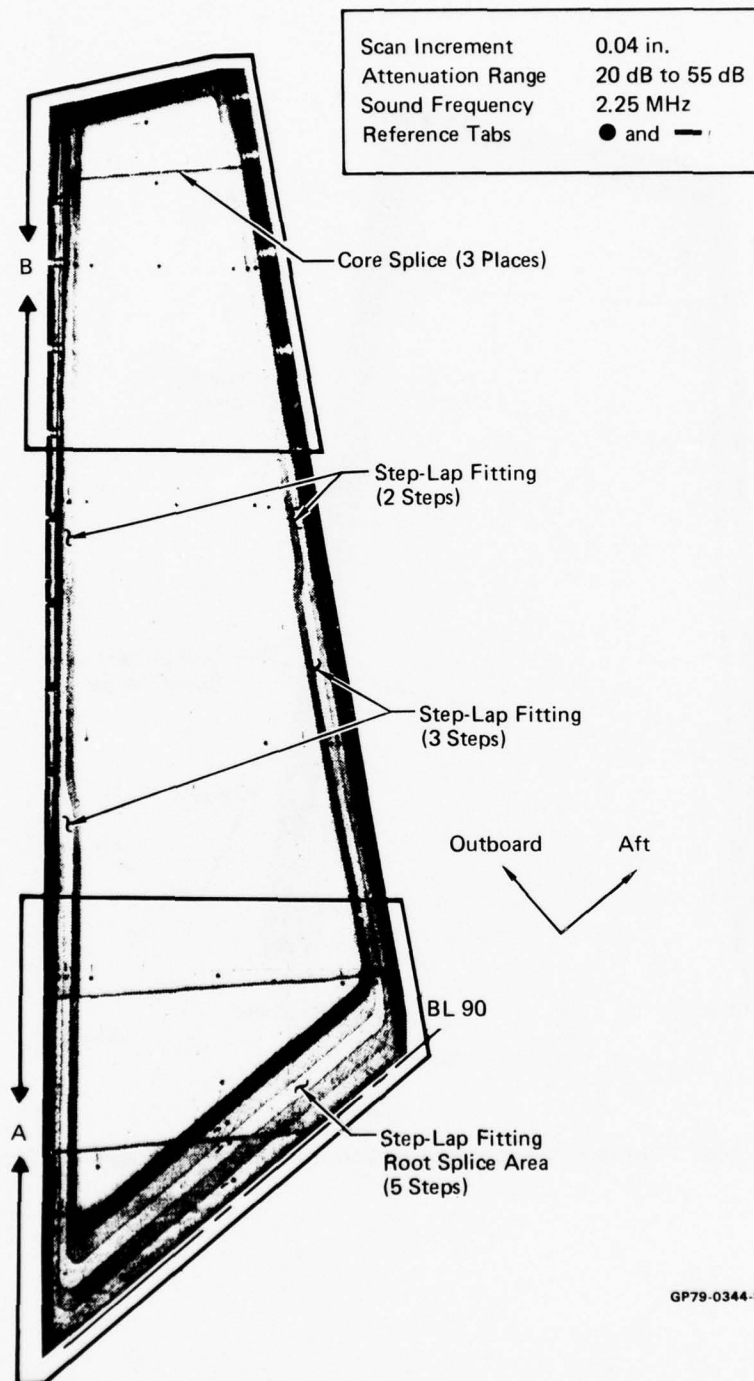




**Figure 4. (Continued) Ultrasonic Inspection Record for Left-Hand Eagle 14 Torque Box**



**Figure 4. (Concluded) Ultrasonic Inspection Record for Left-Hand Eagle 14 Torque Box**



GP79-0344-8

Figure 5. Ultrasonic Inspection Record for Right-Hand Eagle 14 Torque Box

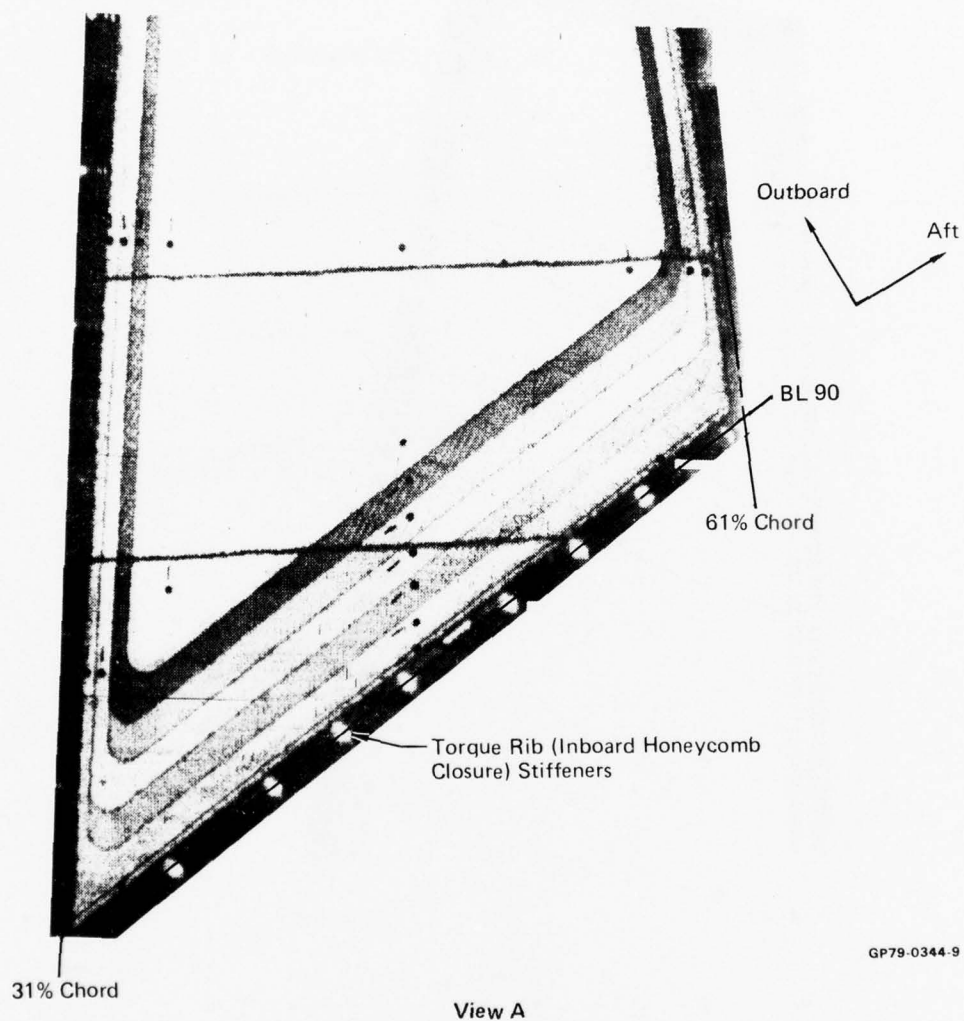
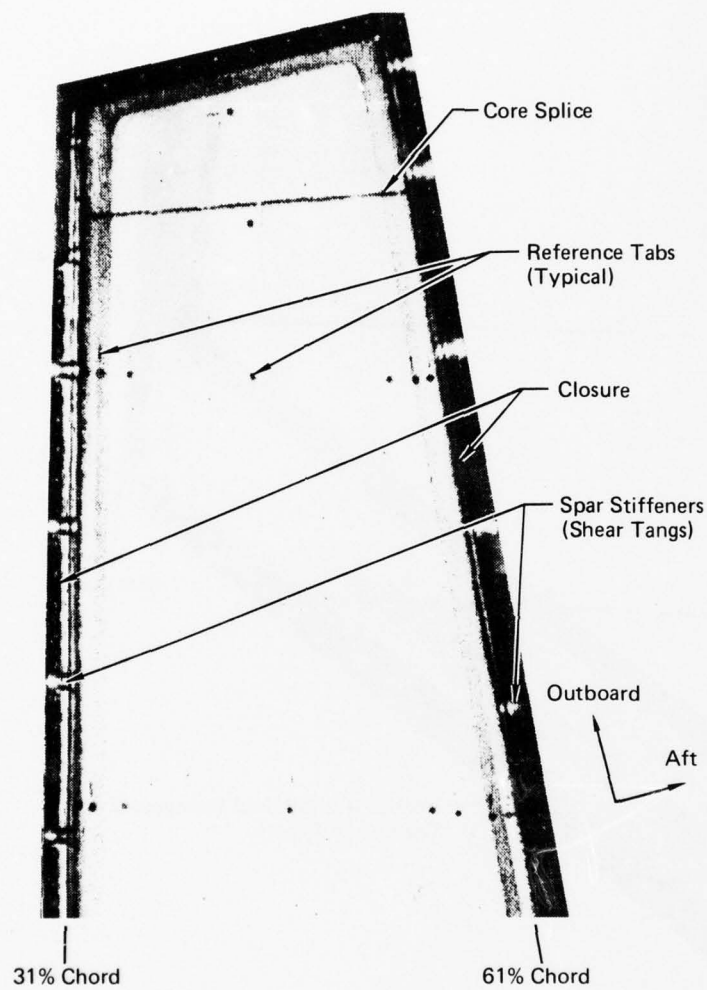


Figure 5. (Continued) Ultrasonic Inspection Record for Right-Hand Eagle 14 Torque Box





View B

GP79-0344-10

Figure 5. (Concluded) Ultrasonic Inspection Record for Right-Hand Eagle 14 Torque Box

No defects were found in the leading edge, trailing edge and tip panels of the Eagle 14 test article.

5. NONDESTRUCTIVE EVALUATION OF THE PDV STABILATOR - Components of the PDV stabilator were nondestructively tested using the same techniques that were used for the Eagle 14 test article. In addition, a thorough visual examination was made for conformance to the requirements of the engineering drawing. Repairs were then defined and completed prior to the use of this stabilator as a static test article.

a. Torque Box - Through-transmission ultrasonics revealed two disbonds, Figure 6, in the root splice area. These comprised approximately 15% of the total bonded area of this root splice. In-motion radiography revealed five small areas of blown core in outboard sections of the torque box. Four of these areas, shown in Figure 7, were adjacent to the front spar. All five were in the vicinity of a core splice.

Disbonds at the root splice (Figure 8) were localized, using pulse-echo ultrasonics, to the skin which had been tension-loaded during the design verification static test. It was conceivable, however, that these could have occurred within this boron/epoxy skin on either side of the metal splice fitting, at either skin-to-fitting bondline, or at the skin-to-core bondline. The depth of disbonds was determined by a contact ultrasonic inspection in which a dual transducer was used to send and receive ultrasonic signals. The sequence and strength of sound echos from the various material interfaces were used in conjunction with the known speed of sound in the various media to locate the disbonds in the skin-to-fitting bondline nearest the honeycomb core. This was verified upon dissecting the root splice after the static test.

None of these defects appeared in the original production inspection records or in the limited inspection conducted after the static and fatigue tests in the design verification program. After static and fatigue tests, the torque box was reinspected using static radiography. Disbonds would not normally be detected in X-rays, so it's possible that these occurred during the structural tests. Blown core, however, would have appeared in X-rays but did not. Thus, these defects occurred after the structural tests possibly as a result of the simulated lightning strike tests.

The disbonds in the PDV root splice were not repaired. Effects of large disbonds were evaluated in Reference 1 for this step-lap joint configuration; results of these tests indicated that PDV disbonds would not have a significant impact on static failure levels. Also, the areas of damaged core in the torque box were not large enough to require a repair.

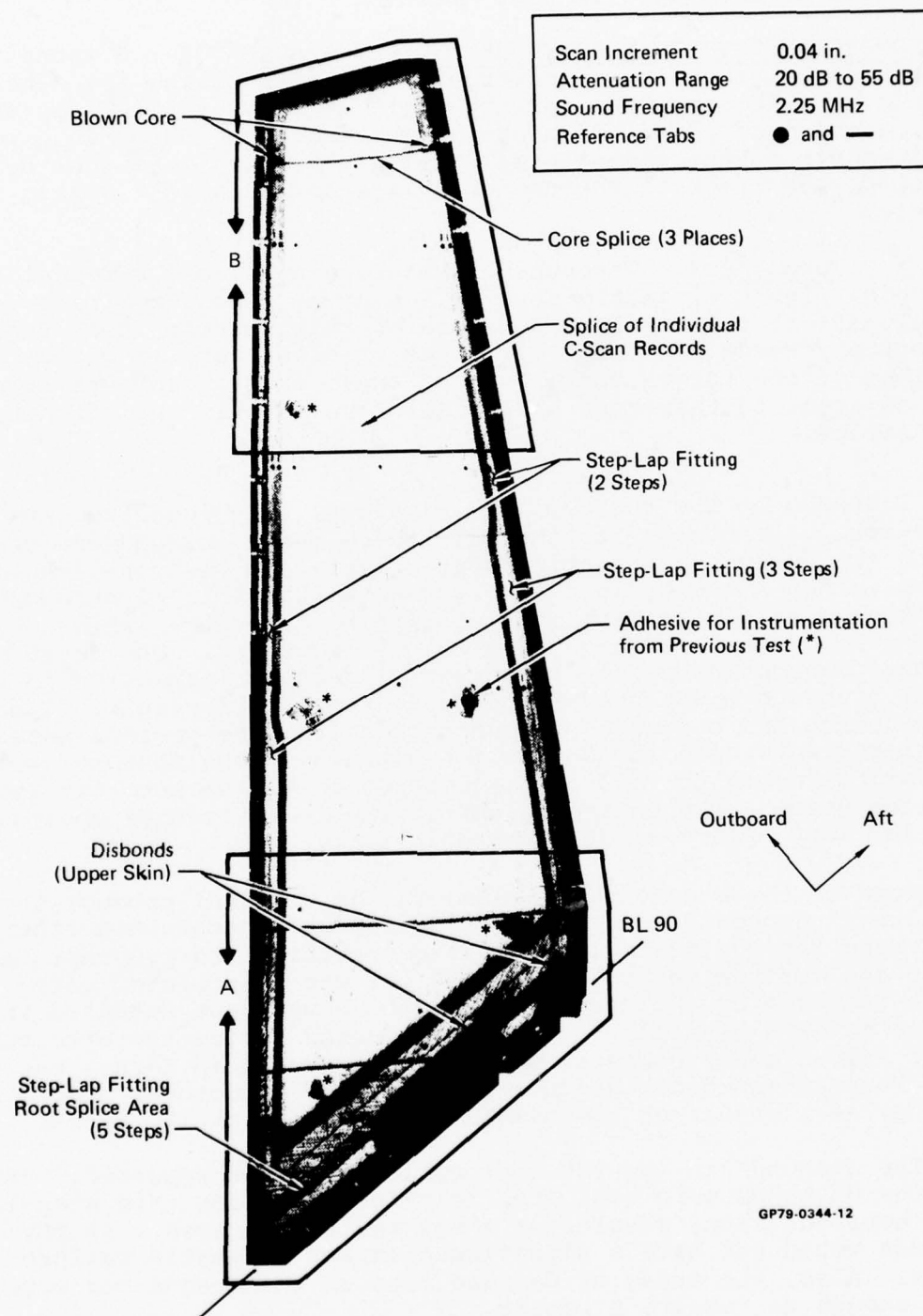


Figure 6. Ultrasonic Inspection Record for PDV Torque Box

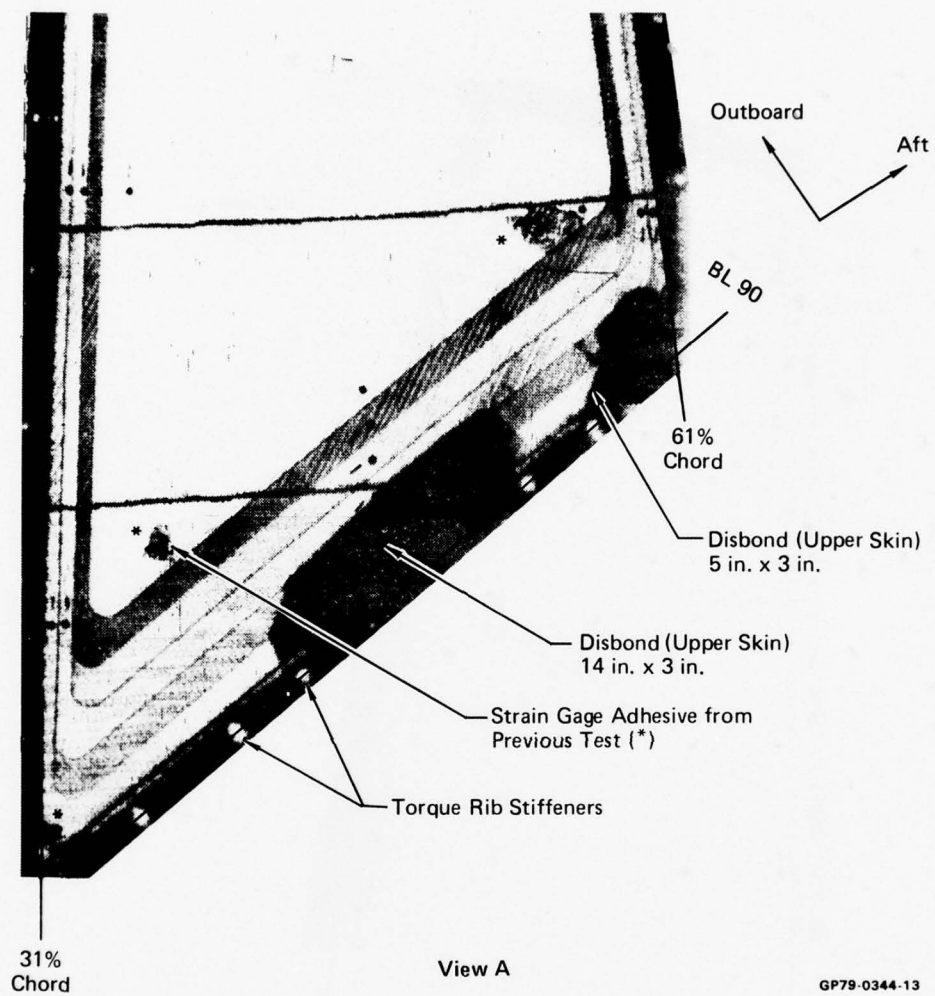


Figure 6. (Continued) Ultrasonic Inspection Record for PDV Torque Box



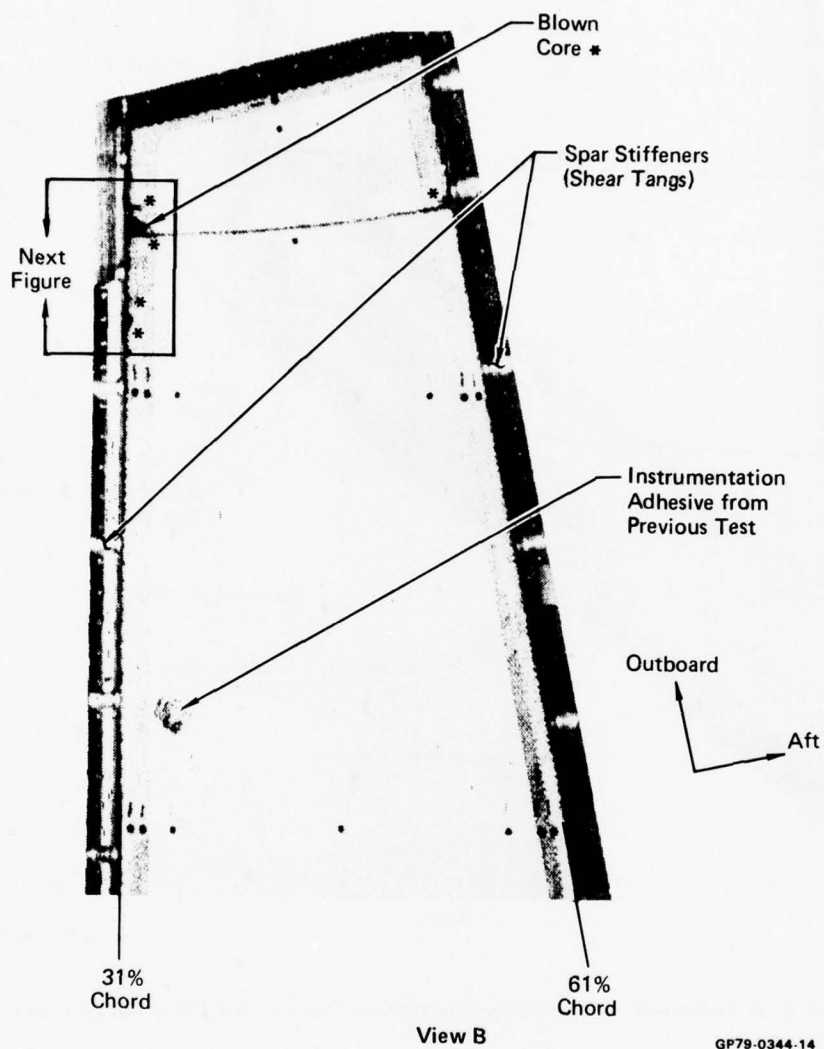
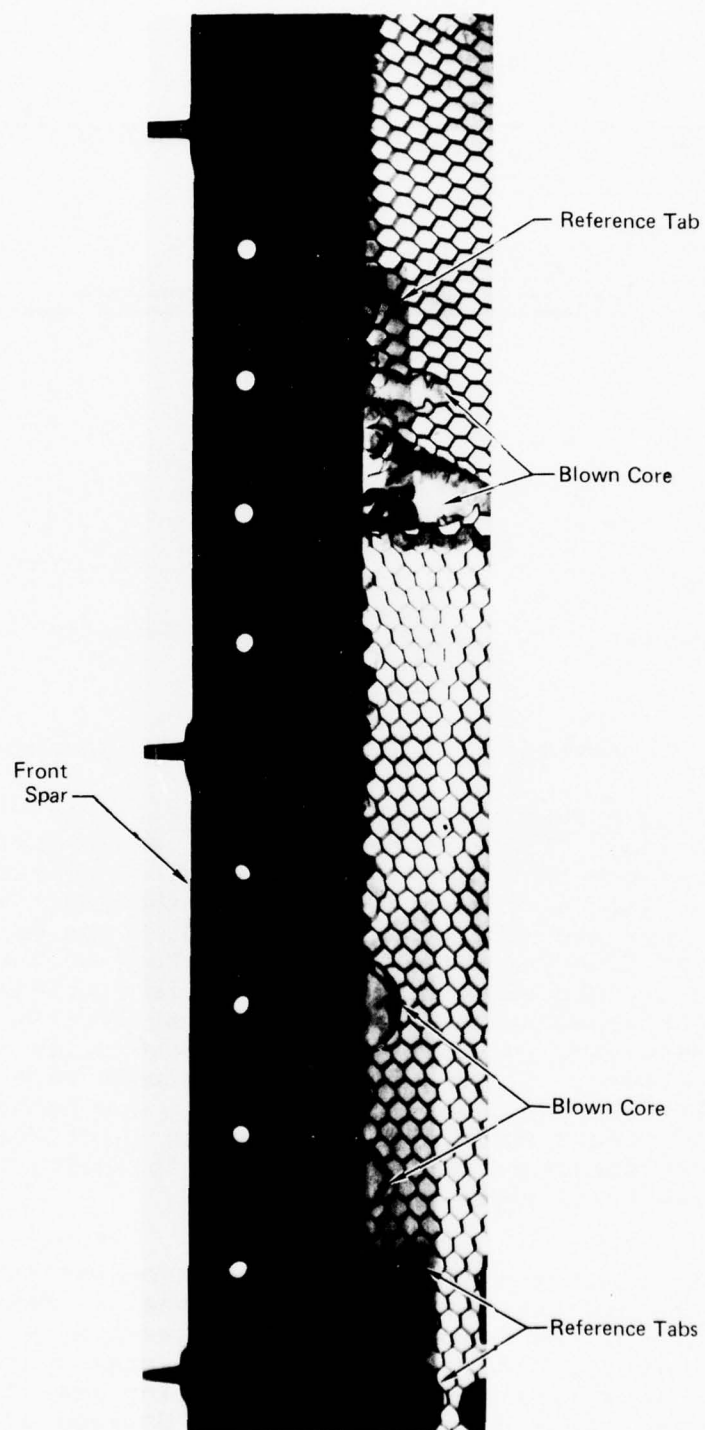
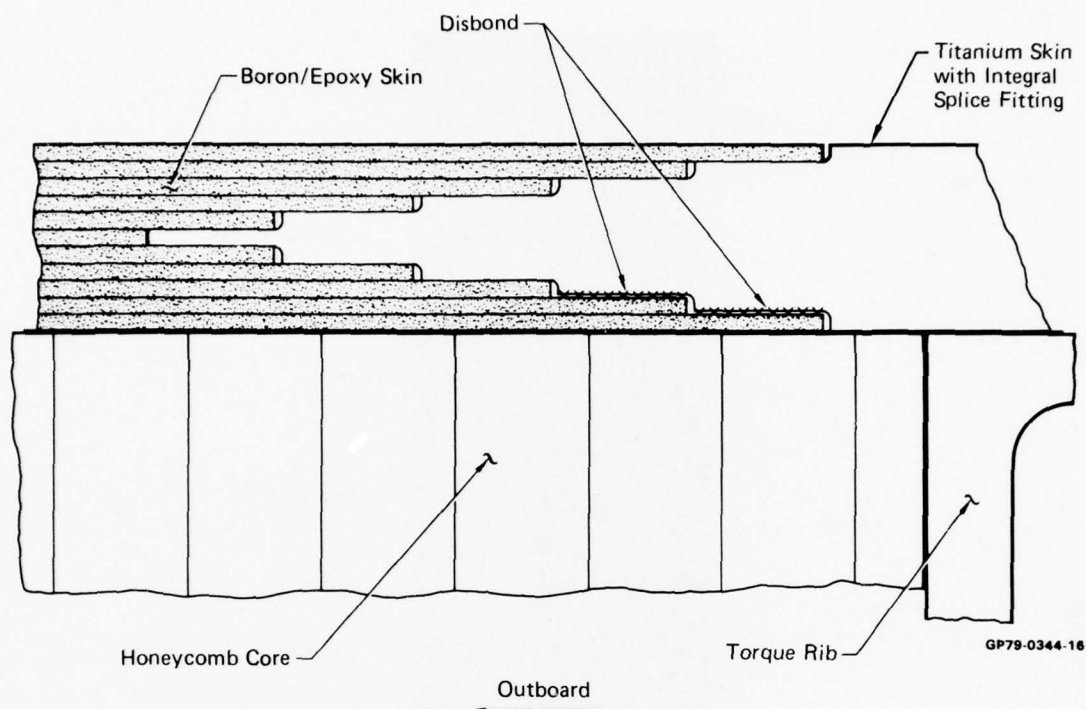


Figure 6. (Concluded) Ultrasonic Inspection Record for PDV Torque Box



GP79-0344-15

**Figure 7. Blown Core Areas in PDV Torque Box**



**Figure 8. Disbonds in PDV Root Splice Found Using Ultrasonics**

b. Metallic Structural Components and Fittings - Visual inspection of leading edge, trailing edge and tip panels and the spindle fitting revealed numerous defects which required repair. These are summarized in Figure 9. Shear ties between the trailing edge panel and the torque box are made through tangs which are machined integral with web stiffeners on the rear spar. Four of these tangs were missing and were replaced with machined clevis fittings which nested over and were attached to the four spar web stiffeners. Oversized repair bolts were used to correct for elongated holes in the spindle-to-skin bolt pattern. Other areas of the spindle were polished to remove surface flaws which were detected in a dye penetrant inspection. Close-tolerance spindle bushings which interface with aft fuselage support structure had been removed following the simulated lightning strike test; these were replaced.

Through-transmission ultrasonic inspection was performed on the leading edge and trailing edge bonded panels. Results confirmed that many of the dents, dings and creases were associated with skin-to-core disbonds. One hole and several dents in the aluminum skins were repaired by locally filling the honeycomb core with adhesive and bonding doublers over the damaged areas. A disbanded skin on the tip panel was rebanded and riveted around the periphery.

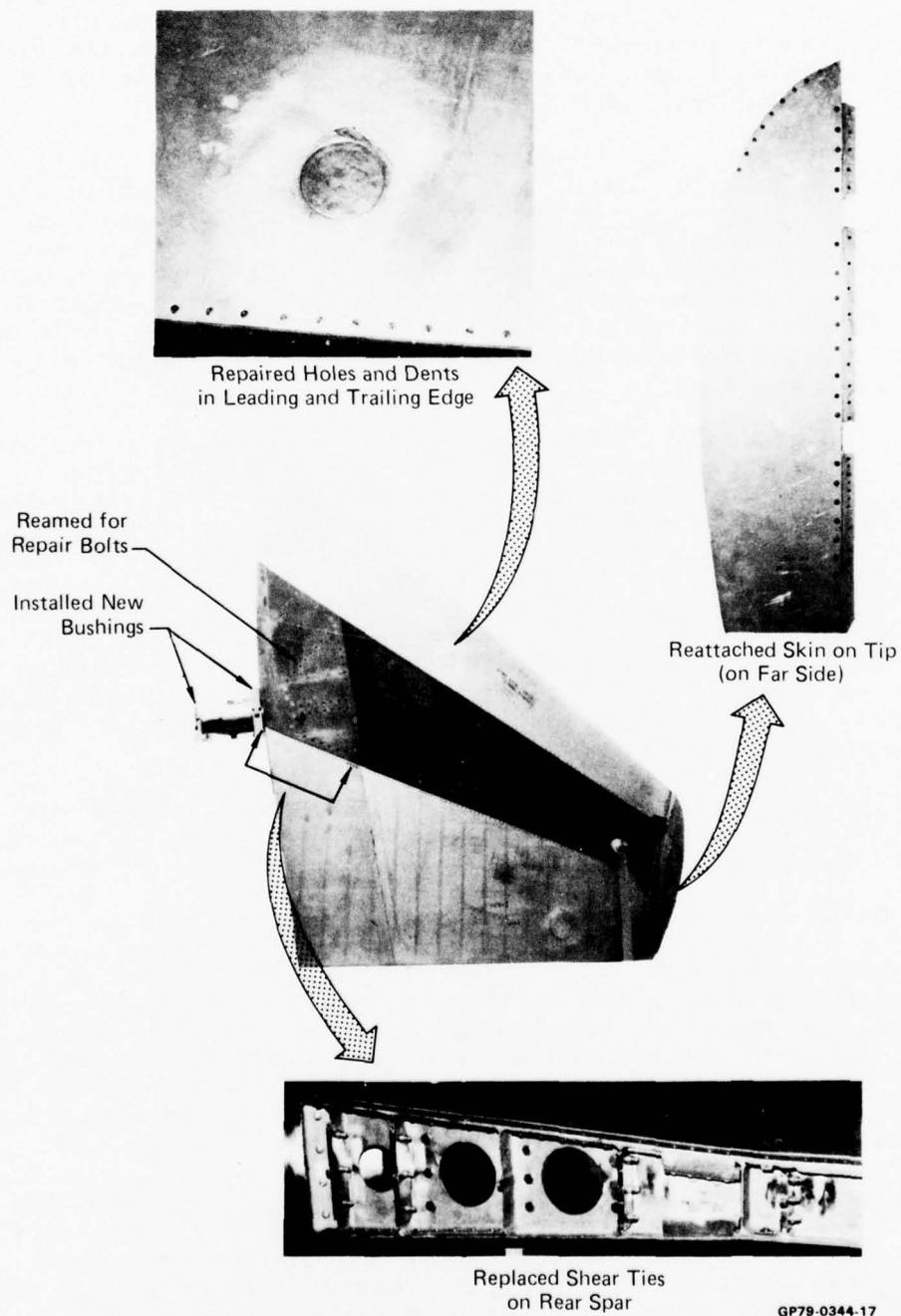


**Figure 9. PDV Stabilator Repairs**



### SECTION III

#### STABILATOR TEST PROGRAM

Full-scale static tests of two F-15 stabilators were conducted in this program to determine their ultimate static strength. The results of these tests were compared with results of a similar design verification test conducted in 1971 to determine the effects of exposures to service and load environments.

1. LOADS USED FOR F-15A STABILATOR DESIGN AND DESIGN VERIFICATION TESTING - The maximum design loads for the F-15 stabilator torque box occur during high speed rolls at altitude. This maneuver causes maximum bending moment and torque as well as 98.5% of the maximum shear expected for the stabilator. Leading edge, trailing edge and tip structural assemblies are designed to loads which occur in a similar maneuver but executed at sea level. Net shear loads on the stabilator for these conditions are up loads and produce compression in the upper surface.

The "snag" leading edge structure typical of all production stabilators (such as Eagle 14) results in a center of pressure aft of its location on the nonsnagged configuration (PDV stabilator). For the torque-box maximum load condition, the torque is increased 16% relative to the torque used in verification testing of the nonsnagged version. This increased torque only affects member loads in the root metal structure. In the earlier design verification test program, however, 200% of static design loads were sustained without failure. This demonstrated strength was well in excess of the room temperature design requirement of 164% and thus qualified the stabilator for the increased loading associated with the snag configuration.

2. TEST LOADS USED IN THIS PROGRAM - Minor modifications were made in the torque-box-critical condition described above to insure that premature failures did not occur in the noncomposite structure.

Loads in the root metal structure were maintained at the levels previously demonstrated in design verification tests by applying a leading-edge-up torque. This torque was applied inboard of the root splice of boron/epoxy skins by means of the torque beam shown in Figure 10. In addition, tension pad loads on the sheet metal leading edge were reduced and adjacent pad loads were increased to maintain the same overall stabilator loading. Pads involved in this redistribution are shaded in Figure 10. Loads on the remaining pads were identical to those used in the design verification test.

Resultant loads for the torque-box-critical condition are shown in Figure 11. F-15 stabilator design loads (solid lines), design verification test loads (dotted lines) and current test loads (dashed lines) matched within 3% in areas of the torque box where analysis indicates lowest margins of safety. These areas are: root

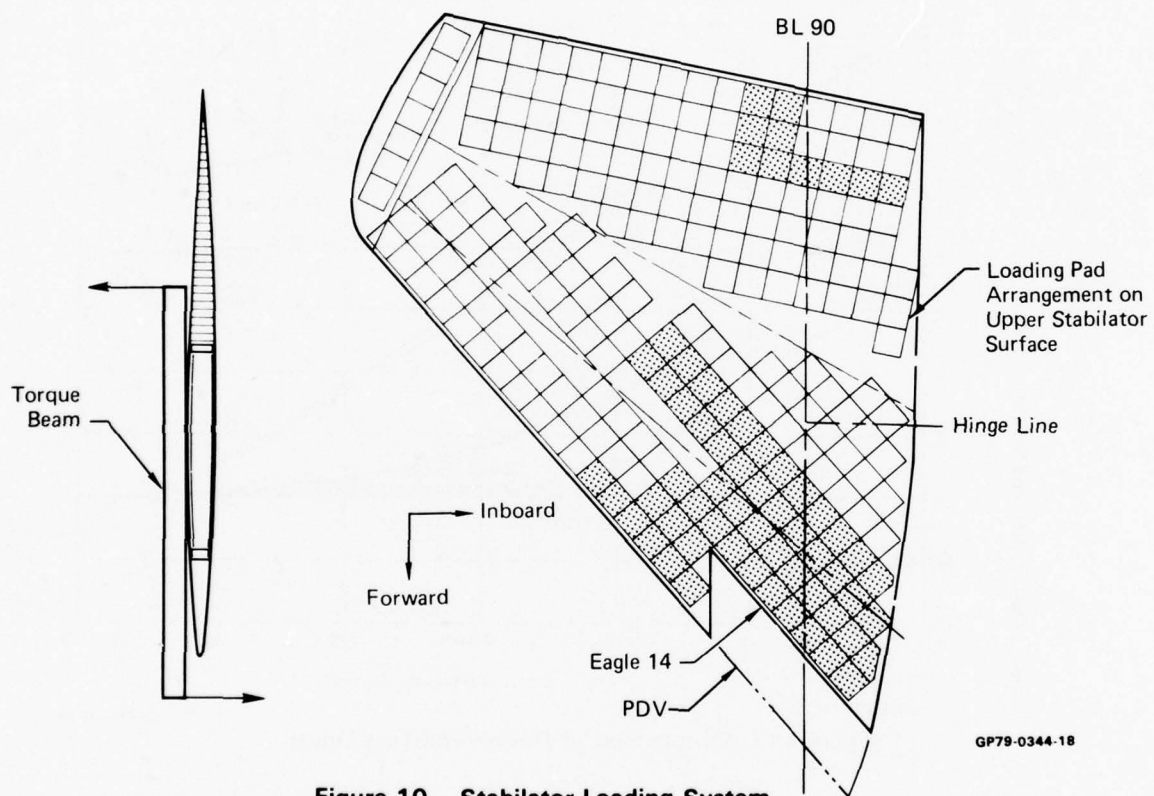
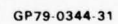


**Figure 10. Stabilator Loading System**



metal structure, hinge line stations 0 to 20; composite skin root splice, load reference stations 0 to 10. Torsion loads in outboard areas of the stabilator were somewhat higher than in the design verification tests as a result of the change in distributed loads required to off-load the sheet metal leading edge of Eagle 14 as described above.

To insure developing comparable loads in the composite skins of both stabilators, the applied load distribution for the test of the Eagle 14 stabilator was also used for the static test of the PDV stabilator. For both static tests, stabilators were cantilevered from the spindle with torsional moments reacted through the control horn fitting. Axial loads at the control horn fitting were measured by a load cell. Distributed loads were applied to the upper stabilator surface (as installed in the test frame) using two load fixture assemblies, each composed of tension pads, wiffle tree, strain link, and a load cylinder. Two load cylinders, slaved to a common servo-controller, were used for applying torque beam loads.

Each stabilator was instrumented with strain rosettes ( $0^\circ$ ,  $45^\circ$ ,  $90^\circ$  gages), uniaxial strain gages and deflection transducers in highly-loaded areas identified from the design verification test data. These locations are shown in Figure 12. A uniaxial gage was

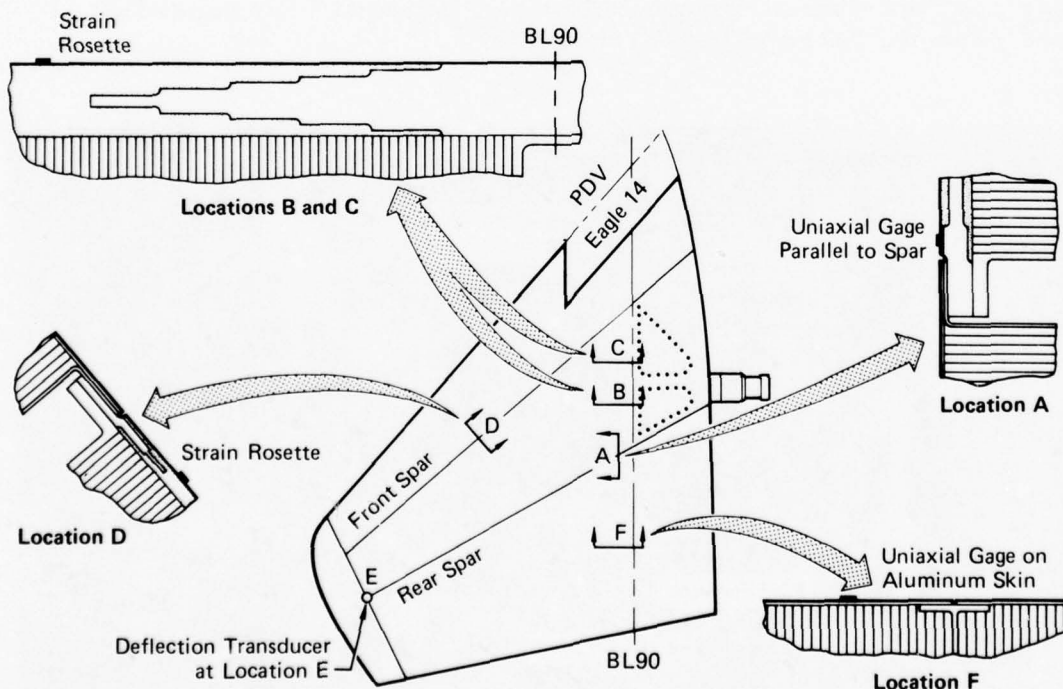


Figure 12. Strain Gage Locations for Data Analysis

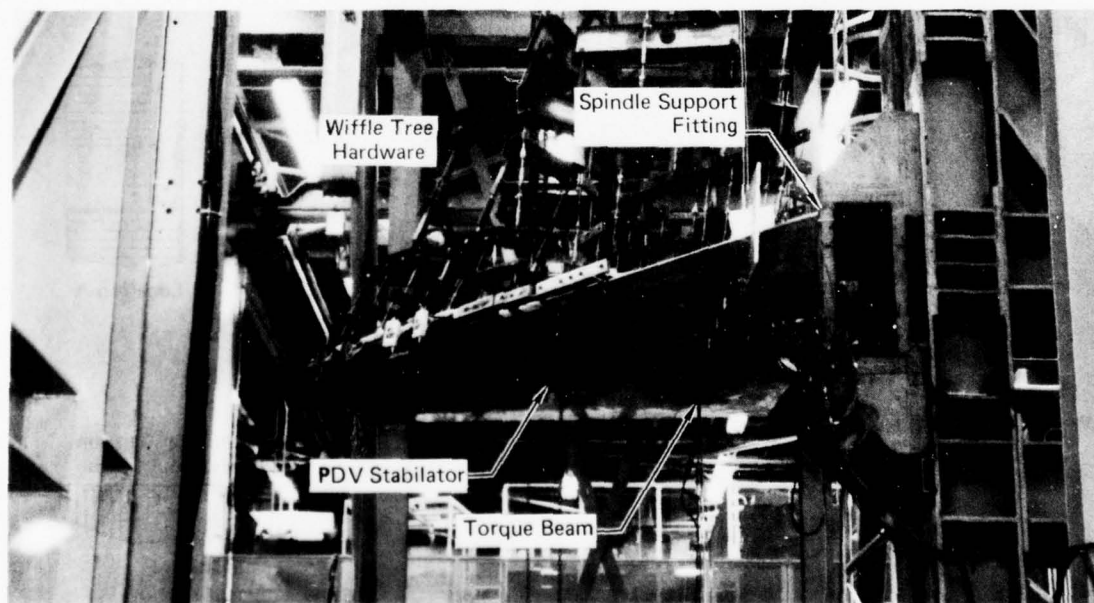
GP79-0344-22



placed on the boron/epoxy skin near the rear spar (location A) to monitor spar cap strains. Strain rosettes were placed on the skin adjacent to the edge of the titanium splice plate (locations B and C) to monitor bonded joint loads. Strains in the boron/epoxy skin next to a highly-loaded area of the leading edge (location D) were also monitored using a strain rosette. Normal displacements at location E were monitored for comparing overall stabilator bending. Other strains and displacements, such as the strain in the trailing edge skin at location F, were recorded for evaluating stabilator failures.

3. STATIC TESTS OF STABILATORS - Full-scale tests were conducted at room temperature so that direct comparison could be made with the results of the room temperature design verification tests. The PDV is shown in the test setup in Figure 13 with the view toward the trailing edge. The Eagle 14 stabilator is shown in Figure 14 loaded to 150% DLL. Lower skins were primarily loaded in tension. For the Eagle 14 test, the lower (tension) skin had been the upper skin on the stabilator during flight service. For the PDV test, the tension skin had also been tension-loaded in design verification testing. All instrumentation was placed on the tension skin.

a. Eagle 14 Test Results - Failure of the Eagle 14 stabilator occurred in the root splice area of the tension skin at 190% of design limit loads. Strain and deflection data are presented in Table 2 for selected load levels. These data are linear with load except for the strain in the rear spar cap which increased at a faster rate as failure became imminent.



GP79-0344-21

Figure 13. Stabilator Static Test Setup

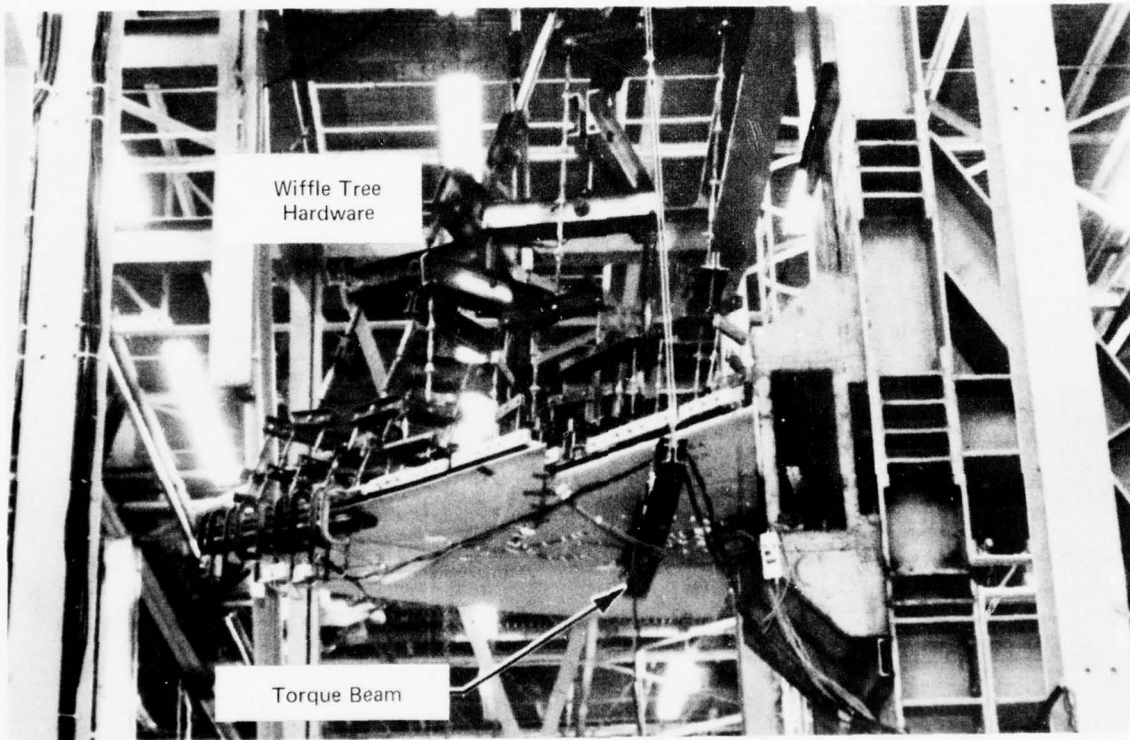


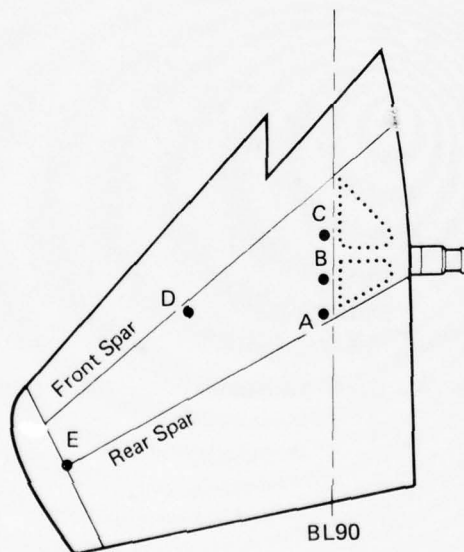
Figure 14. Eagle 14 Stabilator at 150% DLL

GP79-0344-20

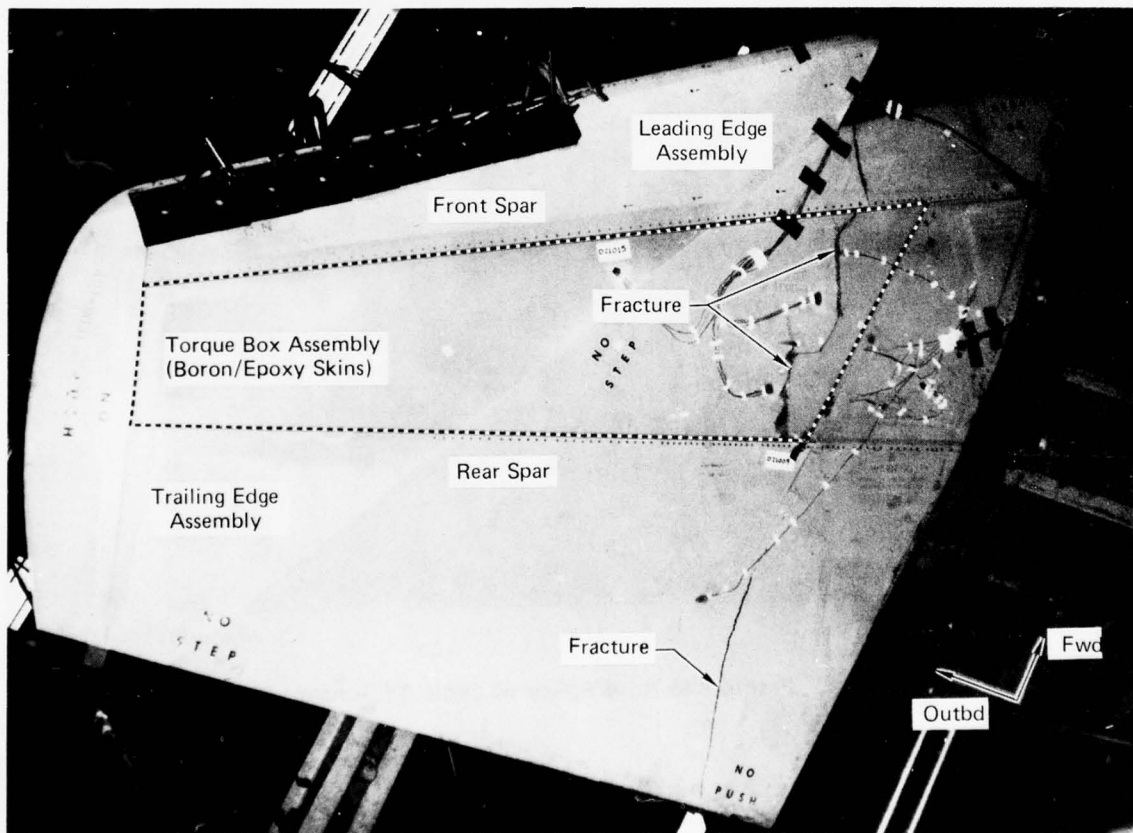
TABLE 2. EAGLE 14 TEST DATA

Location	Design Limit Load Level			
	50%	100%	150%	190% (Failure)
A Strain in Boron/Epoxy Rear Spar at Skin Splice ( $\mu\text{in./in.}$ )	1152	2325	3492	4605
B Principal Strain in 44-Ply Boron/Epoxy Skin at Splice Plate ( $\mu\text{in./in.}$ )	1133	2286	3461	4220
C Principal Strain in 44-Ply Boron/Epoxy Skin at Splice Plate ( $\mu\text{in./in.}$ )	956	1927	2927	3733
D Principal Strain in 28-Ply Boron/Epoxy Skin Near Front Spar ( $\mu\text{in./in.}$ )	1102	2223	3348	4197
E Stabilator Tip Displacement (in.)	4.1	8.3	12.6	16.2

GP79-0344-23



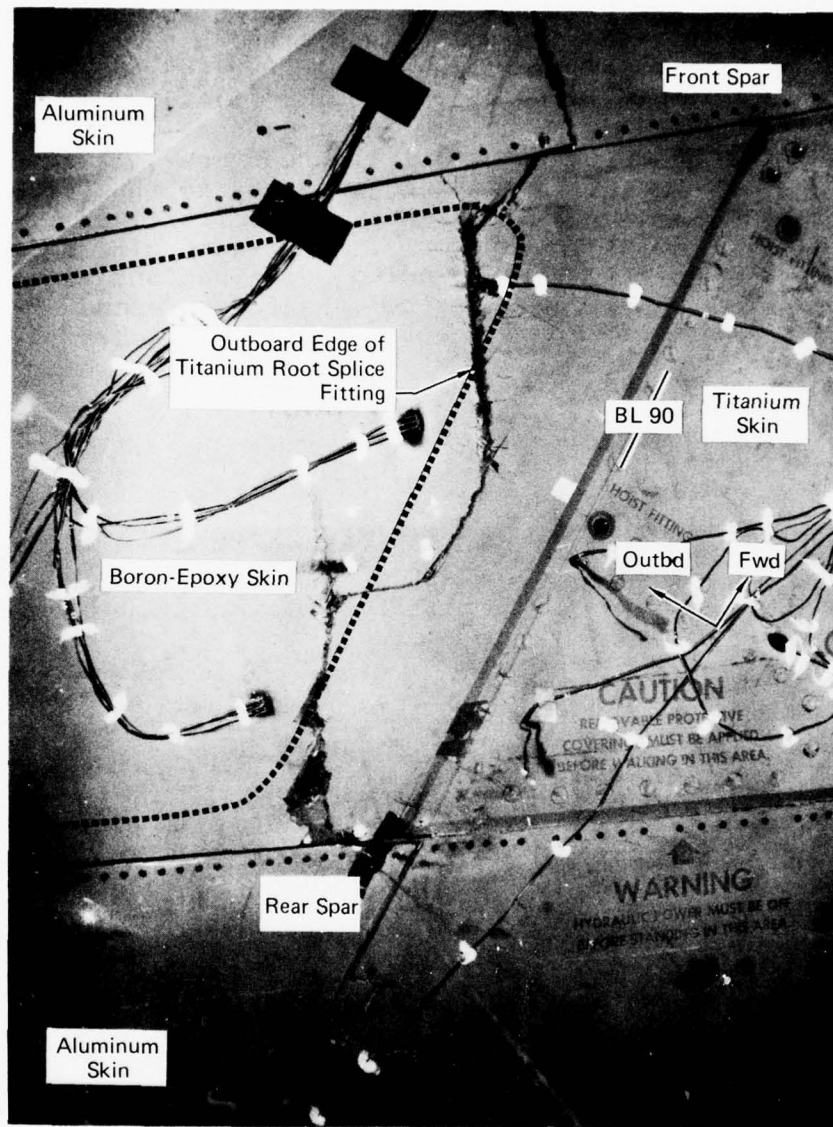
The tension surface failed as shown in Figure 15. Aluminum skins of leading and trailing edge structures were fractured and the boron/epoxy skin in the torque box was cracked in the vicinity of the bonded splice to the inboard titanium skin. The outline of the innermost step of the picture-frame splice fitting is shown in Figure 16 superimposed on the root splice area. The failure extended through the upper flange of the rear spar, through the boron/epoxy skin and splice fitting adjacent to the rear spar, then forward through the boron/epoxy skin to the front spar. The front spar was cracked completely through. Post-test ultrasonic inspection of the boron/epoxy skin revealed delaminations extending approximately 8 inches outboard from the fracture and a 4-inch wide delamination extending along the front spar 20 inches outboard from the fracture.



GP79-0344-25

Figure 15. Tension Skin of Eagle 14 Stabilator After Static Test





GP79-0344-26

**Figure 16. Fracture in Root Splice of Eagle 14 Tension Skin**

The root splice area of the tension skin was machined from the Eagle 14 torque box for further evaluation. Several inboard-out-board cuts were also made. The structure after dissection is shown in Figure 17. In addition to the skin fractures, considerable bond failure also occurred as shown in the cross-sectional schematics in Figure 17 and in the related Figure 18. These bond failures were primarily adhesive and were typical of lap shear failures obtained at room temperature in the qualification of FM400 adhesive.



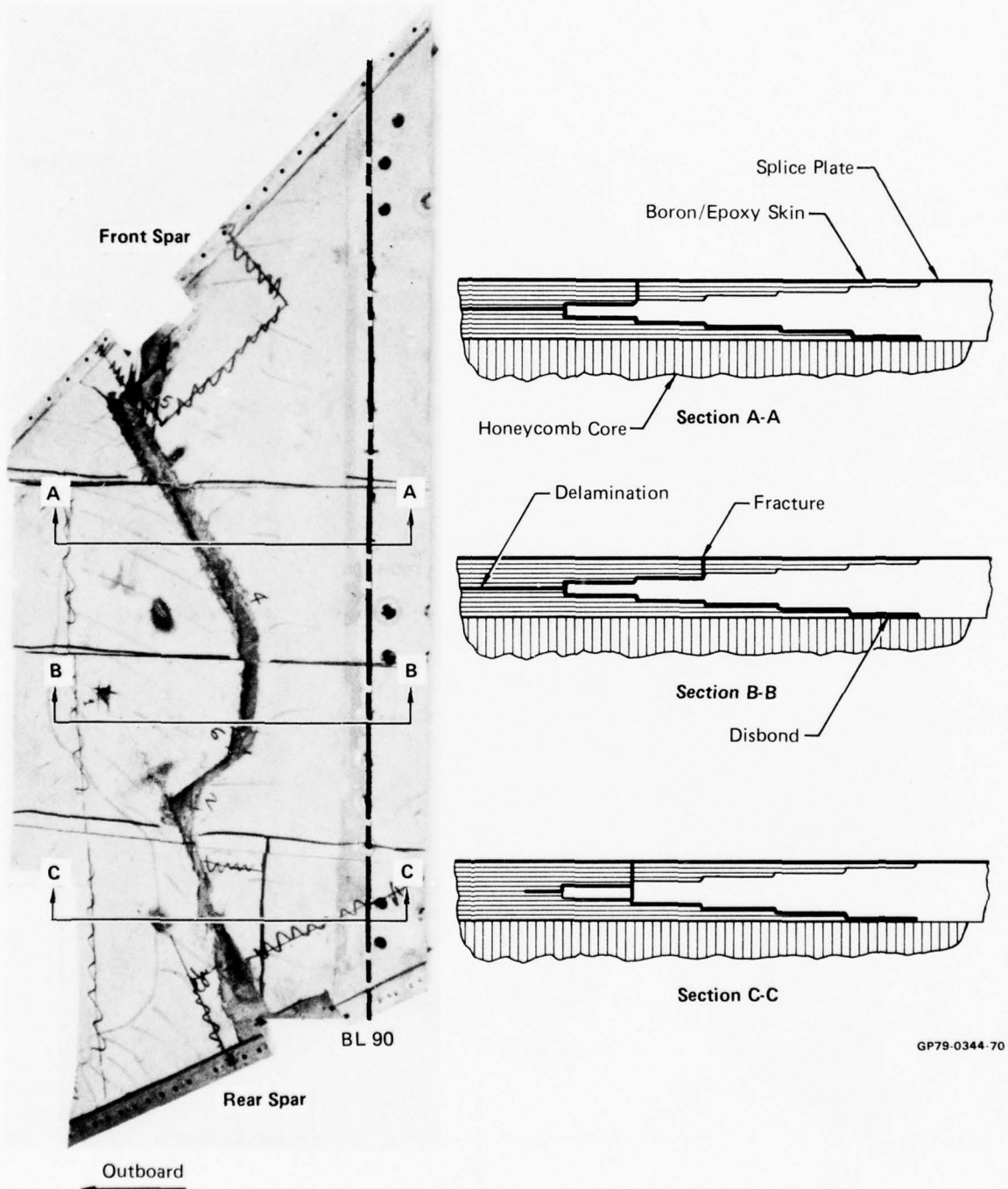


**Figure 17. Disbonds, Fractures and Delaminations in the Failed Eagle 14 Skin**

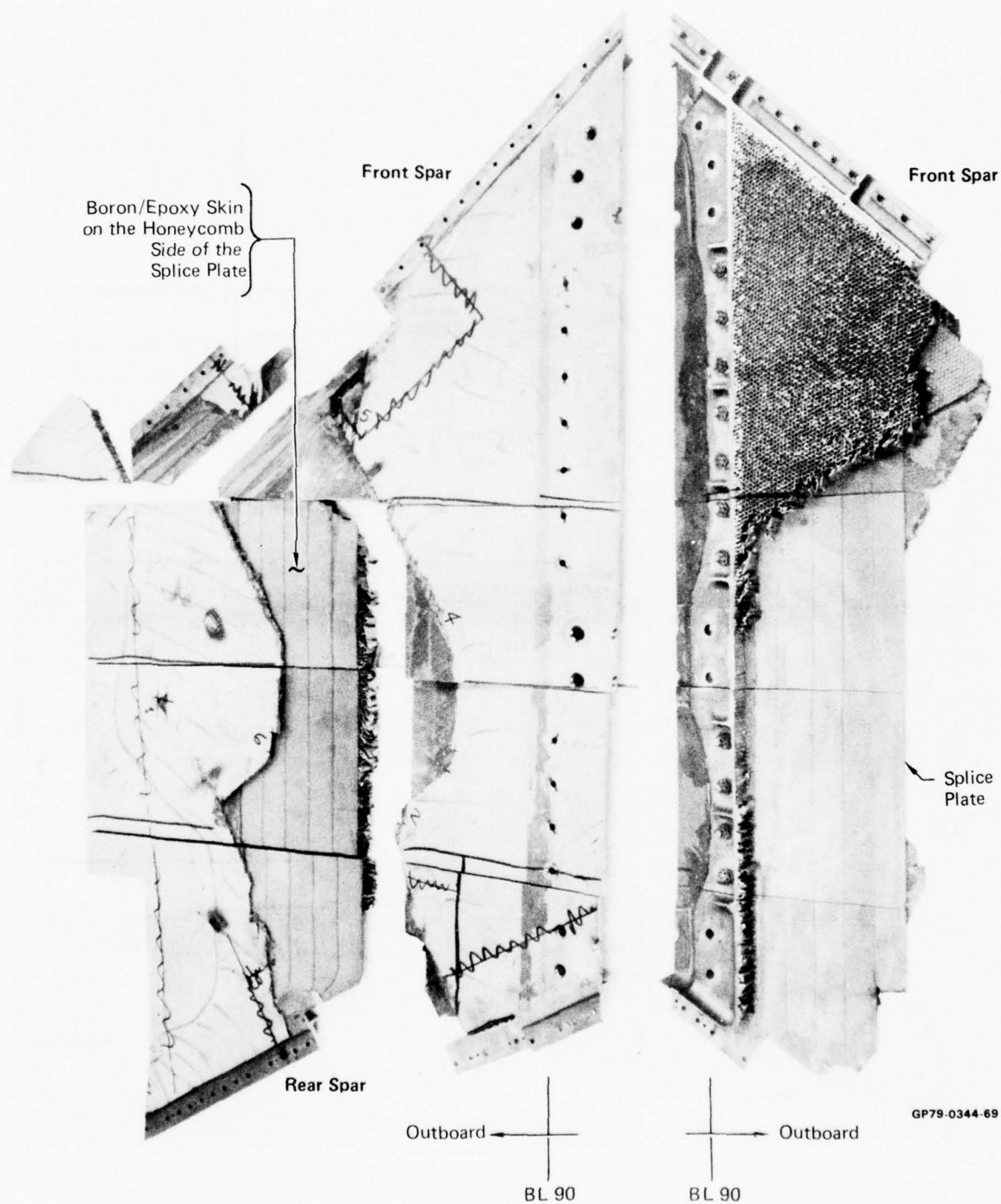


**Figure 18. Disbonds of Eagle 14 Root Splice**

b. PDV Test Results - Ultimate failure of the PDV stabilator occurred in the root splice area of the tension skin at 184% of design load. A local failure in the trailing edge structure had occurred earlier at 169%. Load-strain data were linear up to the occurrence of the initial failure and, after redistribution of trailing edge loads to the torque box (Figure 19), continued linearly until ultimate failure occurred. Strain data are shown in Table 3 for selected load levels.

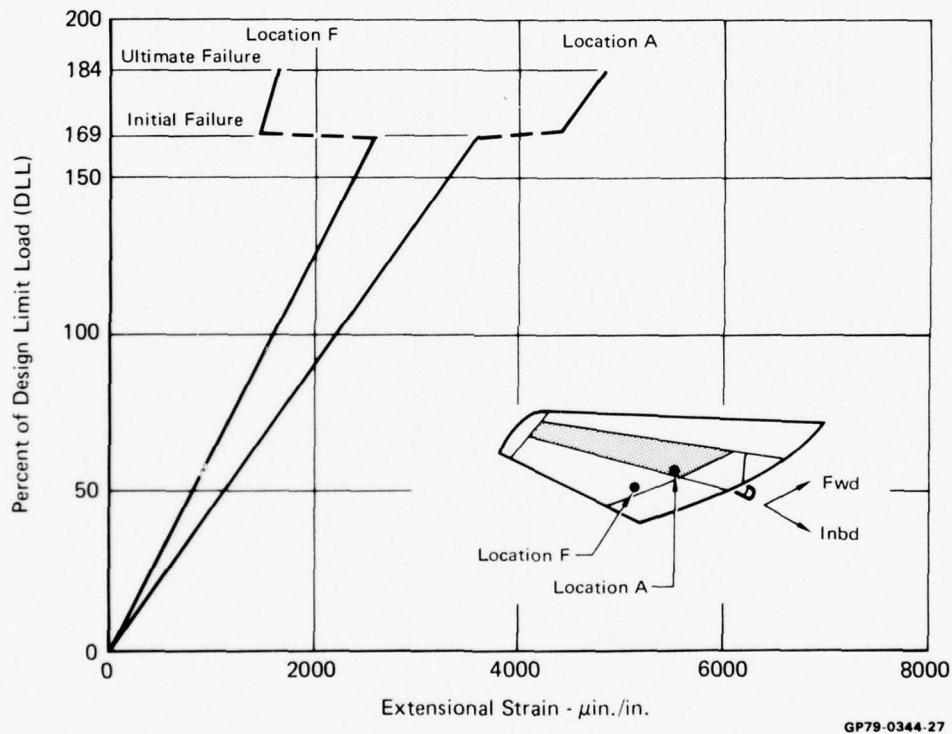
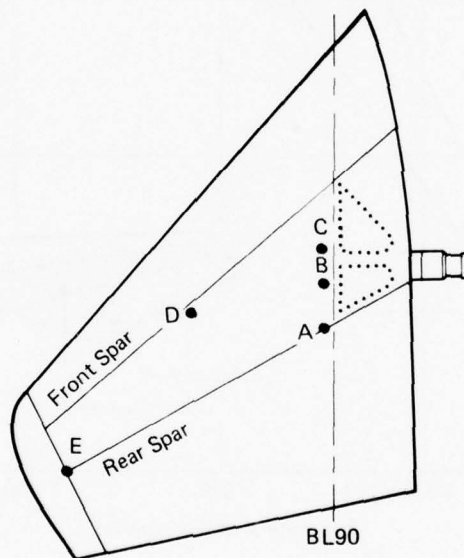


**Figure 19. Strains in PDV Torque Box and Trailing Edge Structure**

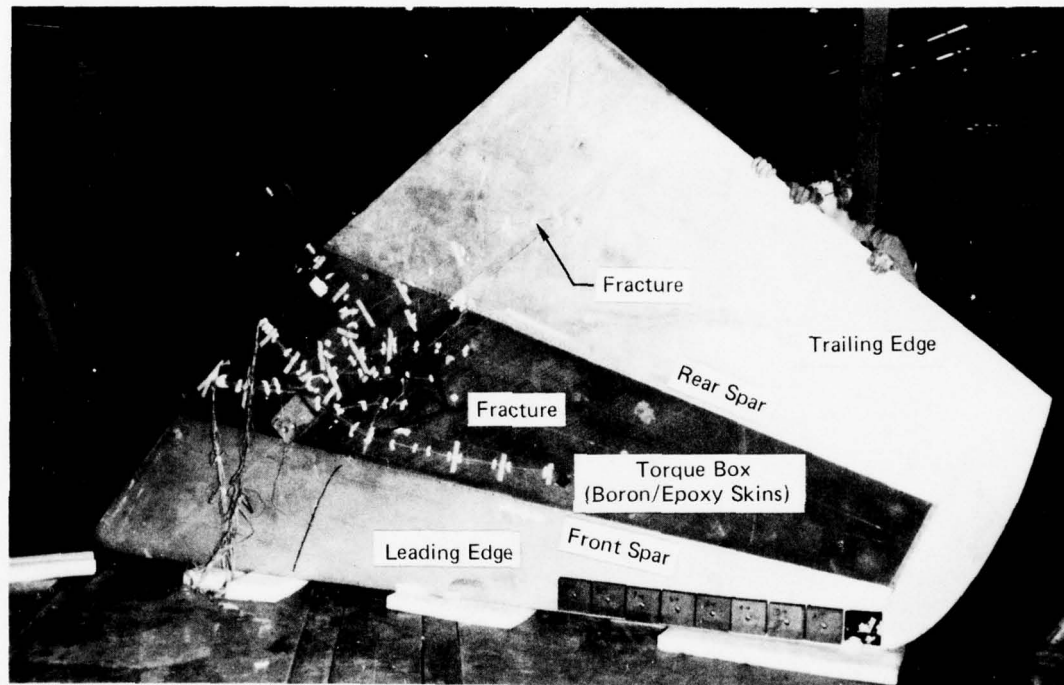
TABLE 3. PDV TEST DATA

Location	Design Limit Load Level			
	50%	100%	150%	184% (Failure)
A Strain in Boron/Epoxy Rear Spar at Skin Splice ( $\mu\text{in./in.}$ )	1119	2239	3364	4891
B Principal Strain in 44-Ply Boron/Epoxy Skin at Splice Plate ( $\mu\text{in./in.}$ )	1121	2242	3345	4632
C Principal Strain in 44-Ply Boron/Epoxy Skin at Splice Plate ( $\mu\text{in./in.}$ )	939	1870	2800	3565
D Principal Strain in 28-Ply Boron/Epoxy Skin Near Front Spar ( $\mu\text{in./in.}$ )	1087	2168	3247	4075
E Stabilator Tip Displacement (in.)	4.2	8.4	12.4	15.5

GP79-0344-24



Fracture of the tension skin was similar to that experienced with the Eagle 14 stabilator test with the exception that the fracture in the PDV stabilator propagated through disbanded areas of the root splice. These disbonds were detected in pretest nondestructive evaluations and are described in Section II. As shown in Figure 20, the skin failure extended from the leading edge to the trailing edge of the stabilator. In addition, a disbond occurred at a splice in the compression skin of the trailing edge structure and is thought to be associated with the local failure noted at 169% DLL.

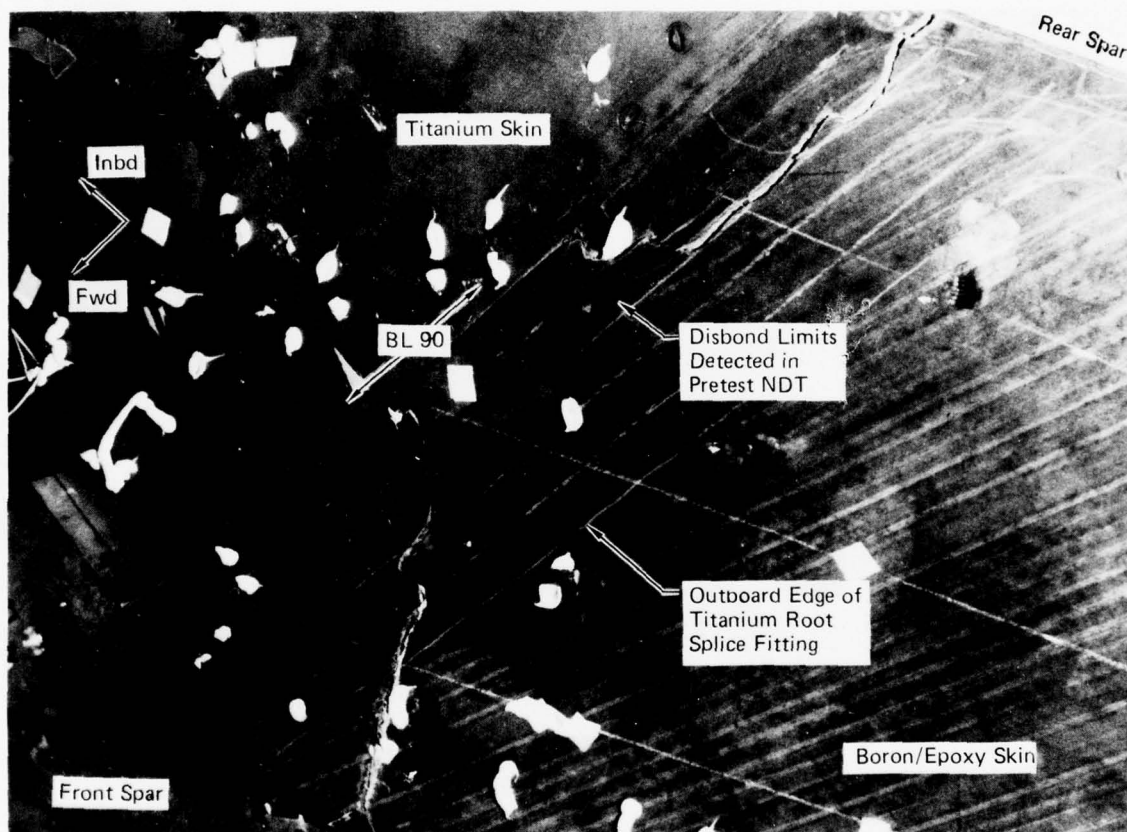


GP79-0344-28

**Figure 20. Tension Skin of PDV Stabilator After Static Test**

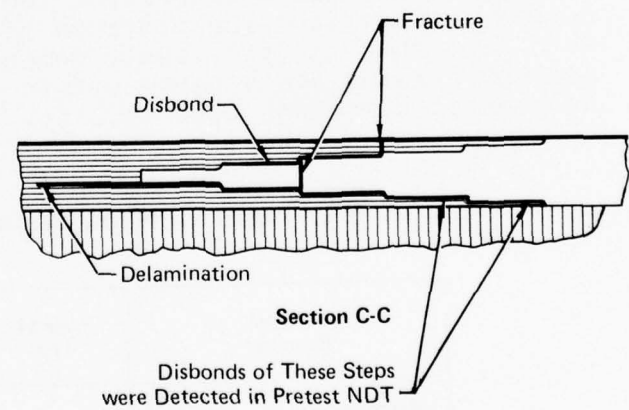
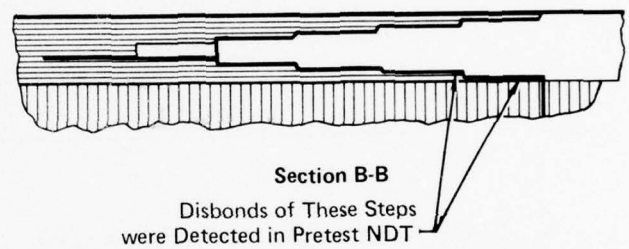
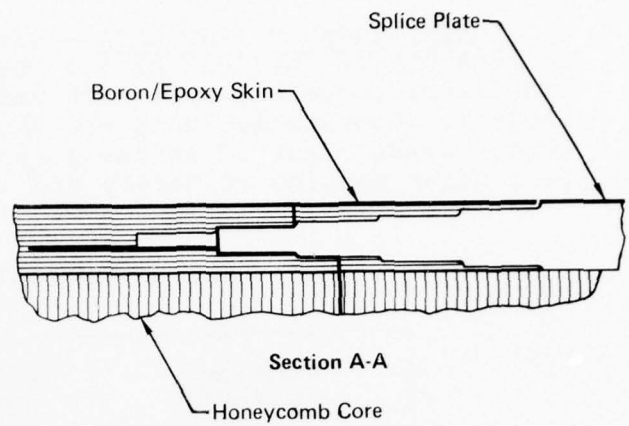
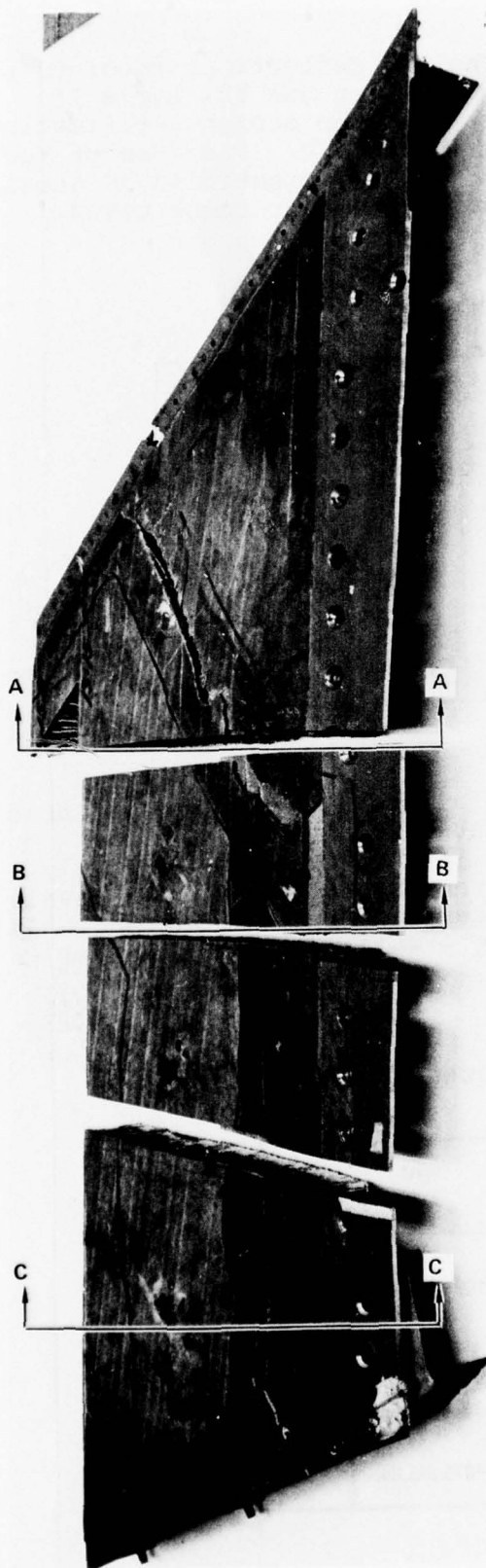
The torque box failure area is shown in Figure 21. To further examine the failure, the fractured portion of the tension skin was machined from the PDV torque box. This is shown in Figure 22 along with cross-sectional schematics showing the extent of the disbonds.





GP79-0344-29

Figure 21. Fracture in Root Splice of PDV Tension Skin



GP79-0344-68

**Figure 22. Disbands, Fractures, and Delaminations in the Failed PDV Skin**

4. CORRELATION OF TEST DATA - Strains and deflections recorded up to 150% DLL in the test of the PDV stabilator and the Eagle 14 stabilator correlate well with values from the design verification program. Comparative data are shown in Table 4. Fracture of the torque boxes occurred in the areas previously identified as areas of minimum margins of safety and instrumented for these tests.

**TABLE 4. TEST DATA CORRELATION**

Data Measured at 150% DLL	Eagle 14 Test	PDV Test	Design Verification Test
Location A: Strain in Rear Spar Cap at Root Splice	3492 $\mu\text{in./in.}$	3364 $\mu\text{in./in.}$	3400 $\mu\text{in./in.}$
Location C: Principal Strain at Tip of Splice Plate	2927 $\mu\text{in./in.}$	2800 $\mu\text{in./in.}$	2750 $\mu\text{in./in.}$
Location D: Principal Strain at Midspan	3348 $\mu\text{in./in.}$	3247 $\mu\text{in./in.}$	3039 $\mu\text{in./in.}$
Location E: Tip Displacement	12.6 in.	12.4 in.	12.2 in.

GP79-0344-30

Strains in boron/epoxy skins at failure are compared in Table 5 with corresponding values recorded at 200% DLL in the design verification test. Values from Eagle 14 and PDV tests typically exceeded those from the previous test although failure load levels were less than the previously demonstrated 200% DLL. The Eagle 14 and PDV strain levels agree within  $\pm 4\%$  - well within the normal scatter of component test results.

**TABLE 5. PEAK STRAIN COMPARISONS**

Measured Parameter	Eagle 14 Test	PDV Test	Design Verification Test
Maximum Load Level (% DLL)	190% (Failure)	184% (Failure)	200% (No Failure)
Location A: Strain in Rear Spar Cap	4605 $\mu\text{in./in.}$	4891 $\mu\text{in./in.}$	4500 $\mu\text{in./in.}$
Location C: Principal Strain at Splice Plate Tip	3733 $\mu\text{in./in.}$	3565 $\mu\text{in./in.}$	3600 $\mu\text{in./in.}$
Location D: Principal Strain at Midspan	4197 $\mu\text{in./in.}$	4075 $\mu\text{in./in.}$	4033 $\mu\text{in./in.}$

GP79-0344-19

The stabilator failure load levels are also consistent with load levels achieved in box beams which were fabricated and tested for the Reference 1 program. These beams were identical in both materials and configuration to the stabilator root splice; test loads from the same torque-box-critical condition were used. A comparison of failure load levels from stabilator and box beam tests is shown in Figure 23.

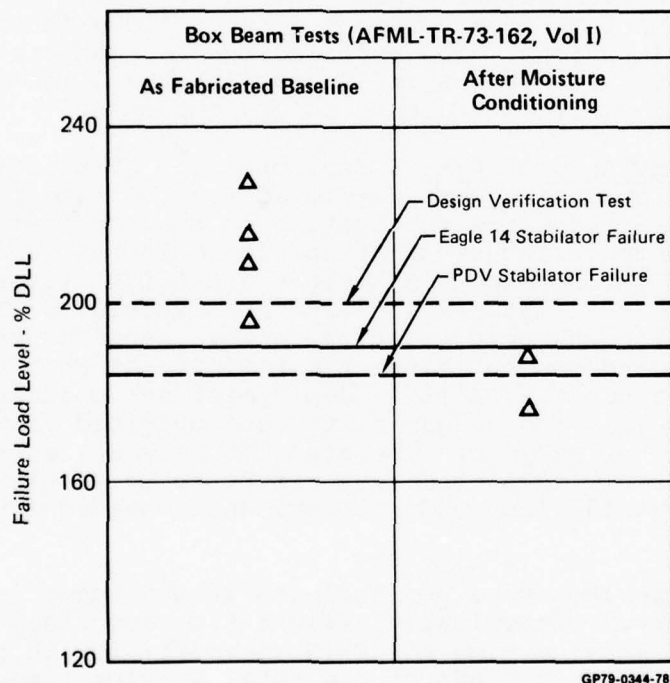


Figure 23. Stabilator and Box Beam Test Results

## SECTION IV

### MOISTURE CONTENTS OF TEST ARTICLE SKINS

The purpose of this phase of the program was to compare measured and predicted moisture levels for the Eagle 14 stabilator and the PDV stabilator after their individual usage environmental exposures. Surface weather data were collected representing the actual environmental history of each stabilator. Steady-state heat balance equations for specific locations in the composite skins were developed utilizing the procedures outlined in Reference 2. Moisture diffusion properties were experimentally determined using coupons representing the material system, laminate configuration, and processing of the stabilator skins. These data were used in a computer routine to generate chronological boundary conditions for upper and lower skins. Boundary conditions were applied sequentially in a numerical solution of Fick's Second Law of Diffusion to calculate skin moisture contents as a function of exposure time. Values predicted to exist at the time of static test were compared with moisture contents measured at the same locations. The correlations between predicted and measured values for the Eagle 14 stabilator and the PDV stabilator were good and verified the methodology employed.

1. ENVIRONMENTAL HISTORIES - Environmental histories of the Eagle 14 and PDV stabilators were developed for the time period from completion of torque box fabrication to the conclusion of static tests. Geographic locations of the Eagle 14 stabilator and summaries of indoor exposure periods and flight times are shown in Table 6. The stabilator skins were not exposed to effects of solar radiation and precipitation during indoor exposure periods. Eagle 14 was indoors until the first flight of Ship 14. For the climatic test program, Ship 14 deployment was documented in References 3 through 5 and hangar times were obtained from personnel assigned to that program. The stabilators were removed from Ship 14 on 7 September 1976 after its return to St. Louis for rework and stored outside (but under cover) until needed for this program.

Flight periods were not included in the Eagle 14 environmental history. Historically, flight time comprises less than 3% of the total service time for F-15 aircraft; for Ship 14, it was 129.4 hours, or only 0.86% of the total service time. Ferry missions comprised 40.5 hours of this total and these are typically conducted at speed and altitude combinations which result in low skin temperatures, thus inhibiting rapid moisture changes in the skins. The remaining 88.9 flight hours were expended in various missions for the climatic test program.



TABLE 6. EAGLE 14 STABILATOR HISTORY

Stabilator Location	Arrival	Departure	Flight Time* (hr)	Exposure Indoors (%)	Activity
St. Louis, Missouri	27 July 1973	29 May 1974	—	100	Torque Box Fabrication Through Stabilator Installation
St. Louis, Missouri	29 May	1 July	8.4	0	Flight Test
Edwards AFB, California	1 July	13 July	5.6	20	Desert Exposure
El Centro NAS, California	13 July	22 July	1.0	0	Desert Exposure
Edwards AFB, California	22 July	27 July	1.4	22	Desert Exposure
El Centro NAS, California	27 July	2 August	3.9	0	Desert Exposure
Edwards AFB, California	2 August	5 August	1.1	0	Desert Exposure
El Centro NAS, California	5 August	20 August	14.8	7	Desert Exposure
Edwards AFB, California	20 August	23 September	8.2	20	Desert Exposure
Eglin AFB, Florida	23 September	10 December	0.7	100	Environmental Laboratory
Edwards AFB, California	10 December	10 January 1975	14.4	20	Desert Exposure
Elmendorf AFB, Alaska	10 January	11 January	—	0	Arctic Exposure
Eielson AFB, Alaska	11 January	19 February	20.4	3	Arctic Exposure
Edwards AFB, California	19 February	8 May	23.8	20	Desert Exposure
Howard AB, Panama Canal Zone	8 May	13 June	16.6	6	Tropics Exposure
Edwards AFB, California	13 June	13 February 1976	9.1	33	Desert Exposure
St. Louis, Missouri	13 February	7 September	—	100	Ship 14 Rework up to Stabilator Removal
St. Louis, Missouri	7 September	25 August 1977	—	0	Outdoor Storage of Stabilator
St. Louis, Missouri	25 August		—	100	Current Program

Climatic Test Program

\* Ferry time included with totals for Edwards AFB

GP79-0344-47

Detailed surface weather data, recorded at the various bases where Ship 14 was stationed, were obtained from the USAF Environmental Technical Applications Center (ETAC). These data are generally recorded hourly at base weather stations on Federal Meteorological Form 1-10; however, the Edwards AFB weather station was closed for part of each day and the El Centro NAS weather station closed permanently in 1960. Missing weather data were estimated using statistical information for these sites. Information from Reference 3 was used to define the environment experienced in the environmental chamber during the Eglin mission. Data for St. Louis were obtained from the National Weather Service at St. Louis.

The PDV stabilator was indoors in various McDonnell production, test, and storage facilities from fabrication through static test as summarized in Table 7. Following the simulated lightning test, the PDV torque box was occasionally removed from storage and

TABLE 7. PDV STABILATOR HISTORY

Date	Activity
20 May 1971	Torque Box Fabrication Completed
18 August - 17 September 1971	Spectrum Fatigue Test, 16,000 EFH
21 September 1971	Static Test to 150% DLL
20 October 1971	Static Test to 200% DLL
November 1971 - May 1972	Laboratory Storage
1 May 1972 - 4 October 1972	Simulated Lightning Strike Test
November 1972 - August 1977	Warehouse Storage
25 August 1977 -	Current Program

GP79-0344-46

used (indoors) for various tooling verification purposes. These activities were not well-documented and have not been included as specific milestones in the PDV history. Necessary climatic data were obtained from the National Weather Service.

The environmental histories of Eagle 14 and PDV stabilators are summarized in Appendices A and B, respectively. Surface weather data were converted to a spectrum of exposures containing a typical daily cycle in temperature, humidity, wind speed, cloud cover and precipitation frequency for each month (or portion of a month) and for each base. Each typical day is broken down to eight 3-hour segments. Data associated with each 3-hour segment in the appendices include latitude, longitude, site factor, month, time of day (local standard time), humidity (HA), cloud cover (MCC), wind speed (VW), precipitation frequency (P), and duration. The site factor is a measure of smoke and haze in the air and is used in conjunction with cloud cover data in the calculation of solar heating effects using the Reference 2 methodology. Precipitation frequency refers to the percent of observations for that 3-hour segment during which precipitation was recorded. As presented in the appendices, the duration of each 3-hour segment refers to the total time (in hours) for which the accompanying ambient weather data apply. The sum of the durations for the eight segments of a typical day comprises the length of deployment to a given base or, in the case of long assignments, comprises one month at a base. An event in the environmental history is defined as the weather data associated with the eight segments of a typical day and the corresponding durations of each segment.

Indoor exposure periods were included in the environmental histories for both stabilators as separate events. For the PDV stabilator, indoor exposure periods at St. Louis comprised the entire history. Skin temperature for these periods was assumed to be equal to the outside ambient temperature or 70°F, whichever was greater. For an ambient temperature less than 70°F, an effective

relative humidity of air surrounding the stabilator was calculated from the ambient humidity assuming a constant water vapor pressure. The expression used is:

$$H_{\text{eff}} = \frac{P_a}{P_{70}} H_a$$

where  $H_{\text{eff}}$  = effective relative humidity (%)

$P_{70}$  = saturation pressure of water vapor at 70°F

$P_a$  = saturation pressure of water vapor at a true ambient temperature (less than 70°F)

$H_a$  = ambient relative humidity (%) corresponding to the true ambient temperature

In Appendices A and B, hangar and indoor periods are coded with "-99" in the cloud cover column (MCC). Humidities, as shown, associated with these periods have been corrected according to the above procedure.

2. COMPOSITE SKIN THERMAL MODELS - One dimensional heat transfer models were used to calculate skin temperatures for various environmental conditions. Models developed to represent the torque box structure in the areas of the stabilator 50% chord line are shown in Figure 24. Using these models, steady-state heat balance equations were derived which account for solar radiation heating and radiation interchange with the surroundings, conduction heat transfer between the upper and lower composite skins, and convective heat loss or gain due to ambient conditions. Radiation terms were linearized for the expected range of temperatures. The resulting steady-state heat balance equations are presented below. Simultaneous solution of these equations yield surface temperatures of upper and lower skins and of the shaded and unshaded ground.

Upper Surface ( $T_u$ )

$$\alpha_u Q = 1.10 \epsilon_u \tau (T_u - T_s) + C (T_u - T_\ell) + h (T_u - T_a)$$

Lower Surface ( $T_\ell$ )

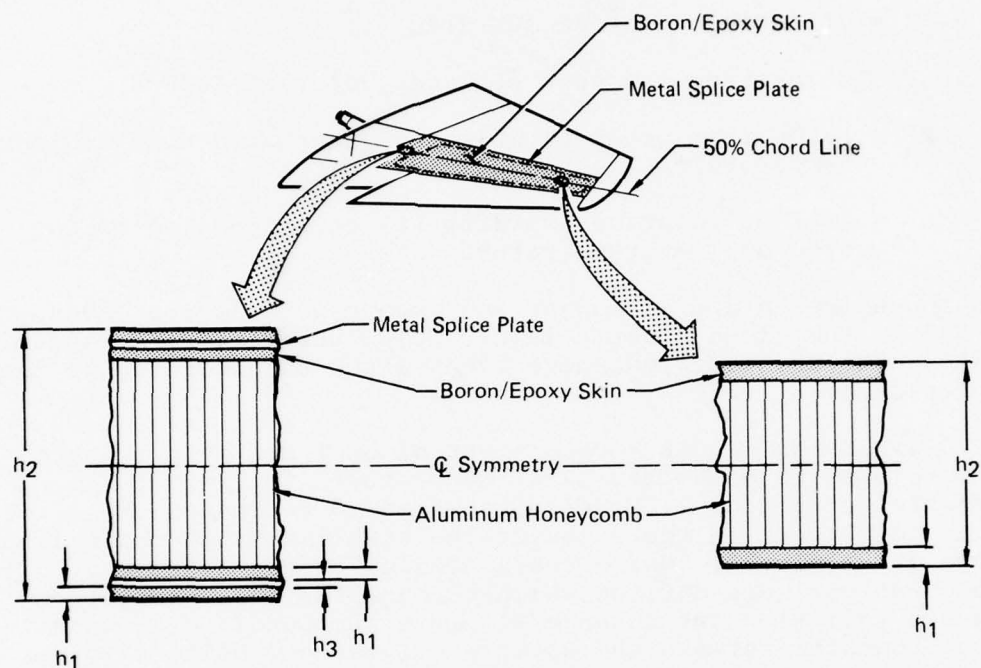
$$C (T_u - T_\ell) + (1-F) (1-\alpha_g) \alpha_\ell Q = h (T_\ell - T_a) + 1.05 \epsilon_\ell F (T_\ell - T'_g) + 1.15 \epsilon_\ell (1-F) (T_\ell - T_g)$$

Shaded Ground Plane ( $T'_g$ )

$$1.05 \epsilon_\ell F (T_\ell - T'_g) = h (T'_g - T_a)$$

Unshaded Ground Plane ( $T_g$ )

$$\alpha_g Q = 1.10 \epsilon_g \tau (T_g - T_s) + h (T_g - T_a)$$



**Torque Box at Root Splice**

Location	h1	h2	h3	Paint*
5-Ply Skin	0.026	3.99	0.182	Blue
20-Ply Skin	0.104	3.80	0.026	Blue

Notes:

Dimensions in inches.

\*Color of paint on Eagle 14.

**Torque Box Away From Root Splice**

Location	h1	h2	Paint*
14-Ply Skin	0.073	1.59	Orange
24-Ply Skin	0.125	2.42	Orange
38-Ply Skin	0.198	3.36	Blue
44-Ply Skin	0.229	3.71	Blue

GP79-0344-46

**Figure 24. Data for Thermodynamic Models of Torque Box**



where  $T_u$  = upper skin temperature  
 $T_l$  = lower skin temperature  
 $T_g$  = ground temperature (unshaded)  
 $T_g'$  = ground temperature (shaded)  
 $T_a$  = ambient temperature  
 $T_s$  = sky radiation sink temperature  
 $Q$  = solar heating rate  
 $h$  = convective heat transfer coefficient (function of wind speed)  
 $C$  = overall conductance between upper and lower surface  
 $F$  = radiation view factor from lower surface to shaded area under stabilator  
 $\tau$  = cloud factor for nocturnal exposure ( $\tau = 1.0$  during daylight hours)  
 $\alpha_u$  = upper skin solar absorptivity  
 $\alpha_l$  = lower skin solar absorptivity  
 $\alpha_g$  = ground solar absorptivity  
 $\epsilon_u$  = upper skin emissivity  
 $\epsilon_l$  = lower skin emissivity  
 $\epsilon_g$  = ground emissivity

Thermodynamic constants for these equations are defined in Tables 8 and 9. Assumptions inherent in the development of these equations are discussed next for each of the heat transfer modes.

a. Solar Heating - The stabilator upper surface and unshaded ground experience direct solar heating and the stabilator lower surface is heated by solar energy reflected from the unshaded ground. The main parameters involved are:

$Q$  = solar heating rate, and  
 $\alpha$  = solar absorptivity



**TABLE 8. EMISSIVITY AND SOLAR ABSORPTIVITY DATA USED FOR STABILATOR AND RUNWAY SURFACES**

Surface	Emissivity, $\epsilon$	Absorptivity, $\alpha$
Eagle 14 Stabilators		
Blue Polyurethane Enamel	0.900	0.64
Orange Lacquer	0.905	0.53
Production Stabilators		
Gray Polyurethane Enamel	0.883	0.86
Runway Surface		
Concrete	0.900	0.61

GP79-0344-43

**TABLE 9. OVERALL CONDUCTANCE AND RADIATION VIEW FACTORS**

Torque Box Location	Conductance Between Skins, C (Btu/hr-ft <sup>2</sup> °F)	Radiation View Factor, F
14-Ply Boron/Epoxy	4.13	0.340
24-Ply Boron/Epoxy	2.82	0.435
38-Ply Boron/Epoxy	2.02	0.528
44-Ply Boron/Epoxy	1.82	0.560
20-Ply Boron/Epoxy at Splice	1.59	0.564
5-Ply Boron/Epoxy at Splice	2.00	0.580

GP79-0344-44

To calculate solar radiation heating rates, clear-sky data given in Reference 6 for horizontal receivers were used. To account for solar heating reductions due to cloud cover, atmospheric haze, smoke and humidity, the methodology of Reference 2 was applied.

Solar absorptivity (and emissivity) values were measured for paint colors used on the F-15 and are presented in Table 8 along with values for concrete from Reference 7. Eagle 14 stabilators were painted blue and orange during the climatic test program to identify Ship 14 as a test airplane. Production stabilators are painted gray. The PDV stabilator was not painted.

b. Radiation Interchange with Surroundings - To calculate the radiation interchange between the stabilator and its surroundings the following parameters were used:

$T_s$  = sky radiation sink temperature  
 $\tau$  = cloud transmissivity factor for nocturnal exposure  
 $F$  = radiation view factor  
 $\epsilon$  = emissivity

Both the stabilator upper surface and the unshaded ground radiate energy to the sky which acts as a hemispherical black body. For calculations for daylight hours, a sky radiation sink temperature,  $T_s$ , of 15°F below the ambient temperature was used. This temperature is typical for partly cloudy skies during daylight hours. For calculations for night hours, a sky temperature of -50°F was used. This temperature was taken from Reference 7 and is based on measurements taken on clear cold nights. To account for cloud cover, radiation terms for the upper surface and unshaded ground were multiplied by a transmissivity factor ( $\tau$ ) that was developed using McCabe's cloud cover and solar transmission data from Reference 2. In calculations for daylight hours, this factor was set equal to 1.0. In calculations for night hours, it equaled 0.2 on a clear night and approached zero as the cloud cover increased.

The stabilator lower surface exchanges radiation with the ground which is made up of both a shaded and unshaded area. To calculate the radiation interchange between the lower surface and these ground areas, a radiation view factor ( $F$ ) was derived assuming the stabilator is positioned parallel to the ground with the shadowed area directly under it. These data are presented in Table 9.

The radiation energy emitted from the stabilator skin and ground plane is directly influenced by the surface emissivity ( $\epsilon$ ). Surface emissivity values were measured for this program and are presented in Table 8. The emissivity of the ground plane was based on data for concrete given in Reference 7.

c. Conduction Heat Transfer - Since the upper and lower composite skins are joined by an aluminum honeycomb core (see Figure 24), heat transfer between these surfaces is principally due to conduction. The overall thermal conductance,  $C$ , is a function of the thermal conductivity of the composite skins and aluminum honeycomb, and the thermal resistance due to the adhesive bond between the skin and honeycomb. Conductance data used for the thermodynamic analyses are presented in Table 9.

d. Convective Heat Transfer - The outer surfaces of the stabilator composite skins and the ground plane experience convective heat loss or gain due to ambient wind and temperature conditions. The following equation was used to calculate the convective heat transfer coefficient ( $h$ ):

$$h = 0.34 (v)^{0.8}$$

where  $v$  = air velocity in ft/sec.

This equation is based on turbulent forced convection on a flat plate taken from Reference 8. When the air velocity is 3.81 ft/sec, the above equation gives a value of approximately 1.0 for the coefficient. Since the coefficient for no-wind conditions (natural convection) results in a coefficient near 1.0, this value was used for calculations whenever the air velocity was less than 3.81 ft/sec.

3. MOISTURE DIFFUSION PROPERTIES - Testing was conducted to characterize the diffusion properties of boron/epoxy (B<sub>4</sub>/5505) for the maximum skin temperatures and range of relative humidities expected in runway environments. Coupons meeting the material and processing specifications used for composite skins were exposed to the hygrothermal laboratory environments shown in Table 10. Moisture contents of the coupons were monitored by tracking weight gain (or loss) relative to initial dry weights. Diffusion properties for temperatures less than 100°F were obtained by extrapolation of the measured data.

**TABLE 10. LABORATORY ENVIRONMENTS USED FOR DETERMINING MOISTURE DIFFUSION PROPERTIES**

Environment			Coupons					
			4 Plies		28 Plies		48 Plies	
Number	T (°F)	RH (%)	Bare	Painted	Bare	Painted	Painted	
1a	182	100	Yes		Yes	Yes	Yes	
1b	180	0	Yes					
2a	140	97	Yes		Yes	Yes	Yes	
2b	140	0	Yes					
3a	100	96	Yes	Yes	Yes	Yes	Yes	
3b	100	0	Yes	Yes				
4	140	71	Yes		Yes			
5	140	37	Yes		Yes			
6	140	53	Yes		Yes			
7a	180	65	Yes					
7b	180	0	Yes					
8a	100	69	Yes	Yes	Yes	Yes	Yes	
8b	100	5	Yes	Yes				
9	100	41	Yes	Yes	Yes	Yes	Yes	
10	140	88	Yes					

GP79-0344-42

Coupons for exposures shown in Table 10 were machined from cured and postcured 4-ply, 28-ply and 48-ply panels. Prepreg material was AVCO 5505 boron/epoxy. Coupons from the 4-ply panel were 2 x 2 x .02 (4 plies) inches. These were used primarily to obtain equilibrium moisture data because of their short time to saturation but were also used for measuring diffusion coefficients for absorption and desorption cycles. Coupons from the thicker panels were 5 x 5 x .15 (28 plies) inches and 5 x 5 x .25 (48 plies) inches and consisted of two typical stabilator skin layups. These were used for measuring diffusion coefficients for absorption environments. Some coupons were also painted to duplicate the stabilator surface finish (1 coat of epoxy primer, 2 coats of polyurethane enamel).

Properties determined from these tests include equilibrium moisture content (a function of relative humidity) and diffusion coefficient (a function of the coupon temperature). An example of the moisture absorption data obtained with unpainted 4-ply coupons at 100°F and 96% RH is shown in Figure 25. Equilibrium moisture content is shown as the horizontal asymptote for the data. The diffusion coefficient for this temperature was calculated using the following linear solution to Fick's Second Law of Diffusion:

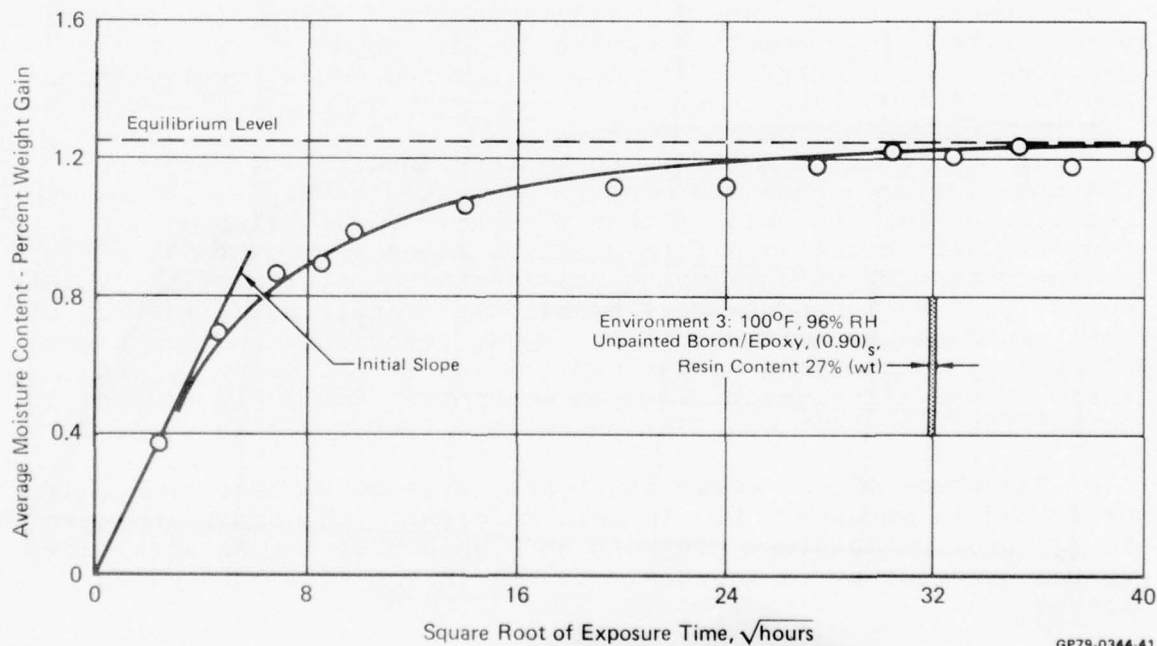


Figure 25. Moisture Absorption in 4-Ply Boron/Epoxy Coupons



$$\frac{M_t}{M_{eq}} = \frac{4}{h} \left( \frac{Dt}{\pi} \right)^{1/2}$$

$$\text{thus } D = \frac{h^2 \pi}{16 M_{eq}^2} \left( \frac{M_t}{\sqrt{t}} \right)^2$$

where  $D$  = diffusion coefficient ( $\text{in}^2/\text{hr}$ )

$h$  = coupon thickness (in)

$t$  = exposure time (hr)

$M_t$  = average through-the-thickness moisture content (%) at the time " $t$ " (assuming initial moisture content at  $t = 0$  was zero)

$M_{eq}$  = equilibrium moisture content (%)

The value of  $M_t/\sqrt{t}$  is the slope of the initial straight line segment of the Figure 25 profile. The straight line was fitted to weight gain data recorded up to 50% of  $M_{eq}$  using linear regression methods.

Diffusion coefficients were measured for absorption (Table 10 environments 1a, 2a, 3a, 4, 5, 6, 7a, 8a, 9, 10) and desorption (environments 1b, 2b, 3b, 7b, 8b) exposures. Absorption exposures were started after complete drying of the coupons; desorption exposures were started after coupons reached equilibrium with the previous environment.

a. Equilibrium Moisture Contents - Equilibrium moisture contents for unpainted coupons are presented in Figure 26 for the relative humidities used in this program. Equilibrium moisture contents were normalized to a baseline fiber volume of 54% (30% resin content by weight) which represents the minimum fiber volume normally found in boron/epoxy stabilator skins. Normalization of data was based on moisture in the epoxy resin only and was accomplished by multiplying actual equilibrium weight gains by the ratio of baseline-to-actual resin contents. For 4-ply coupons, actual resin content was 27%; hence, the factor was 30/27 or 1.11.

The shape of the curve in Figure 26 is consistent with that presented in Reference 9. In this reference, the sharp increase in equilibrium moisture contents at high humidities is attributed to the presence of an inorganic filler in the AVCO 5505 resin system.



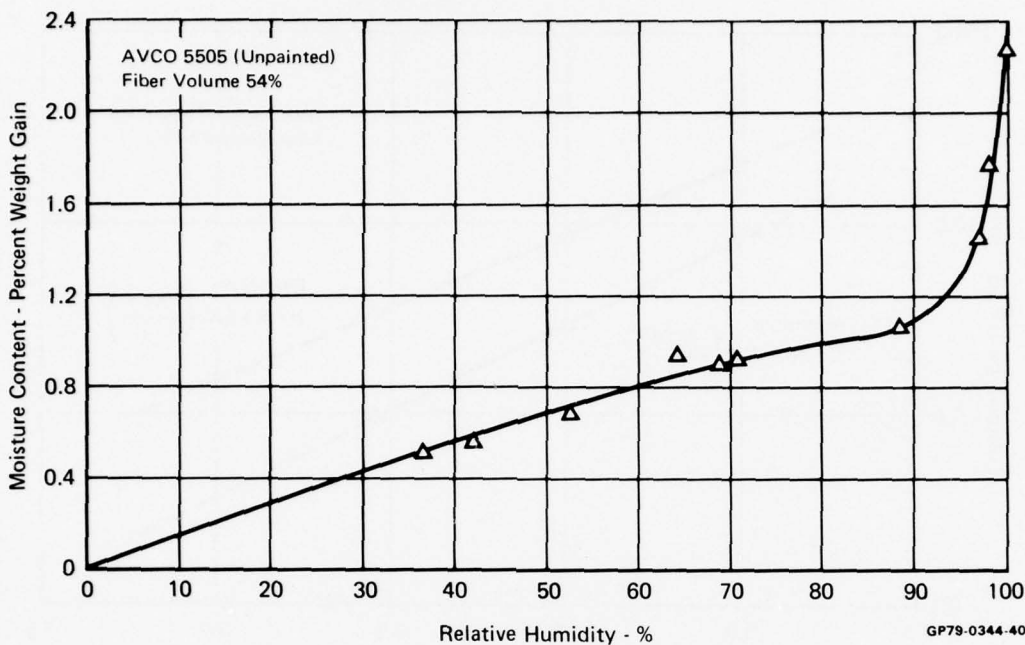


Figure 26. Equilibrium Moisture Contents for Stabilator Composite Skins

b. Diffusion Coefficients - Diffusion coefficients for absorption and desorption environments are presented in Figure 27 for unpainted coupons. Data were normalized to a baseline fiber volume of 54%, in this case using Reference 10 techniques. The edges of thicker coupons were sealed with aluminum-backed tape, thus limiting diffusion to the through-the-thickness direction. The 4-ply coupons, however, were too thin to use this sealing method, so the procedures described in Reference 11 were used to analytically account for the moisture absorbed through coupon edges. The equations shown in Figure 27 were determined using linear regression techniques for fitting straight lines to logarithm of diffusivity and inverse temperature data.

Diffusion coefficients for boron/epoxy follow the trends reported for graphite/epoxy (in Reference 12 for example) in that desorption coefficients typically exceed absorption coefficients. This inequality, according to Reference 13, indicates a interdependence between diffusion coefficients and moisture concentration. For the analytical work in this program, diffusivity was assumed to be independent of concentration and absorption coefficients were used to define moisture histories of the stabilator skins in that the overall trend was absorption, with desorption limited primarily to surface plies.

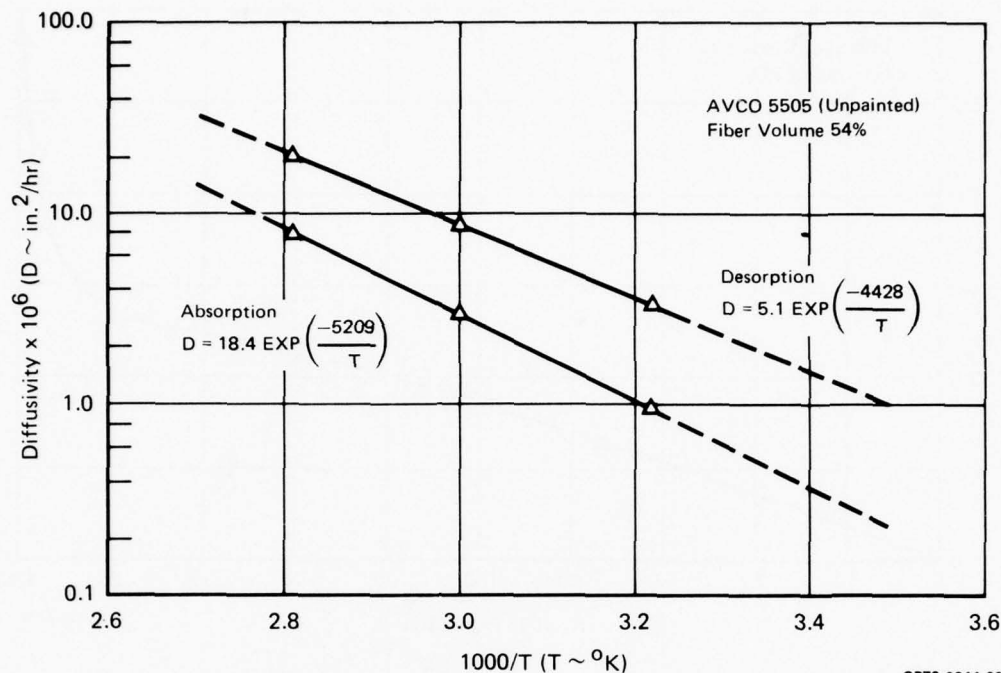
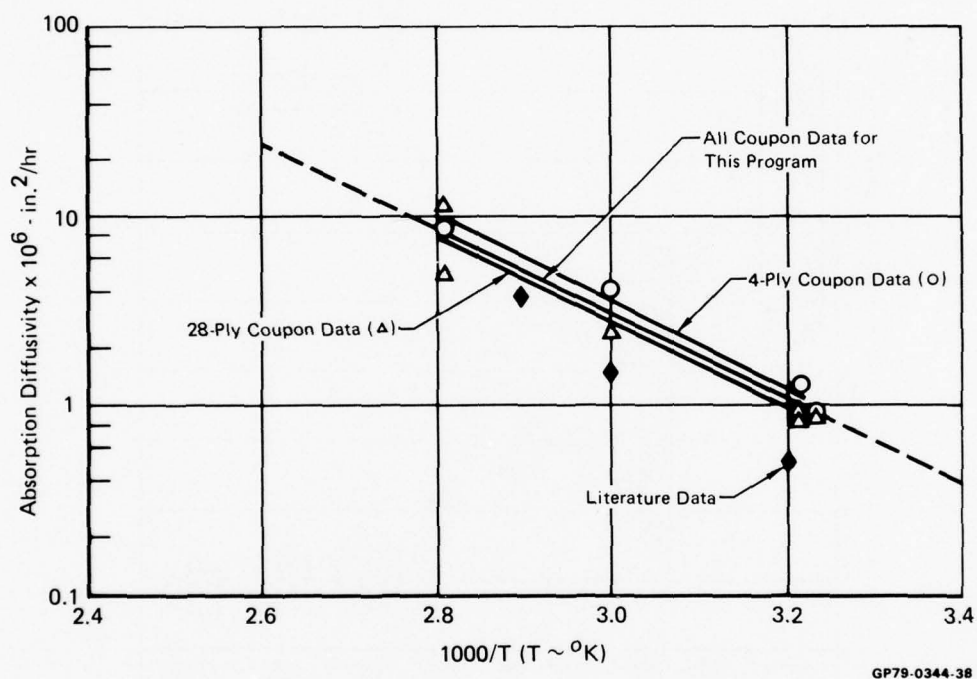


Figure 27. Diffusivity for Stabilator Composite Skins

The absorption coefficients obtained in this program are greater than those presented in Reference 9 for AVCO 5505 composites. A comparison of these data is shown in Figure 28. The source of this difference is not known, although edge effects and different resin contents between the two groups of coupons may be contributing factors. When curve fit with straight lines, absorption coefficients from 4-ply coupon data correlate very well with coefficients from 28-ply coupon data.

c. Effects of Painted Surface - Paint coatings which duplicated the F-15 surface finish had no effect on the moisture content of the boron/epoxy. Absorption was neither accelerated nor decelerated, as concluded by comparing weight gains in painted and unpainted coupons. The layer of paint, typically .002-inch, reached equilibrium at 3% to 4% weight gain (increase in paint weight) for relative humidities between 95% and 100%.

Effective diffusion coefficients for painted and unpainted coupons are compared in Figure 29. There were no significant differences in these values at any temperatures. The 4-ply painted coupon data at high temperatures showed significant scatter as a result of visible bubbles of moisture forming at the paint/laminate interface. Similar bubbles also occurred in the paint of thicker coupons later in their exposure period.



**Figure 28. Program and Literature Diffusivity Data for Unpainted AVCO 5505 Boron/Epoxy**

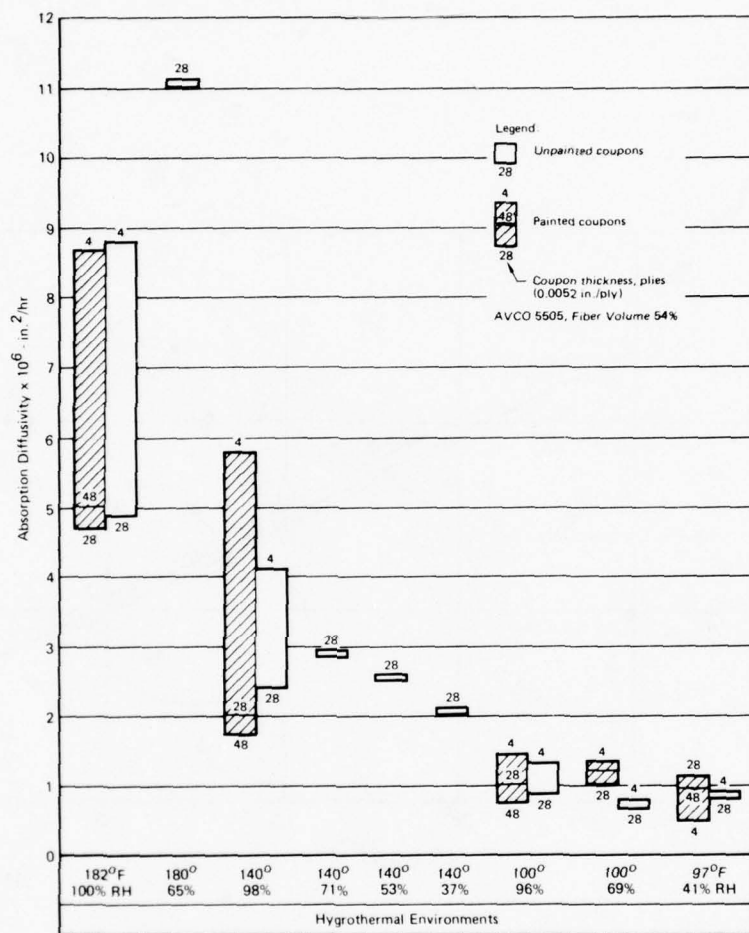


**Figure 29. Range of Effective Diffusivities for Painted and Unpainted Boron/Epoxy**

The reason for scatter in the data from unpainted coupons, however, is not fully understood. Coupons used to obtain data for several of the Table 10 environments were sectioned and photomicrographed upon completion of testing. Cracks were found in the surface ply of 4-ply and 28-ply coupons which had been exposed to

the 182°F environment. These cracks, as shown in Figure 30, extended across the surface parallel to fibers and into the laminate only to the boron fiber in the surface layer. No trans-laminar cracks were found. It is not known whether these cracks were present at the time of exposure to 182°F or whether the presence of such cracks could cause the data scatter.

4. PROCEDURES FOR CALCULATING MOISTURE CONTENTS - Relative humidity of air adjacent to the skin was calculated from ambient conditions assuming that the temperature of this surface air equaled the skin temperature. The expression used is:

$$P_S H_S = P_A H_A$$

where

$P_S$  = saturation pressure of water vapor at the skin temperature

$H_S$  = relative humidity of surface air, %

$P_A$  = saturation pressure of water vapor at ambient temperature

$H_A$  = relative humidity of ambient air, %

Upper and lower bounds for calculated skin temperatures and surface air humidities are presented in Figures 31 and 32 for the Eagle 14 environmental history shown in Appendix A. Skin temperatures and surface air humidities for the PDV stabilator are identical to the ambient temperatures and humidities in the PDV environmental history, Appendix B.

As described in Section IV(2), the effects of solar radiation and wind were incorporated in the calculation of skin temperatures. Surface humidities and skin temperatures were converted to diffusion coefficients and surface moisture concentrations, using the data in Figures 26 and 27, assuming that the moisture diffusion characteristics of the epoxy matrix was not altered by prior exposures. To account for the effects of precipitation, the upper and lower skin temperatures were assumed equal to the ambient temperature and the surface relative humidity was set at 100%. Moisture concentrations at the skin surface, which exists in equilibrium with the surface relative humidity, and diffusion coefficients were then corrected for precipitation effects using:

$$M_C = (1-P) M_S + PM_{100}$$

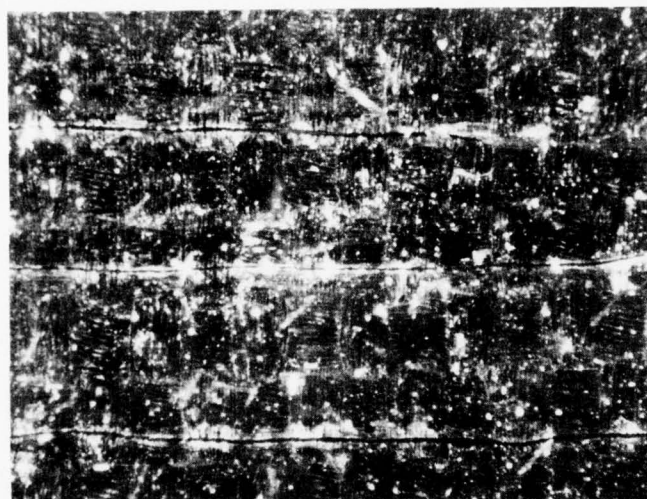
$$D_C = (1-P) D_S + PD_A$$

where

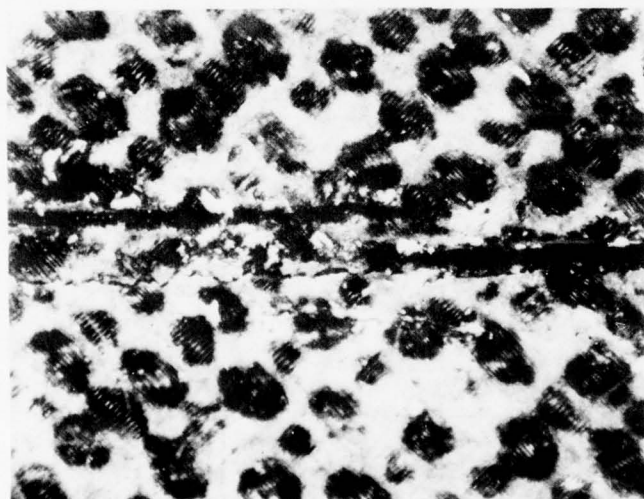
$P$  = frequency of occurrence of precipitation, decimal fraction

$M_C$  = surface moisture concentration corrected for precipitation





4-Ply Coupon, Unpainted  
(0, 90)<sub>s</sub>  
50 x Magnification

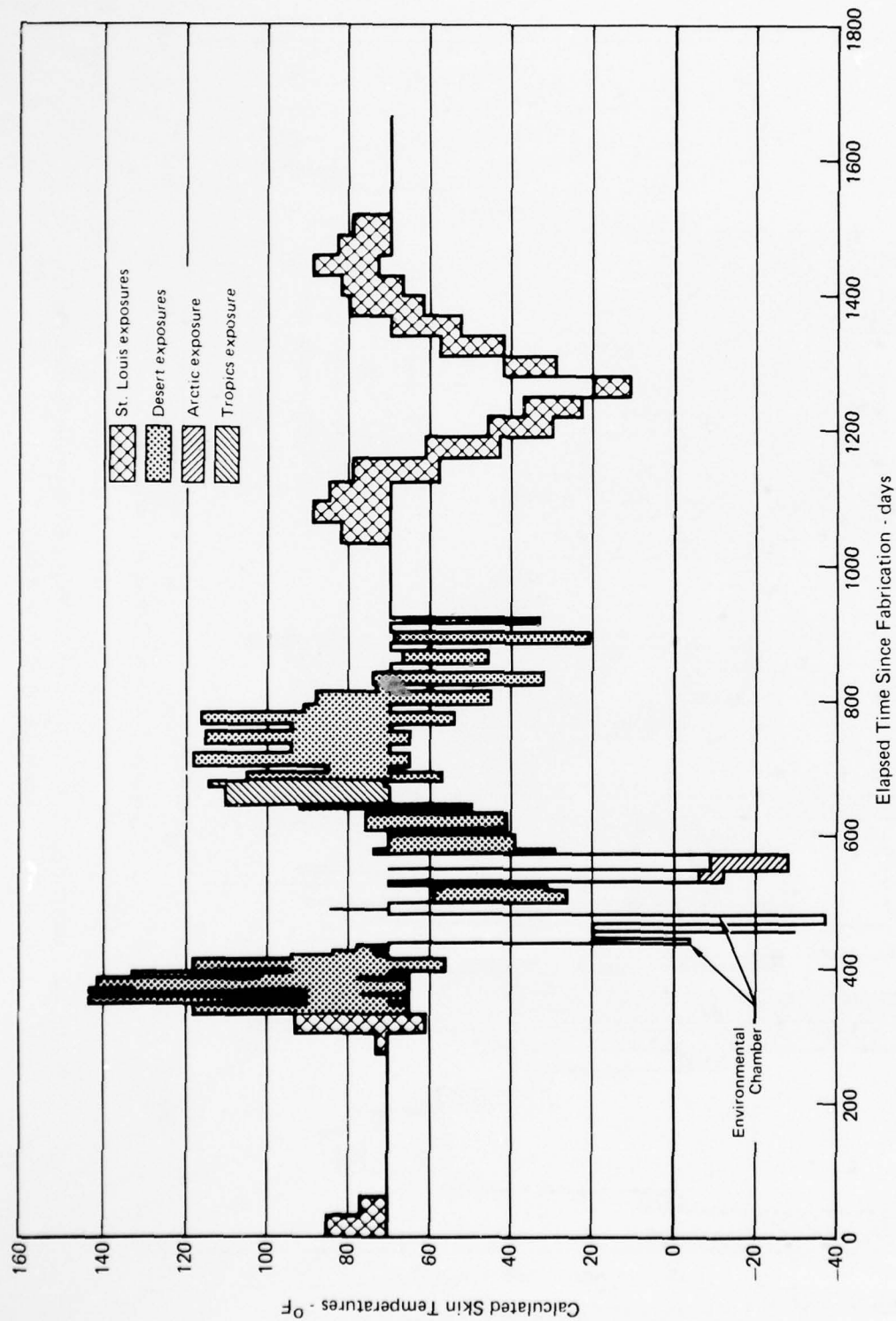


28-Ply Coupon, Unpainted  
[± 45, 90, (0<sub>2</sub>, ± 45)<sub>2</sub>, 0, ± 45]<sub>s</sub>  
50 x Magnification



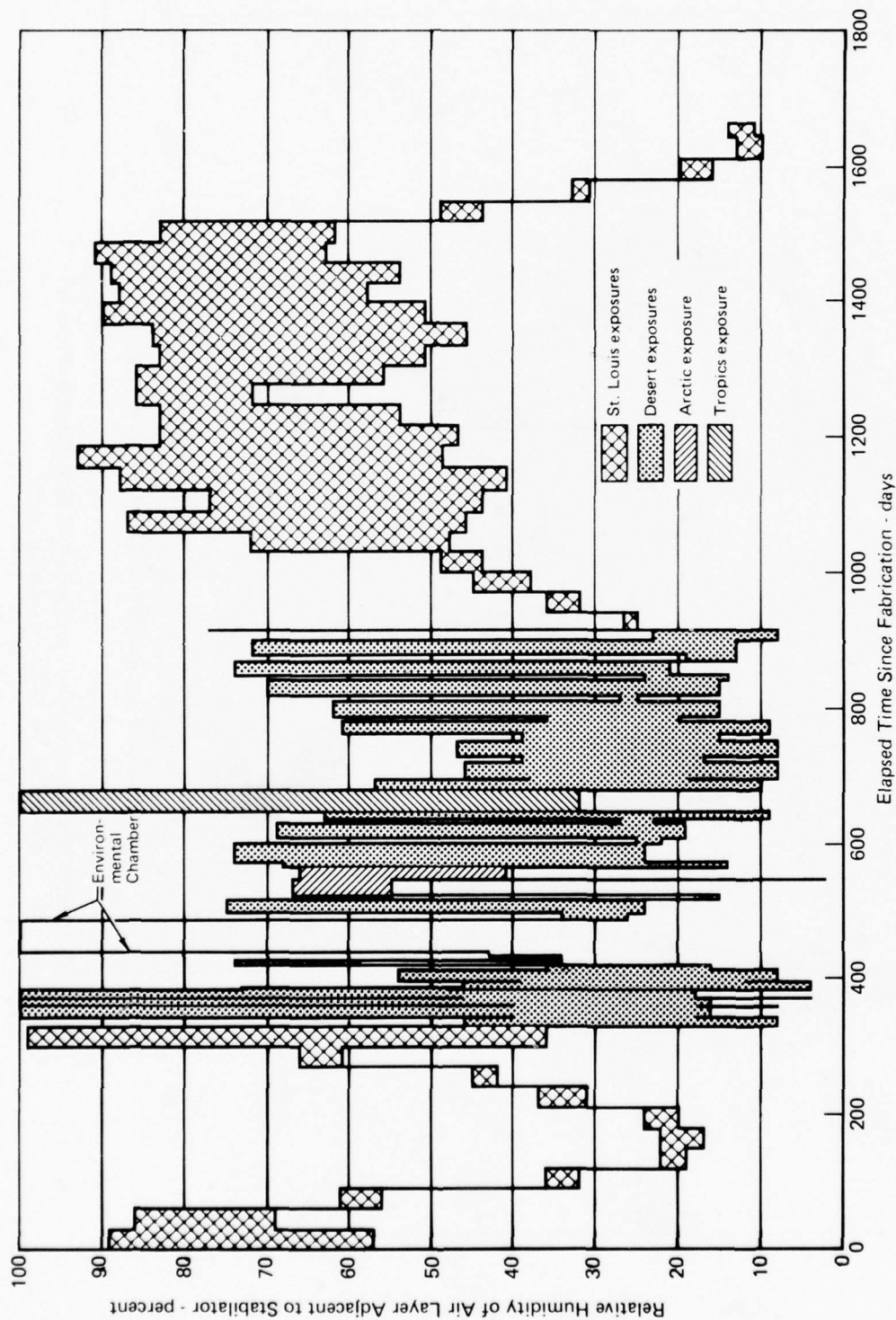
GP79-0344-36

Figure 30. Surface Cracks After Exposures to Severe Laboratory Environments



GP79-0344-36

Figure 31. Upper and Lower Bounds on Predicted Skin Temperatures for the Eagle 14 Environmental History



GP79 0344.34

Figure 32. Upper and Lower Bounds on Predicted Surface Air Humidities for the Eagle 14 Environment History

$M_s$  = equilibrium moisture content corresponding to surface air humidity (no precipitation)  
 $M_{100}$  = equilibrium moisture content corresponding to a 100% RH  
 $D_c$  = diffusion coefficient corrected for precipitation  
 $D_s$  = diffusion coefficient based on skin temperature  
 $D_A$  = diffusion coefficient based on ambient temperature

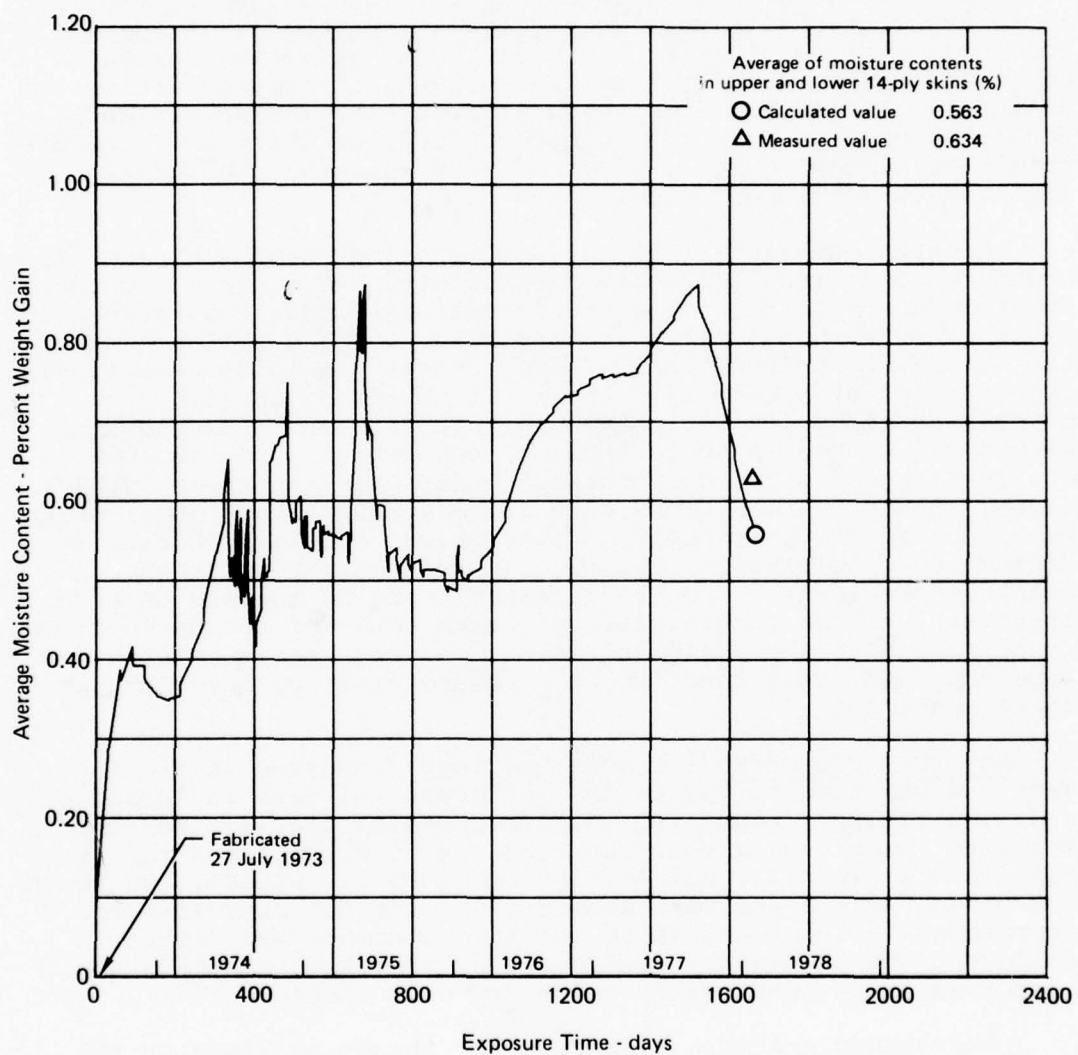
The diffusion coefficients and surface moisture concentrations associated with each event (typical day data) in the environmental history were further modified to effective values representing the solar heating and non-solar heating portions of that day. Procedures used are presented in Reference 14 and consisted of time-weighted averages for diffusivity and a combination of time-weighted and diffusivity-weighted averages for equilibrium moisture content.

Moisture contents were calculated using chronological sets of boundary conditions (effective diffusivity and effective surface moisture concentration) and the associated exposure durations in conjunction with one-dimensional models of the stabilator structure at selected locations. Since the rate of moisture diffusion through air is four-to-five orders of magnitude greater than through boron/epoxy, air columns within the aluminum honeycomb were not included in the diffusion model which consisted of two equal-thickness slabs of boron/epoxy representing upper and lower skins. Boundary conditions calculated for upper and lower skins were applied simultaneously in a numerical solution of Fick's Second Law of Diffusion resulting in through-the-thickness moisture gradients. The gradient remaining at the end of each event was used as the initial concentrations for the calculations associated with the following event. Average moisture contents were obtained, as a function of exposure time, by integrating these gradients.

5. MOISTURE HISTORIES - The methodology discussed in previous sections was used to reduce the environmental data in Appendices A and B, ultimately resulting in moisture-time profiles for three spanwise locations on both the Eagle 14 stabilator and the PDV stabilator. Thin (14 plies), intermediate (24 plies), and thick (38 plies) skin areas were chosen along the 50% chordline to correspond to locations where moisture contents were measured following the stabilator static tests. Moisture contents are expressed as percent weight gains for each coupon.

Calculated moisture histories for these locations in the Eagle 14 stabilator are presented in Figures 33 through 35, in terms of the average of upper plus lower skin values at each location. The peak moisture contents resulted from exposures to environments in St. Louis, the environmental chamber at Eglin AFB, and the Panama Canal Zone at Howard AB. Minimum moisture contents occurred at conclusions of desert exposures at El Centro NAS and





GP79-0344-53

**Figure 33. Predicted Moisture - Time Profile and Measured Value for 14-Ply Eagle 14 Skins**



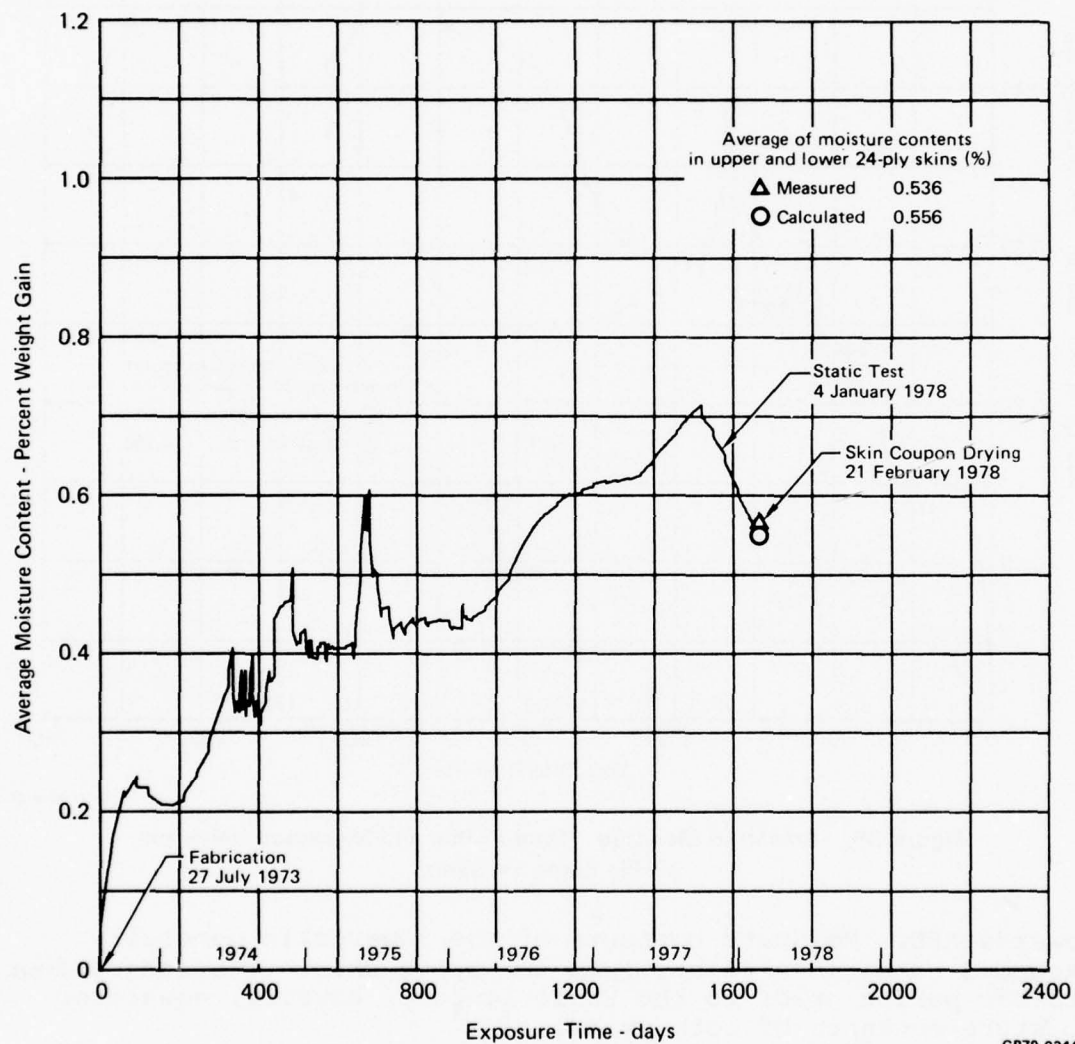
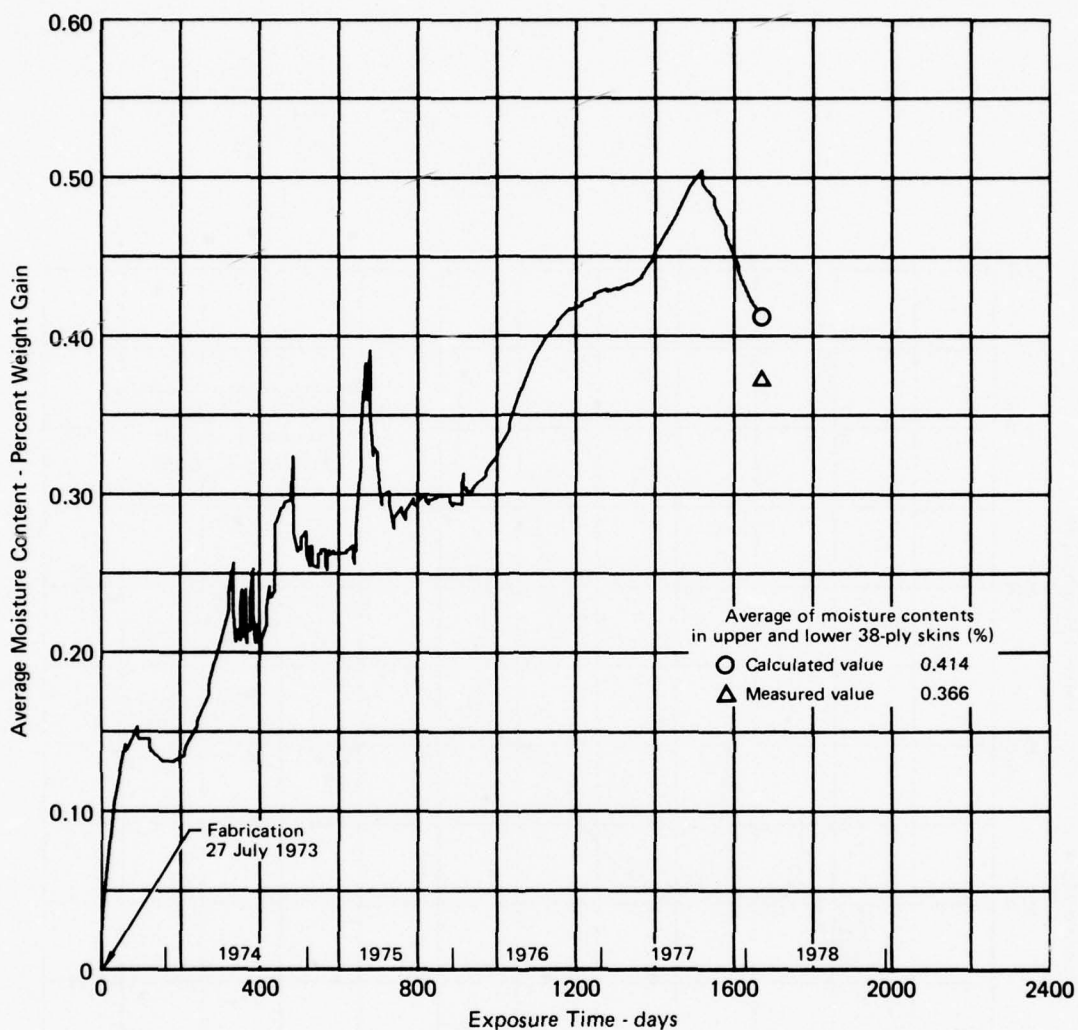


**Figure 34. Predicted Moisture - Time Profile and Measured Value for 24-Ply Eagle 14 Skins**



GP79-0344-55

**Figure 35. Predicted Moisture - Time Profile and Measured Value for 38-Ply Eagle 14 Skins**

Edwards AFB. Moisture contents of the lower skin generally exceeded comparable values from the upper skin. The long indoor storage period prior to the Eagle 14 test, however, equalized moisture contents of both skins.

Moisture histories are shown in Figures 36 through 38 for three locations in the PDV stabilator. No difference was predicted between moisture contents of upper and lower skins. Peaks and valleys in these profiles represent seasonal variations in weather conditions, as modified to account for indoor exposure only. Maximum moisture contents typically occurred at the conclusion of summer exposures.

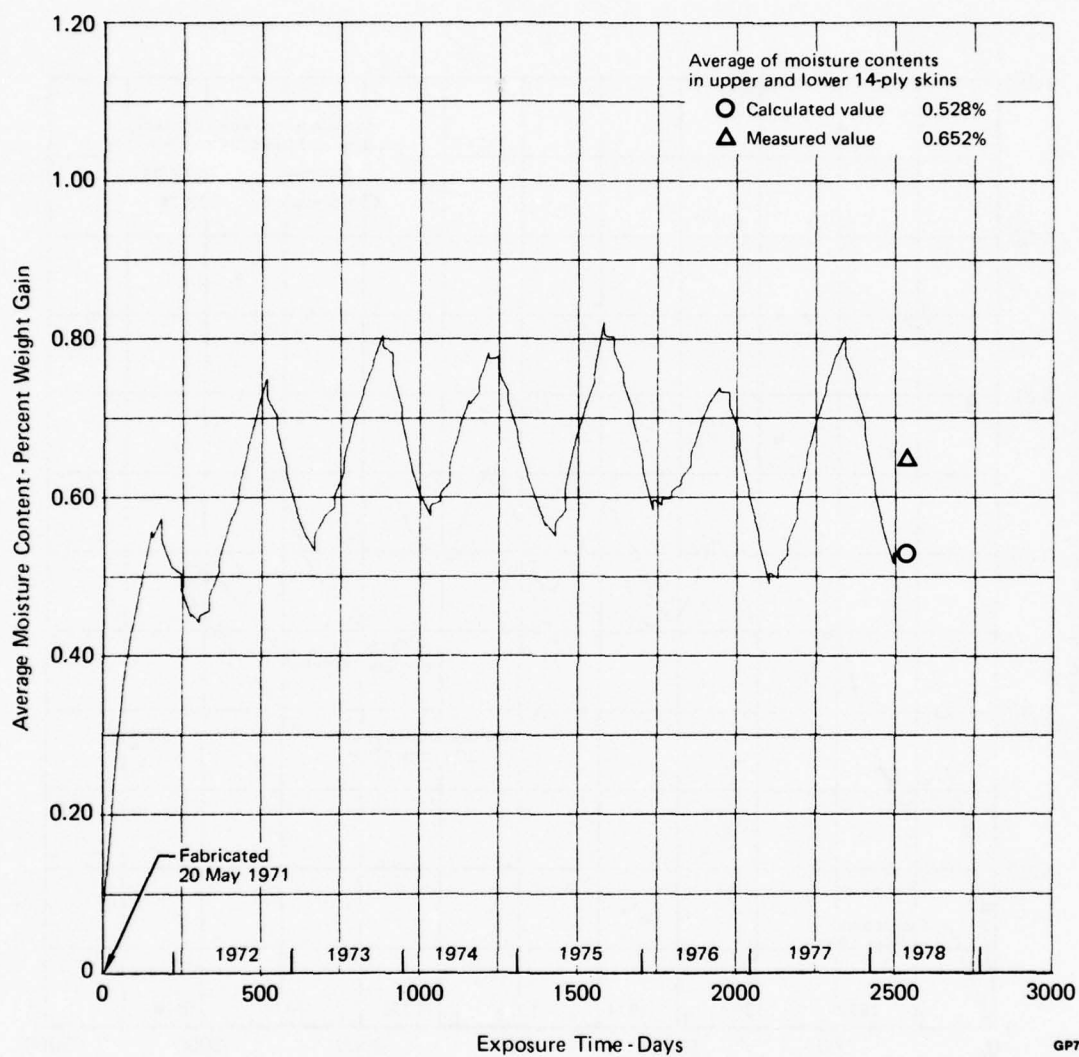
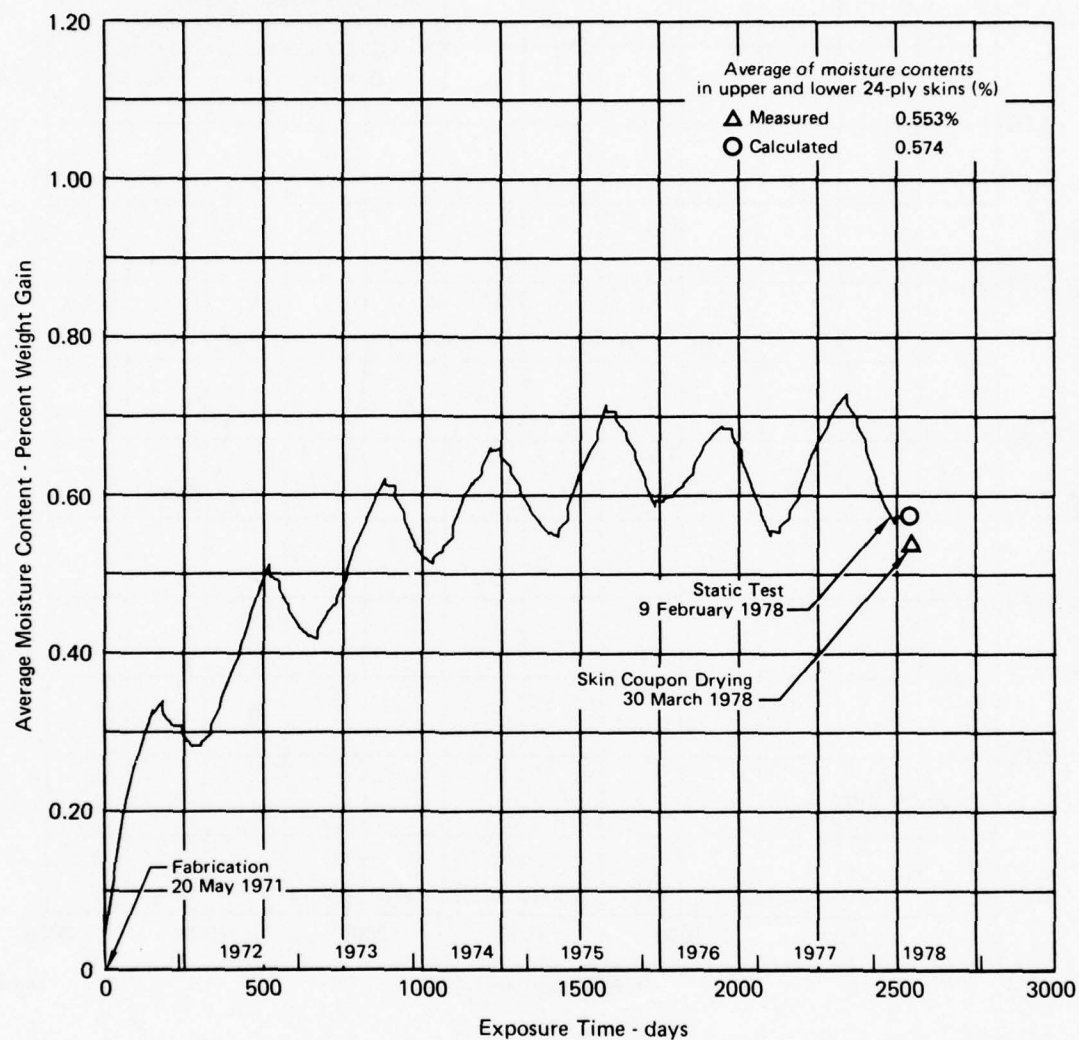
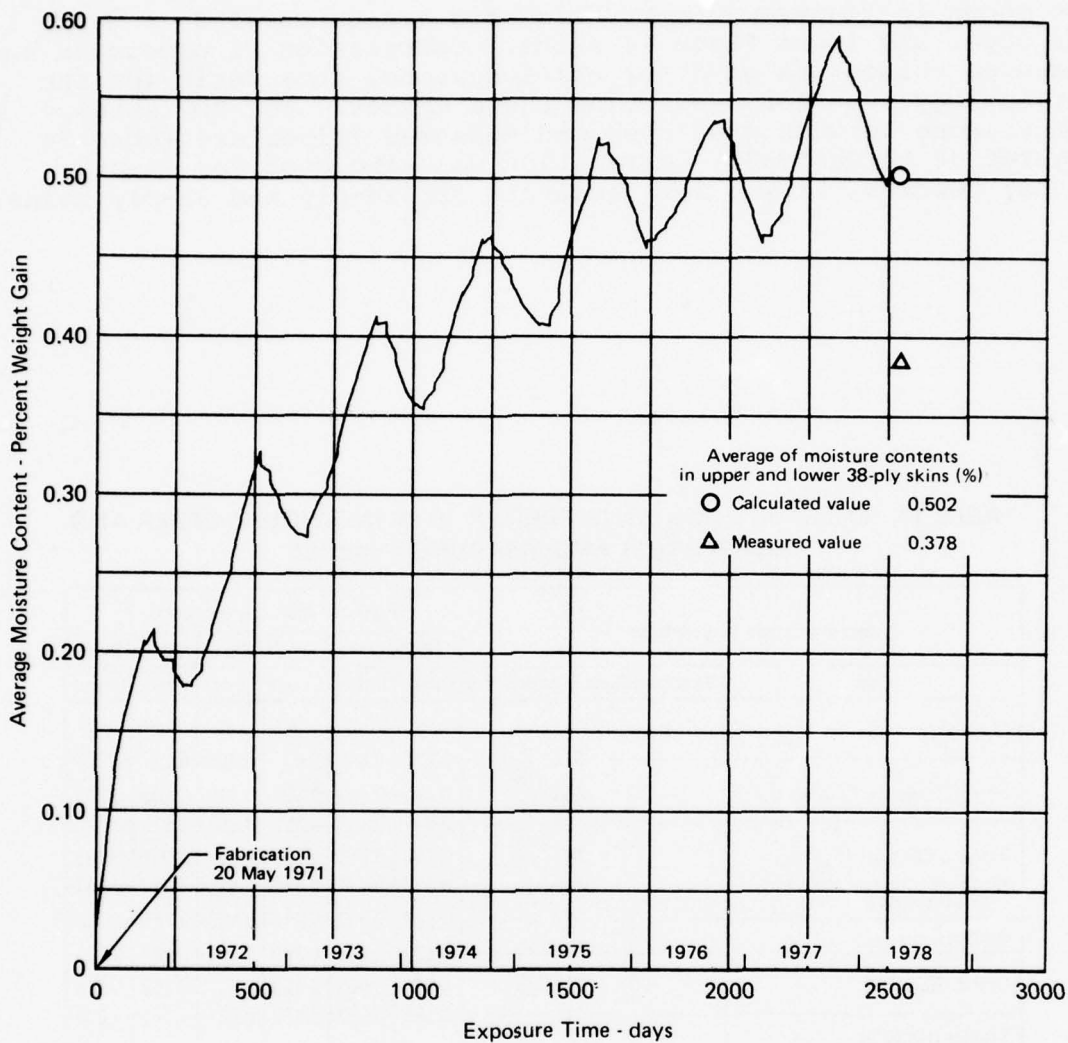


**Figure 36. Predicted Moisture - Time Profile and Measured Value for 14-Ply PDV Skins**



GP79-0344-51

**Figure 37. Predicted Moisture - Time Profile and Measured Value for 24-Ply PDV Skins**



GP79-0344-52

**Figure 38. Predicted Moisture - Time Profile and Measured Value for 38-Ply PDV Skins**

6. CORRELATION OF MEASURED AND PREDICTED MOISTURE CONTENTS - Upon completion of static tests, coupons were machined from 14-ply, 24-ply and 38-ply areas of the upper and lower skins of both stabilators. The skin-to-honeycomb adhesive was removed, and the coupons were dried at 250°F. Moisture contents of the boron/epoxy was determined by comparing in situ weights with the weights after drying. The resin content measured for each coupon was used for normalizing the moisture value to a baseline resin content of 30% by weight.



Comparisons between predicted and measured moisture contents are shown in Figures 33 through 35 and are summarized in Table 11 for upper and lower Eagle 14 skins. Correlation of predicted and measured values was good for all locations, thus verifying the methodology used for predicting these values. For PDV skins, comparisons between predicted and measured values are shown in Figures 36 through 38. Correlation was also good for 24-ply skins; however, it was less accurate for 14-ply and 38-ply skins.

**TABLE 11 MOISTURE CONTENTS PREDICTED IN INDIVIDUAL UPPER AND LOWER SKINS AND MEASURED VALUES**

Location of Eagle 14 Stabilator		Predicted Moisture Contents <sup>△1</sup>					
		14-Ply Skin		24-Ply Skin		38-Ply Skin	
Base	Exposure Time (Cumulative)	Upper	Lower	Upper	Lower	Upper	Lower
St. Louis	Day 1	0	0	0	0	0	0
	334 <sup>△2</sup>	0.674	0.646	0.421	0.400	0.267	0.251
Desert (Edwards, El Centro)	405 <sup>△3</sup>	0.411	0.423	0.303	0.316	0.185	0.201
	418	0.491	0.498	0.350	0.360	0.216	0.228
Climatic Chamber (Eglin)	484 <sup>△2</sup>	0.749	0.754	0.506	0.513	0.315	0.325
	496	0.577	0.581	0.410	0.418	0.257	0.267
Desert (Edwards)	527	0.582	0.582	0.414	0.419	0.260	0.267
Arctic (Eielson)	567	0.536	0.539	0.390	0.490	0.245	0.255
Desert (Edwards)	620 <sup>△3</sup>	0.546	0.555	0.402	0.412	0.252	0.265
	644	0.585	0.593	0.426	0.436	0.266	0.279
Tropics (Howard)	680 <sup>△2</sup>	0.880	0.862	0.611	0.601	0.389	0.386
Desert (Edwards)	890 <sup>△3</sup>	0.483	0.486	0.426	0.433	0.281	0.294
	925	0.503	0.505	0.440	0.446	0.293	0.303
St. Louis	1519 <sup>△2</sup>	0.875	0.875	0.715	0.715	0.502	0.505
	1663	0.563	0.563	0.556	0.556	0.413	0.415
Measured Moisture Contents	1663	0.652	0.615	0.525	0.547	0.362	0.370

Notes:



Expressed as percent of skin dry weight



Maximum value

Minimum value

GP79-0344-33

## SECTION V

### SKIN MOISTURE PROFILES FOR PROJECTED F-15 DEPLOYMENTS

Deployments of the F-15 force were projected for a 25-year service life using the recorded movements of F-4 aircraft. The various aircraft deployments were evaluated on the basis of moisture absorbed at specific locations in the composite skins resulting in the selection of median and worst-case deployments. Peak moisture contents were identified for the actual worst-case condition for use in structural element tests.

1. F-15 DEPLOYMENT PROJECTIONS - Deployments of F-15's were projected for a 25-year service life using data recorded for F-4 aircraft. Service life was broken down into active duty as an operational Tactical Air Command (TAC) fighter and reserve duty with the Air National Guard (ANG). Deployment data from F-4C and F-4D aircraft were used to estimate the active duty period at 15 years. F-4E aircraft were involved in peacetime deployments around the world, and their monthly movement patterns were used to project deployments of F-15's during active duty. At the time of this study, 539 F-4E aircraft had recorded deployments of five years or longer. Fifteen-year deployments for 539 F-15 aircraft were generated using three cycles of these 5-year F-4E data. Resulting patterns were then adjusted to include known differences between these two aircraft types, thus accounting for shifts in pilot training and aircraft staging bases and in depot-level repair facilities and movement from politically sensitive areas of the world. Permanent deployments to test facilities were also eliminated since only operational aircraft were being considered.

To complete the F-15 service lives, deployments associated with the 10-year reserve duty period were postulated from current and planned usage of F-4 aircraft in the ANG. Eight ANG bases were identified as having F-4's, or as likely recipients of F-4's. Individual F-15's were randomly distributed to these bases and assumed to remain there for the 10-year period.

Bases included in active and reserve duty phases are shown in Table 12. Deployments of individual F-15's were not necessarily unique during active duty since aircraft within a squadron tended to travel as a unit when reassigned to a new home base. Use of these 539 deployments, however, does account for the distribution of operational F-15's in the force and allows selection of a median and worst-case deployment representative of the force usage. In addition, the total number of deployments approximates the number of F-15's expected to be on operational status during active duty. Examples of European, Asian and North American deployments are presented in Table 13.

**TABLE 12. BASES USED FOR F-15 DEPLOYMENT PROJECTIONS**

Active Duty Bases		
Netherlands	West Germany	United States
Soesterburg AB	Bitburg AB	Eglin AFB, Florida
Okinawa (Japan)	Hahn AB	Elmendorf AFB, Alaska
Kadena AB	Ramstein AB	Holloman AFB, New Mexico
Philippines	Zweibruchen AB	Homestead AFB, Florida
Clark AB		Langley AFB, Virginia
		Luke AFB, Arizona
South Korea		MacDill AFB, Florida
Kunsan AB		Moody AFB, Georgia
Osan AB		Nellis AFB, Nevada
Spain		St. Louis, Missouri
Torrejon AB		Warner-Robins AFB, Georgia
Reserve Duty Bases		
Fargo, North Dakota	New Orleans, Louisiana	
Fort Smith, Arkansas	St. Louis, Missouri	
Hickam AFB, Hawaii	Selfridge, Michigan	
Kelly AFB, Texas	Springfield, Illinois	

GP79-0344-48

**TABLE 13. PROJECTED 25-YEAR F-15 DEPLOYMENTS**

Year	Month											
	Jan	Feb	Mar	Apr	May	Jun	Jul	Aug	Sep	Oct	Nov	Dec
Deployment - Europe												
1, 6, 11	TORR	TORR	SOES									SOES
2, 7, 12	SOES											SOES
3, 8, 13	SOES	SOES	SOES	TORR	BITB							BITB
4, 9, 14	BITB											BITB
5, 10, 15	BITB	HAHN						HAHN	TORR	TORR	HAHN	HAHN
16 - 25	SELF											SELF
Deployment - Far East												
1, 6, 11	KADE											KADE
2, 7, 12	KADE					KADE	KUNS	KUNS	CLAR	OSAN	OSAN	OSAN
3, 8, 13	OSAN											OSAN
4, 9, 14	OSAN											OSAN
5, 10, 15	OSAN							OSAN	CLAR			CLAR
16 - 25	FORT											FORT
Deployment - United States												
1, 6, 11	LANG			LANG	HOME					HOME	NELL	NELL
2, 7, 12	NELL											NELL
3, 8, 13	LANG	WARN						WARN	LANG			LANG
4, 9, 14	NELL					NELL	MACD					MACD
5, 10, 15	MACD											MACD
16 - 25	FARG											FARG

Note: Bases are identified using the initial four letters of the base name.

GP79-0344-49

2. MOISTURE-TIME PROFILES - Surface weather data for the bases associated with projected F-15 deployments are presented in Appendix C. These are statistical data from information recorded at these bases over several years. An environmental spectrum was constructed for each deployment by compiling events in chronological order. Each event was one month in duration. Environmental data for each event were taken from monthly weather data for a specific base (Table 13). There were 300 events in each spectrum for a service life of 25 years.

Data from each spectrum were converted to skin temperatures and surface air humidities using the heat balance equations which were developed for the stabilator skins (Section IV(2)). Emissivity and solar absorptivity constants for gray polyurethane enamel were incorporated in these equations, thus conforming to the surface finish used for production stabilators. Skin temperatures and surface air humidities were then converted to diffusion coefficients and surface moisture concentrations using data from Figures 26 and 27 and corrections were made for precipitation effects (Section IV(4)). The moisture diffusion characteristics of the epoxy matrix were assumed unaltered by service life exposures in generating these boundary conditions. Boundary conditions for each event were applied in a numerical solution for through-the-thickness moisture gradients and the integrated average content (Section IV(4)) resulting in a detailed moisture-time profile upon evaluation of all spectrum events.

Numerical calculation methods were used to evaluate, in detail, selected deployments. For determining peak moisture contents in all 539 deployments, a closed-form solution (Reference 10) to Fick's second law was used, namely:

$$M_f = (M_{eq} - M_i) \left\{ 1 - \exp \left[ - 7.3 \left( \frac{Dt}{h^2} \right)^{.75} \right] \right\} + M_i$$

where  $t$  = event duration =  $t_f - t_i$

$M_f$  = average moisture content at time  $t_f$

$M_{eq}$  = surface moisture concentration for this event

$M_i$  = initial moisture content at time  $t_i$

$h$  = thickness

$D$  = diffusion coefficient for this event

Peak moisture contents for 14-ply skins were calculated for each environmental spectrum (deployment) using the above closed-form solution. Median and worst-case deployments were then identified by evaluating the median and maximum, respectively, of peak moisture contents from all 539 spectra. Distributions of these peak values are presented in Figure 39 for upper and lower skins. Median and maximum values for upper and lower skins are essentially the same; however, the distribution in the upper skin is more complex due to solar heating effects.

a. Median Deployment - Median of peak moisture contents occurred from exposures during stateside deployments. A representative median deployment is presented in Figure 40 along with the



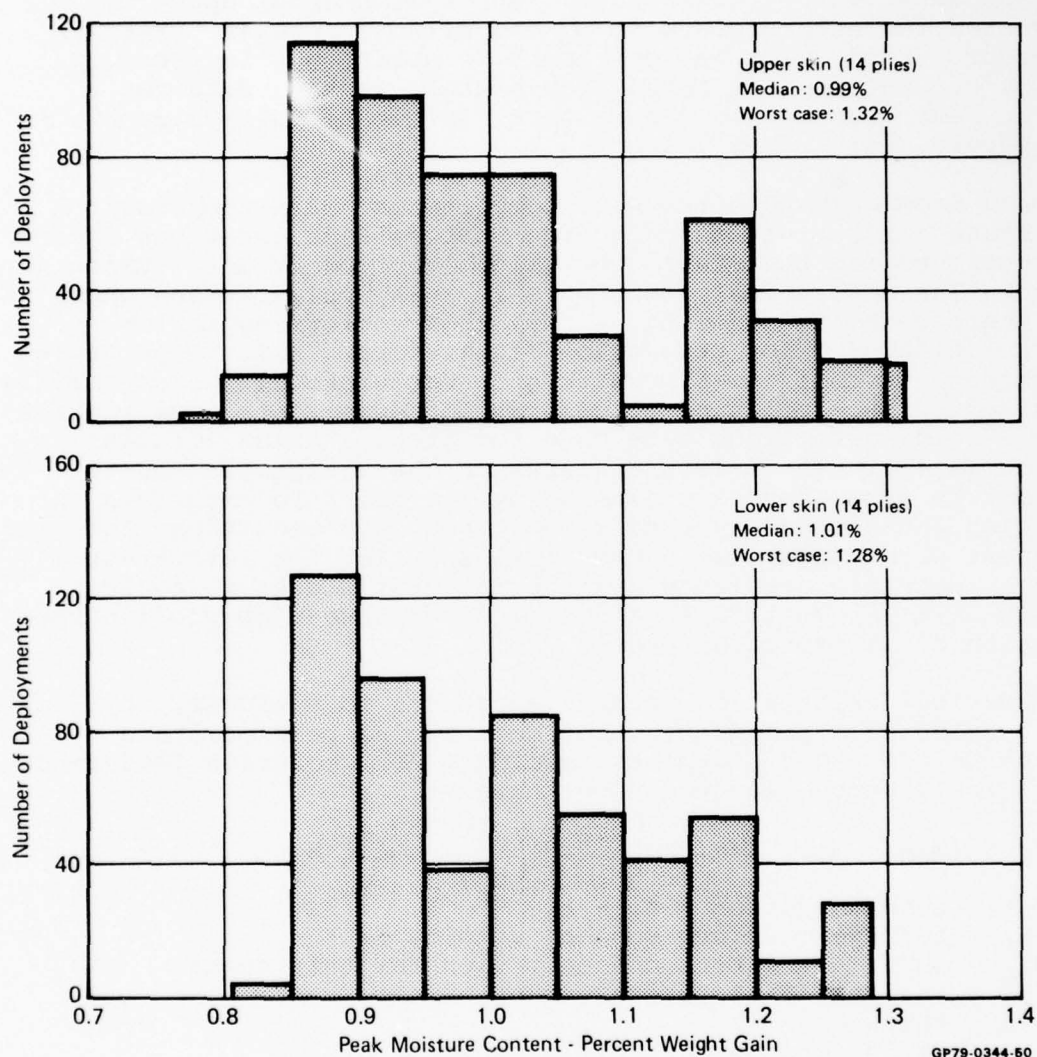


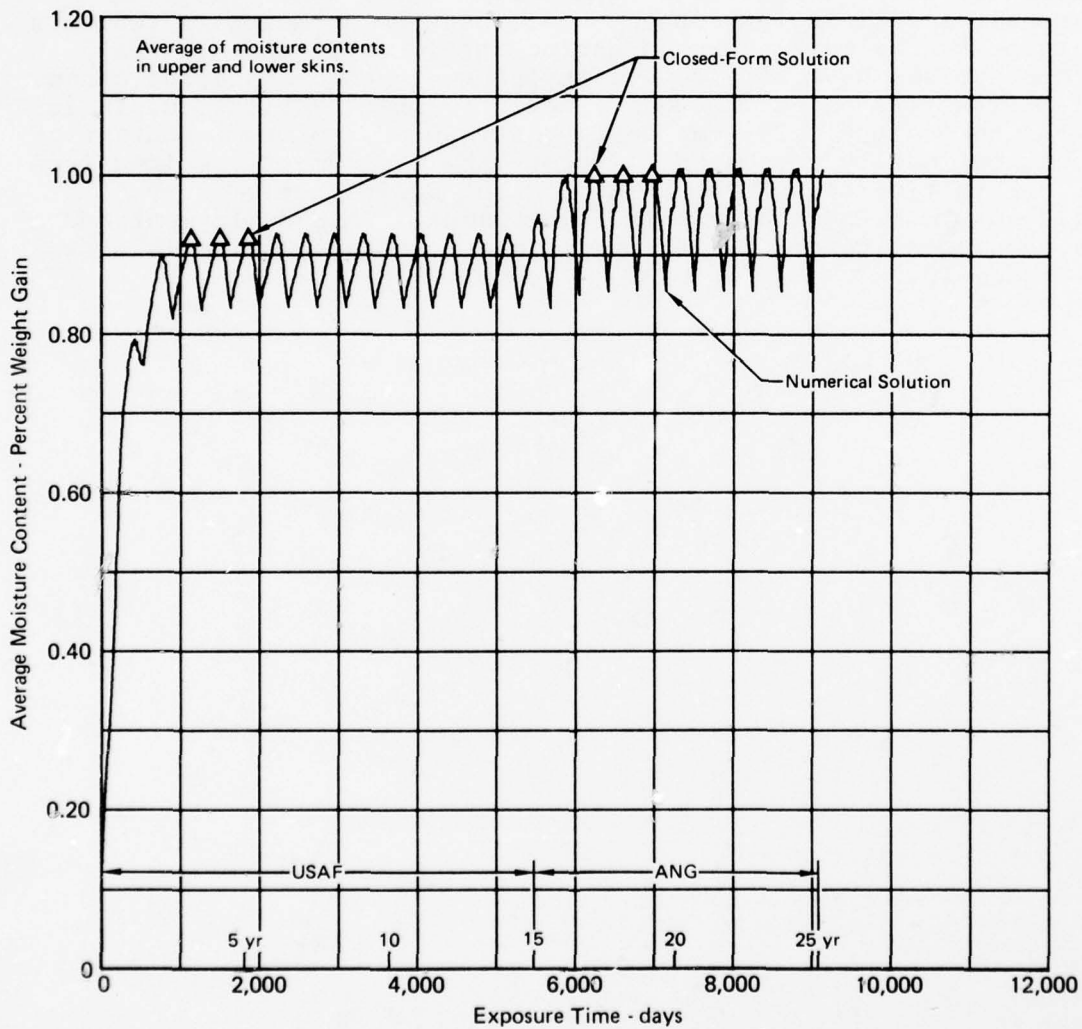
Figure 39. Distribution of Peak Moisture Contents Predicted for F-15 Deployments



### Median-Case Deployment

Year	Month											
	Jan	Feb	Mar	Apr	May	Jun	Jul	Aug	Sep	Oct	Nov	Dec
1, 6, 11	LANG											LANG
2, 7, 12	LANG											LANG
3, 8, 13	LANG											LANG
4, 9, 14	LANG											LANG
5, 10, 15	LANG											LANG
16 - 25	SAIN											SAIN

Note: Bases are identified using the initial four letters of the base name.



GP79-0344-56

Figure 40. Moisture-Time Profile in 14-Ply Skins Predicted for a Median - Case Deployment

corresponding moisture-time profile for 14-ply skins. Good correlation is shown between peak moisture contents from closed-form and numerical solutions.

b. Worst-Case Deployment - The maximum of peak moisture contents occurred in environmental spectra associated with European deployments. A representative worst-case deployment is shown in Figure 41 along with the corresponding moisture-time profile for 14-ply skins, which was calculated using numerical methods. The peak moisture contents from the closed-form solution correlated well with the more detailed numerical results.

Thin skins responded quickly to environments and reached service equilibrium levels within the first five years of active duty. During the next 10 years, moisture contents of these skins oscillated about the service equilibrium level as a result of seasonal variations in weather conditions. Peak moisture contents in thin skins always occurred during active duty since several European bases have more severe environments than stateside bases. Thick skins (44 plies), however, never reached service equilibrium levels throughout a 25-year deployment. Since moisture content of these continually increased, a worst-case deployment resulted from the combination of a European deployment during active duty followed by the most severe ANG deployment. This deployment and the corresponding moisture-time profile for 44-ply skins is shown in Figure 42.

### Worst-Case Deployment

Year	Month											
	Jan	Feb	Mar	Apr	May	Jun	Jul	Aug	Sep	Oct	Nov	Dec
1, 6, 11	SOES	←										SOES
2, 7, 12	SOES	←										SOES
3, 8, 13	BITB	←										BITB
4, 9, 14	BITB	←	RAMS	←								RAMS
5, 10, 15	RAMS	←										RAMS
16 - 25	FORT	←										FORT

Note: Bases are identified using the initial four letters of the base name.

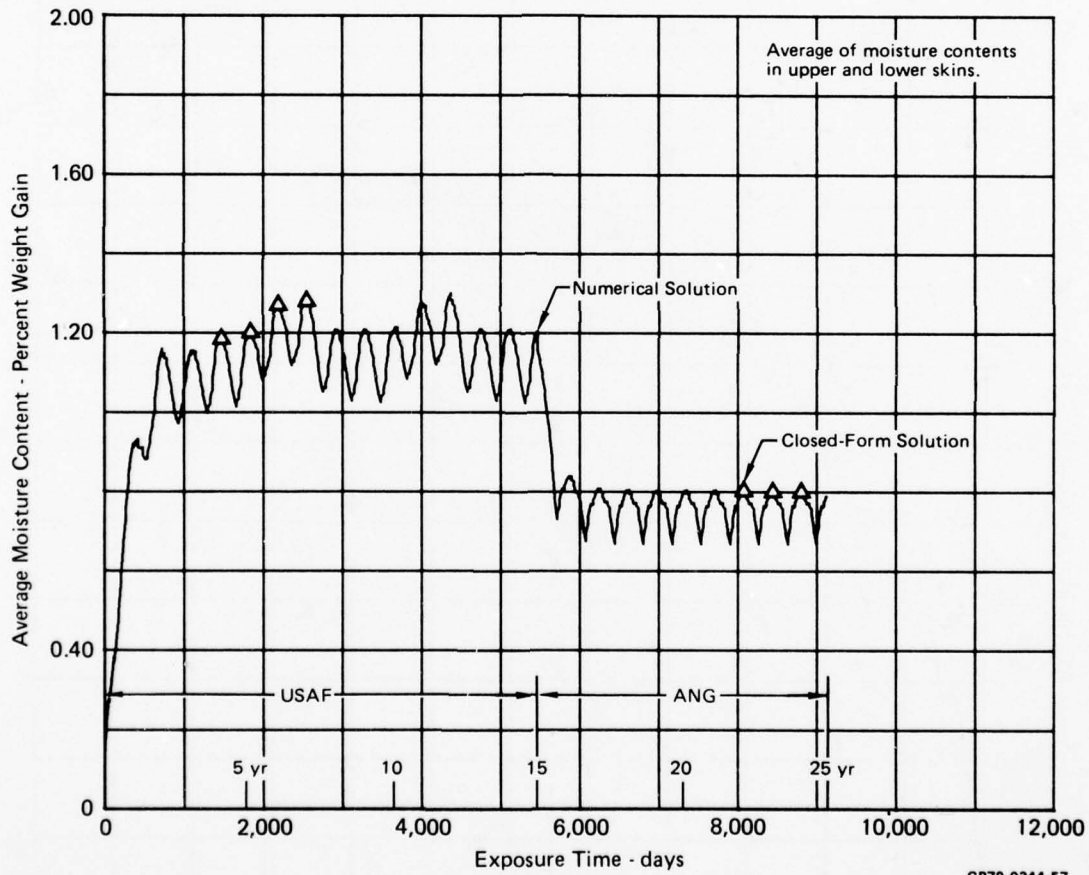
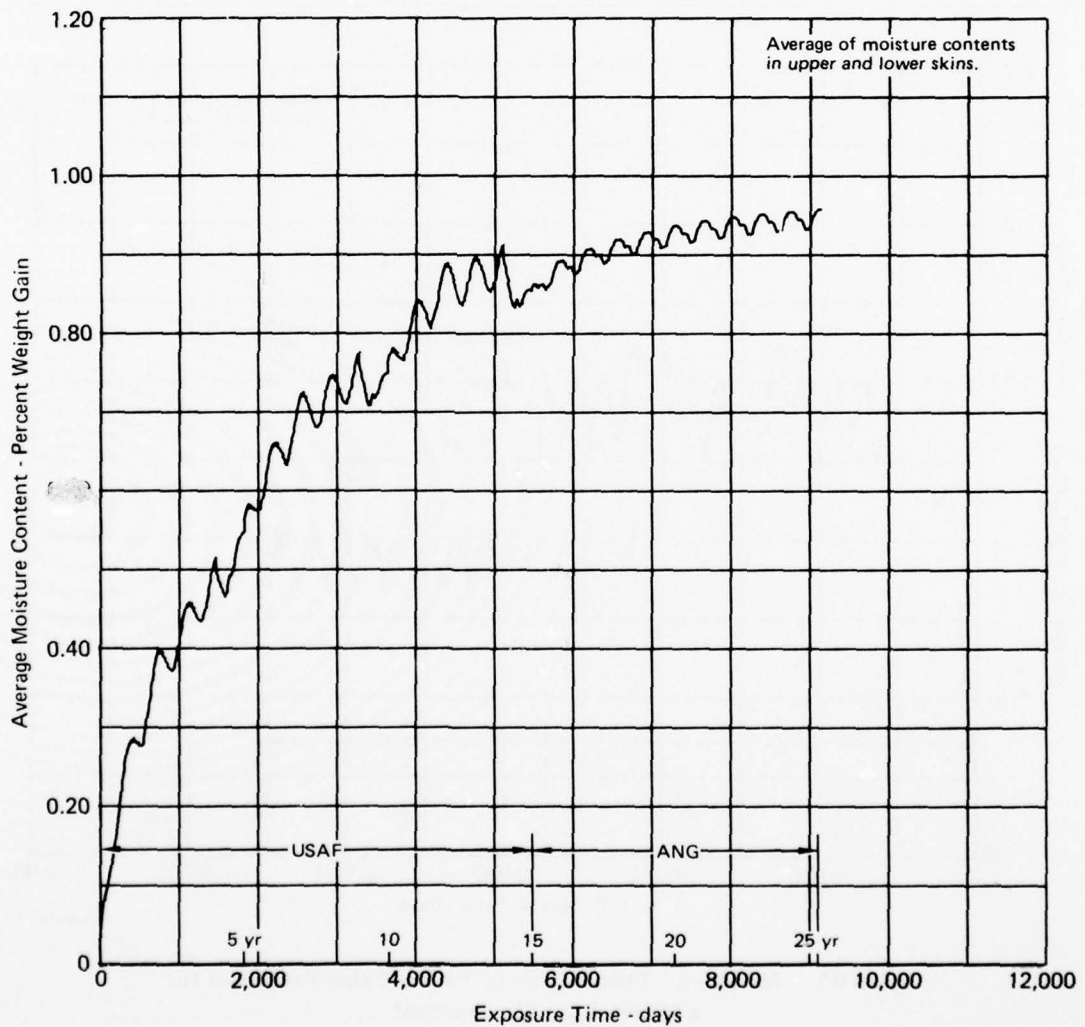


**Figure 41. Moisture - Time Profile in 14-Ply Skins Predicted for a Worst-Case Deployment**

# Worst-Case Deployment

Year	Month											
	Jan	Feb	Mar	Apr	May	Jun	Jul	Aug	Sep	Oct	Nov	Dec
1, 6, 11	RAMS	ZWEI										ZWEI
2, 7, 12	RAMS			RAMS	HAHN	HAHN	SOES					SOES
3, 8, 13	SOES	BITB										BITB
4, 9, 14	BITB											BITB
5, 10, 15	HOME											HOME
16 - 25	NEWO											NEWO

Note: Bases are identified using the initial four letters of the base name.



GP79-0344-58

Figure 42. Moisture - Time Profile in 44-Ply Skins Predicted for a Worst-Case Deployment



## SECTION VI

### ELEMENT TEST PROGRAM

At the conclusion of static tests, specimens were machined from the boron/epoxy skins of both stabilators. These were used to evaluate moisture contents at static test, structural properties, and physical and chemical characteristics of the epoxy resin. Moisture contents measured in the skins verified the predictive methodology (Section IV). Structural properties were determined to aid in the interpretation of static test results and to evaluate the effects of extreme environments. Physical and chemical characteristics were determined to discern degradation occurring as a result of prior stabilator usage.

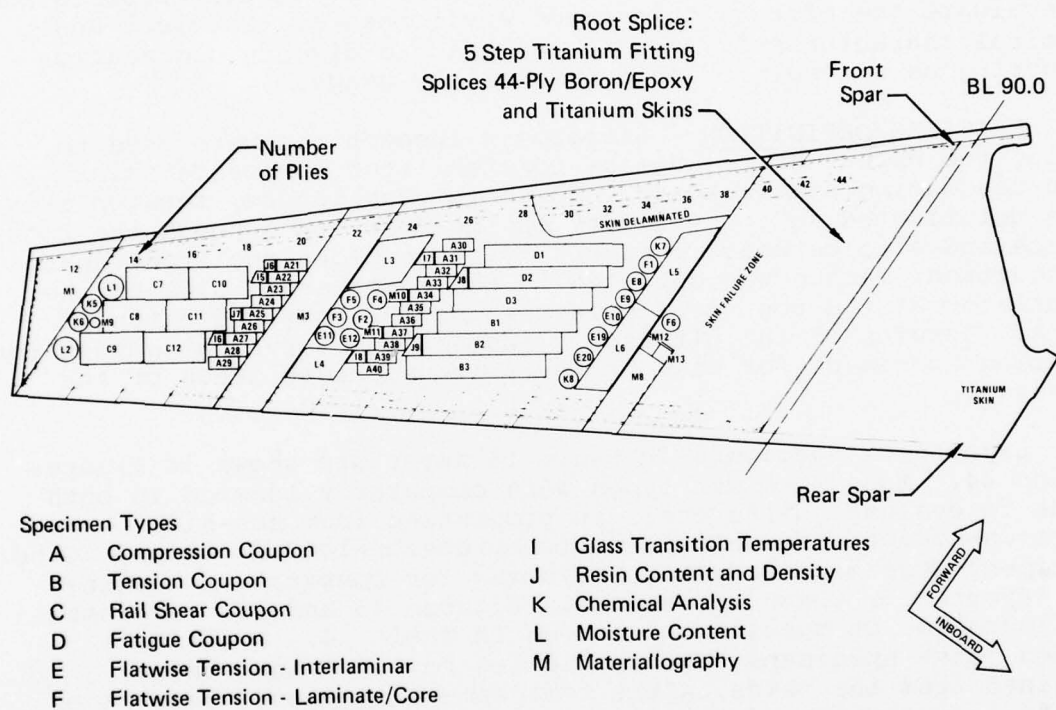
1. SPECIMEN DEFINITION - Ultrasonic inspections were used to define the extent of the damage to stabilator composite skins incurred during static tests. For both stabilators, tension skins were delaminated in the vicinity of the fracture through the root splice and also outboard from the fracture along the front spar. In addition, damage was detected in the compression side of the stabilator at the root splice between boron/epoxy and titanium skins. Results of the ultrasonic inspections served as guides for locating specimens for element tests in undamaged areas of the skins.

Layouts of specimens in Eagle 14 skins are shown in Figures 43 and 44. Many specimen types were comparably located in both skins to evaluate differences in properties from sun-side (tension-loaded) and shade-side (compression-loaded) skins. Other specimens were machined from PDV skins for comparative testing, and layouts for these are shown in Figures 45 and 46. Laminate configuration of specimens is shown in Table 14. Additional bonded joint specimens were fabricated to supplement those machined from the skins, where test damage precluded removal of the full complement of specimens. Configuration and materials used for the bonded joint were identical to the construction of the stabilator root splice.

2. RESULTS OF STRUCTURAL ELEMENT TESTS - These tests were conducted under temperature and absorbed moisture conditions simulating those expected in service. Data presented in this section represents test averages; detail test results are included in Appendix D.

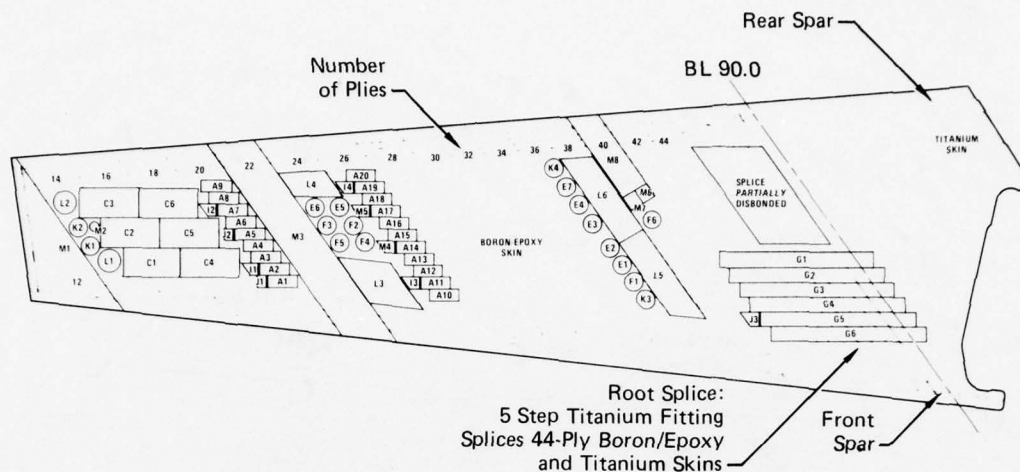
Specimens were tested after conditioning to one of four moisture contents: dry, in situ, Eagle 14, and maximum. Specimens tested dry were desiccated at 250°F. Specimens with in situ moisture levels were tested upon dissection from stabilator skins at the conclusion of static tests. A third group of specimens





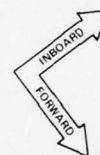
GP79-0344-64

Figure 43 Specimen Layout on the Eagle 14 Tension Skin



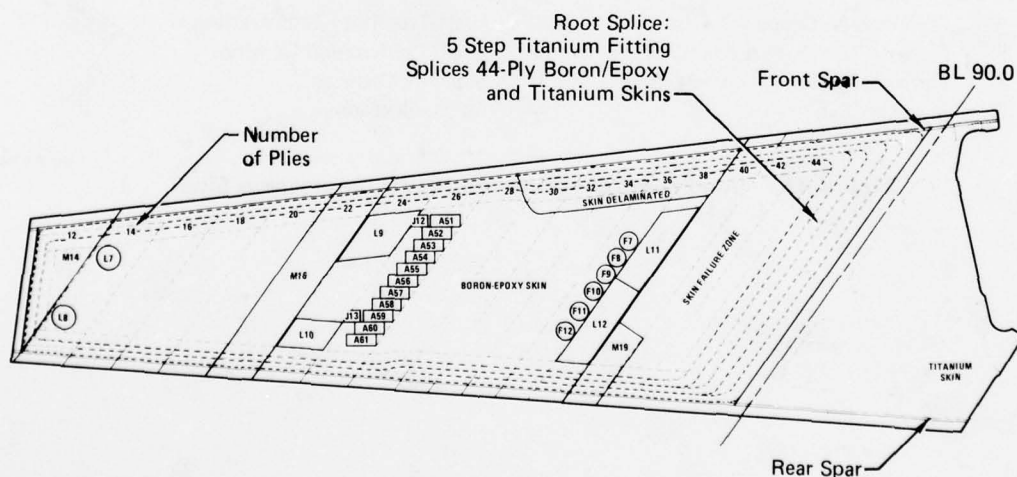
#### Specimen Types

- |   |                                  |   |                               |
|---|----------------------------------|---|-------------------------------|
| A | Compression Coupon               | I | Glass Transition Temperatures |
| B | Tension Coupon                   | J | Resin Content and Density     |
| C | Rail Shear Coupon                | K | Chemical Analysis             |
| D | Fatigue Coupon                   | L | Moisture Content              |
| E | Flatwise Tension - Interlaminar  | M | Materiallography              |
| F | Flatwise Tension - Laminate/Core |   |                               |
| G | Step Lap Joint                   |   |                               |



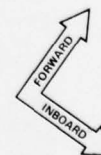
GP79-0344-66

**Figure 44 Specimen Layout on the Eagle 14 Compression Skin**



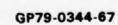
#### Specimen Types

- |   |                                  |   |                           |
|---|----------------------------------|---|---------------------------|
| A | Compression Coupon               | J | Resin Content and Density |
| E | Flatwise Tension Interlaminar    | K | Chemical Analysis         |
| F | Flatwise Tension - Laminate/Core | L | Moisture Content          |
| I | Glass Transition Temperatures    | M | Materiallography          |



GP79-0344-66

**Figure 45 Specimen Layout on the PDV Tension Skin**



78

TABLE 14. CONFIGURATION OF STABILATOR COMPOSITE SKIN

Number of Plies in Each Step	1	Root 44 Plies	Layup of Each Step of Boron/Epoxy Skin														Tip 12 Plies	
			42	40	38	36	34	32	30	28	26	24	22	20	18	16		14
Layup for Laminate Half- Thickness	2	+45	✓	✓	✓	✓	✓	✓	✓	✓	✓	✓	✓	✓	✓	✓	✓	✓
		-45	✓	✓	✓	✓	✓	✓	✓	✓	✓	✓	✓	✓	✓	✓	✓	✓
		90	✓	✓	✓	✓	✓	✓	✓	✓	✓	✓	✓	✓	✓	✓	✓	✓
		0	✓	✓	✓	✓	✓	✓	✓	✓	✓	✓	✓	✓	✓	✓	✓	✓
		0	✓	✓	✓	✓	✓	✓	✓	✓	✓	✓	✓	✓	✓	✓	✓	✓
		+45																
		-45	✓															
		0	✓	✓														
		0	✓	✓	✓	✓	✓											
		+45	✓	✓	✓	✓	✓											
		-45	✓	✓	✓	✓	✓											
		0	✓	✓	✓	✓	✓	✓										
		0	✓	✓	✓	✓	✓	✓	✓									
		+45	✓	✓	✓	✓	✓	✓	✓	✓								
		-45	✓	✓	✓	✓	✓	✓	✓	✓	✓							
		0	✓	✓	✓	✓	✓	✓	✓	✓	✓	✓			✓	✓		
		0	✓	✓	✓	✓	✓	✓	✓	✓	✓	✓	✓		✓			
		+45	✓	✓	✓	✓	✓	✓	✓	✓	✓	✓	✓	✓				
		-45	✓	✓	✓	✓	✓	✓	✓	✓	✓	✓	✓	✓	✓			
		0	✓	✓	✓	✓	✓	✓	✓	✓	✓	✓	✓	✓	✓	✓		
		+45	✓	✓	✓	✓	✓	✓	✓	✓	✓	✓	✓	✓	✓	✓	✓	✓
		-45	✓	✓	✓	✓	✓	✓	✓	✓	✓	✓	✓	✓	✓	✓	✓	✓
		Q Sym																

<sup>△1</sup> Nominal thickness 0.0052 in./ply.

<sup>△2</sup> 0° - direction is parallel to 50% chord line.

GP79-0344-84

were conditioned to moisture contents predicted to exist in Eagle 14 skins at the time of static test (Section IV). These moisture contents are shown in Figure 47. The last group of specimens were conditioned to the maximum moisture contents expected for F-15 deployments (Section V). These are shown in Figure 48.

a. Bonded Joint Specimens - These tests were performed at room temperature and at two elevated temperatures. A temperature of 200°F had been used in conjunction with maximum applied loads for the F-15 design analysis; consequently, most testing was conducted at 200°F in this program. Three tests were conducted at 317°F, the maximum temperature calculated for the stabilator root splice. Test results are summarized in Table 15 in the order of increasing specimen moisture content. In exploratory tests with specimens N4-N9, the tensile loading mode was more critical than the compression mode and was selected for use with the remaining specimens.



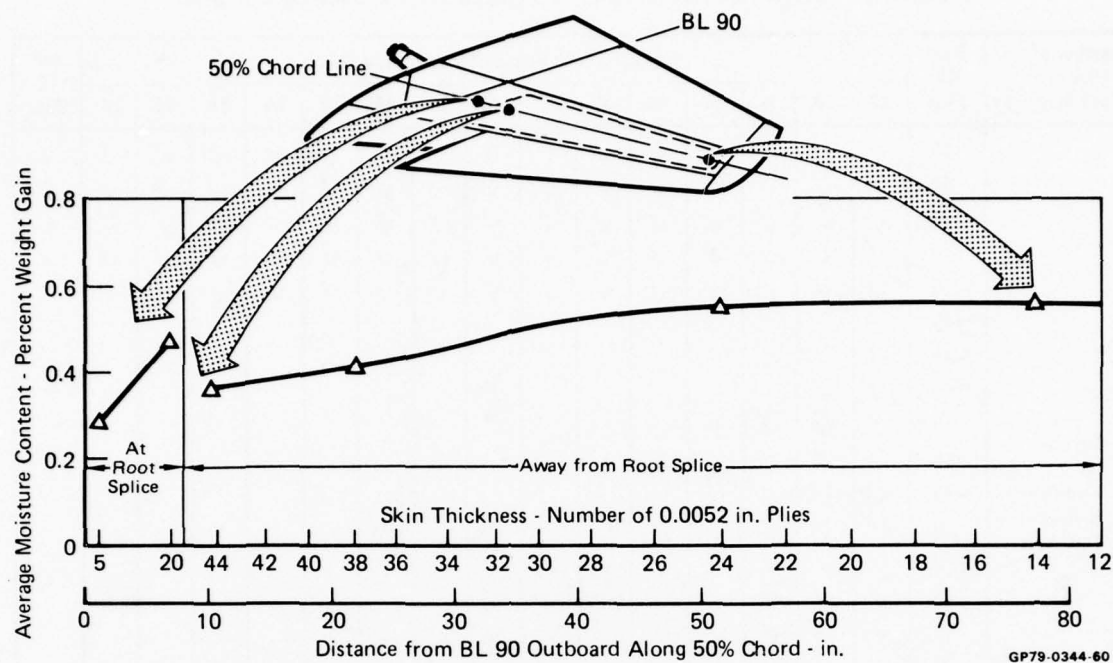


Figure 47. Eagle 14 Moisture Contents at Conclusion of Static Test

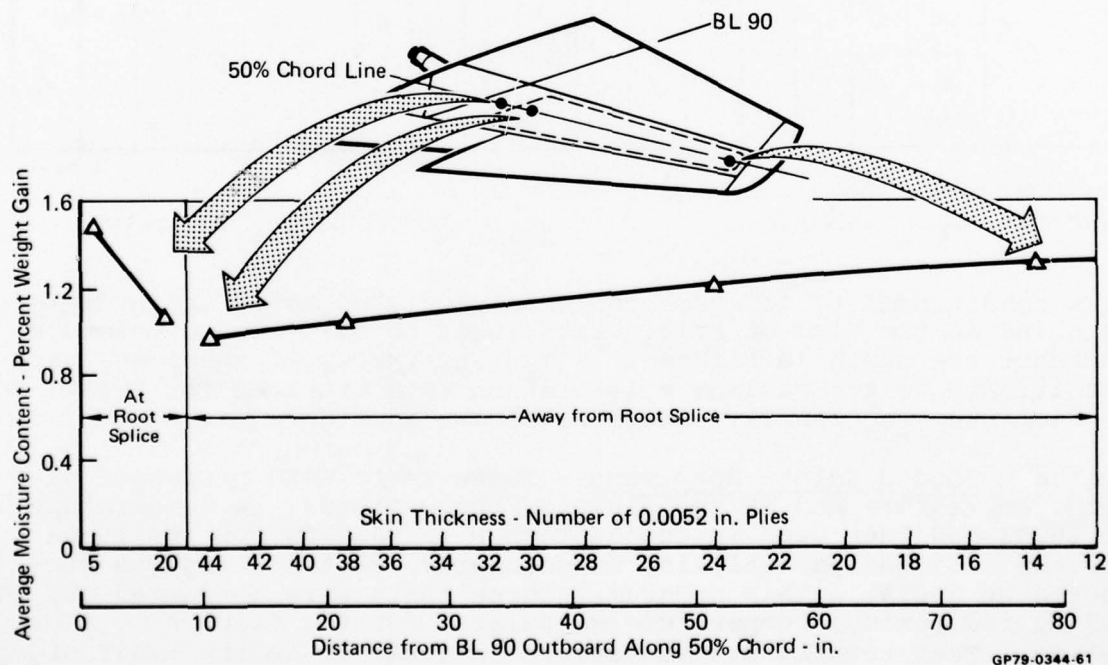
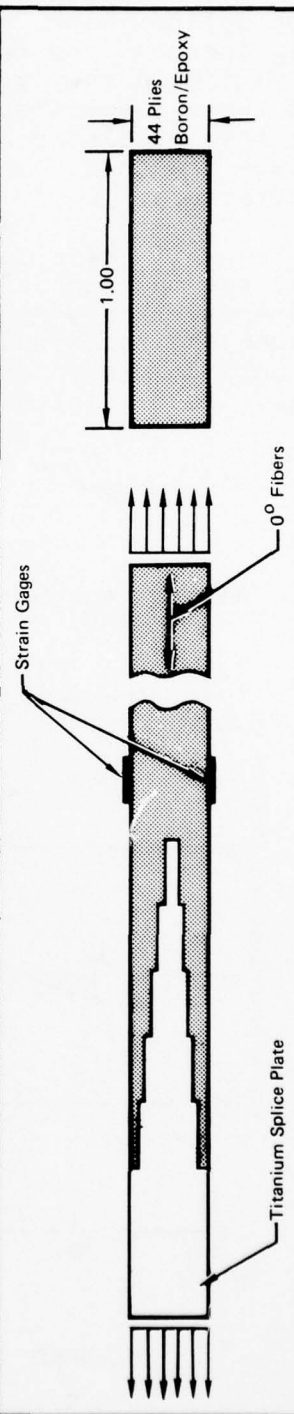


Figure 48. Maximum Moisture Contents Calculated for Use in Element Tests

TABLE 15 RESULT OF BONDED JOINT TESTS

Origin of Specimens	Specimen ID	Test Conditions			Failure Conditions			Primary Modulus, E (msi)
		Mode of Loading	Temperature (°F)	Moisture Content	Normal Stress (ksi)	Normal Strain (in./in.)	Mode of Failure	
New Eagle 14 Stabilator	N17, N18 G1, G2	Tension Tension	200 200	Dry In Situ	87.2 70.9	6800 5290	Fracture of 44-Ply Boron/Epoxy Joint Disbond, Thin Titanium Step Fractured	14.1 14.5
New	N1 - N3	Tension	R.T.	Moisture Contents Predicted for the Eagle 14 Skins	84.6	6680	Fracture of 44-Ply Boron/Epoxy	14.0
New	N4 - N6	Tension			80.1	6270	Fracture of 44-Ply Boron/Epoxy	14.7
New	N7 - N9	Compression			-81.0	-8170 (Max)	Fracture of 44-Ply Boron/Epoxy Due to Beam-Column Bending	13.6
Eagle 14 Stabilator	G3 - G6	Tension	200		72.7	5410	Joint Disbond and Fracture of Boron/Epoxy	14.2
New	N10, N12, N13 N11	Tension	200	Maximum	80.3	6410	Fracture of 44-Ply Boron/Epoxy	13.9
New		Compression	200	Maximum	-69.9	-7260 (Max)	Fracture of 44-Ply Boron/Epoxy Due to Beam-Column Bending	13.8
PDV Stabilator	G10, G12 - G15 N14 - N16	Tension	200	Maximum	71.2	5780	Fracture of 44-Ply Boron/Epoxy	13.8
New		Tension	317	Maximum	50.6	4280	Joint Disbond and Fracture of Boron/Epoxy	12.7



GP79-0344-81

Results of tension tests are presented in Figure 49. All specimens were ultrasonically inspected prior to testing; specimens from Eagle 14 and PDV stabilators exhibited minor disbonding of the splice joint. These defects, however, did not significantly increase the scatter of test data from stabilator specimens, although they may have contributed to the difference between these results and test results for new specimens. Failure modes for stabilator specimens involved disbonding along with laminate fracture. The failure mode for new specimens was laminate fracture.

b. Rail Shear Specimens - These tests were performed at 340°F, the maximum expected temperature for outboard areas of the boron/epoxy skin. Because these specimens from stabilator skins exceeded the recommended thickness for rail shear tests, they were used only to obtain modulus data for comparison with design values. Test results are presented in Table 16.

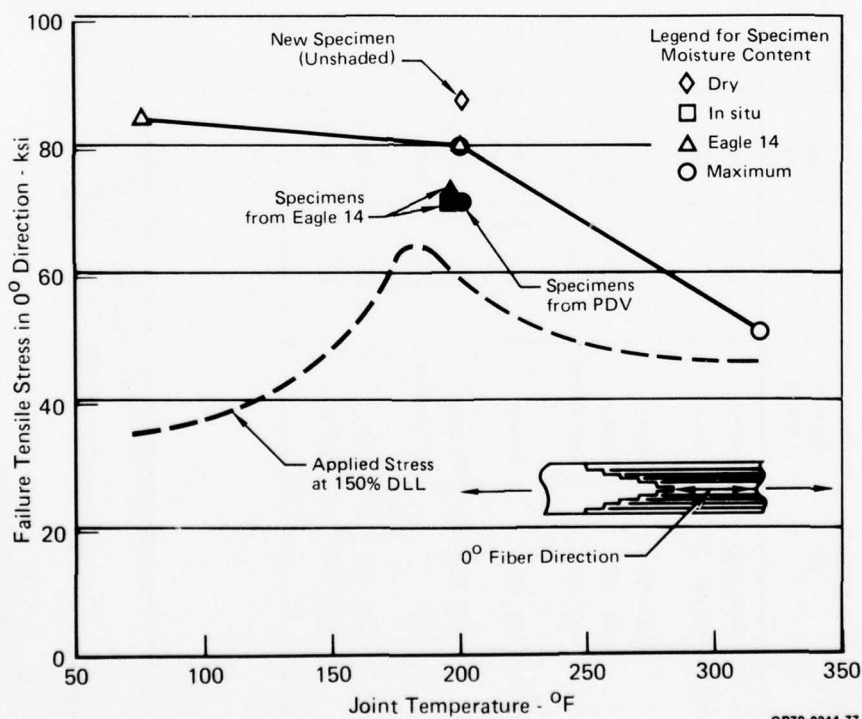


Figure 49 Tensile Strength of Bonded Root Splice

**TABLE 16. SHEAR MODULUS MEASURED IN RAIL SHEAR TESTS**

Location of Specimens in Eagle 14 Skins	Specimen ID	Test Conditions		Primary Modulus, G (msi)	Modulus Ratio
		Temperature (°F)	Moisture Content		
Compression Skin	C1, C2, C3	340	In Situ	3.9	0.89
Tension Skin	C7, C8, C9	340	In Situ	4.3	0.98
Design Value		340	Dry	4.4	1.00
Compression Skin	C4, C5, C6	340	Maximum	2.4	0.62
Tension Skin	C10, C11, C12	340	Maximum	2.9	0.74
Design Value		340	Dry	3.9	1.00

GP79-0344-79

c. Tension Specimens - These tests were conducted at 340°F after the specimens (B1, B2, B3) had been conditioned to the maximum expected moisture contents. Average test results are: failure stress, 76.5 ksi; primary modulus, 15.3 msi. The average strain at failure exceeded 5500 uin/in. This value represents the maximum scale values on the strain recorder since, at failure, strains in two of the three tension tests exceeded scale values. Comparable design allowables (dry) are: failure stress, 73.9 ksi; primary modulus, 14.2 msi; failure strain, 5200 uin/in.

d. Compression Specimens - Tests of boron/epoxy specimens were conducted at room temperature and at 340°F, the maximum temperature calculated for outboard areas of the skins. Test results are summarized in Table 17. Strengths obtained in room temperature and elevated temperature tests of dry specimens were consistent and exceeded design allowable strengths; however, considerable scatter occurred in the strengths obtained in tests of moisture-conditioned specimens. This scatter is thought to be



TABLE 17. RESULT OF COMPRESSION TESTS

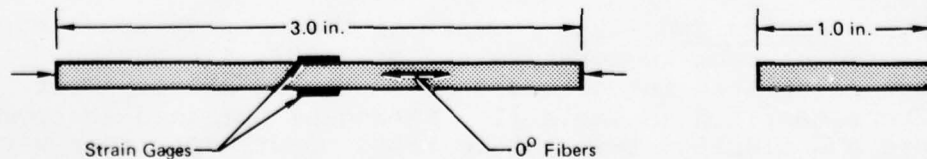
Origin of Specimens	Specimen ID	Test Conditions		Failure Conditions			Primary Modulus, E (msi)
		Temperature (°F)	Moisture Content	Compressive Stress (0°) (ksi)	Compressive Strain (0°) (μin./in.)	Mode of Failure	
PDV Stabilator							
26-Ply Compression Skin	A44 - A46	RT	Dry	100.8	7120	Block Compression	14.3
Tension Skin	A51 - A54	340	Dry	75.4	5790	Block Compression	13.8
Compression Skin	A42	RT	Maximum	99.3	7070	Block Compression	14.4
Compression Skin	A47 - A50	340	In Situ	42.0	3590	Compression, Beam-Column	12.9
Tension Skin	A58 - A61	340	In Situ	53.0	4350	Block Compression	13.1
Compression Skin	A41, A43, A62	340	Maximum	50.5	8140	Compression, Beam Column	18.4
Tension Skin	A55 - A57	340	Maximum	23.0	1490	Compression, Beam Column	16.0
Eagle 14 Stabilator							
26-Ply Compression Skin	A13 - A15	340	Dry	67.8	5260	Block Compression	13.7
Tension Skin	A30 - A32	340	Dry	67.4	5220	Block Compression	13.7
Compression Skin	A18 - A20	340	In Situ	43.2	3720	Compression, Beam-Column	13.0
Tension Skin	A38 - A40	340	In Situ	59.5	4800	Block Compression	13.0
Compression Skin	A16, A17	340	Eagle 14	17.1	1610	Beam-Column	—
Tension Skin	A36, A37	340	Eagle 14	19.9	2000	Beam-Column	—
Compression Skin	A10 - A12	340	Maximum	52.9	3890	Compression, Beam Column	16.3
Tension Skin	A33 - A35	340	Maximum	16.5	1620	Beam-Column	—
20-Ply Compression Skin	A7 - A9	340	In Situ	36.2	2760	Compression, Beam-Column	13.5
Tension Skin	A27 - A29	340	In Situ	45.3	2980	Compression, Beam-Column	13.7
Compression Skin	A4 - A6	340	Eagle 14	51.4	3250	Block Compression	19.8
Tension Skin	A24 - A26	340	Eagle 14	52.5	3710	Block Compression	19.0
Compression Skin	A1 - A3	340	Maximum	35.5	2280	Compression, Beam Column	21.3
Tension Skin	A21 - A23	340	Maximum	73.1	4730	Block Compression	19.3
30-Ply Tension Skin (Residual Compression)	D1 - D3	340	Maximum	60.2	4120	Compression, Beam Column	18.9

3.0 in.

1.0 in.

Strain Gages

0° Fibers



GP79-0016-6

AD-A076 493

MCDONNELL AIRCRAFT CO ST LOUIS MO

F/6 11/4

EFFECT OF SERVICE ENVIRONMENT ON F-15 BORON/EPOXY STABILATOR.(U)

JUN 79 T V HINKLE

F33615-77-C-3124

UNCLASSIFIED

AFFDL-TR-79-3072

NL

2 OF 2  
ADA  
076493



END  
DATE  
FILMED  
11-80  
DTIC

the result of variable beam-column loads, induced by the test fixture, acting in conjunction with moisture-reduced interlaminar shear properties. The failure mode of specimens under beam-column loadings was delamination at locations of maximum shears.

Results of elevated temperature tests are presented in Figure 50 along with design stress levels in the skin. Results of bonded joint compression tests are also presented in this figure. During the moisture-conditioning prior to these tests, specimens which were machined from tension skins exhibited higher moisture contents and greater scatter in moisture contents than their compression skin counterparts. This may have been caused by micro-cracks in the epoxy resin which occurred in tension skins during the stabilator static tests. The element tests were conducted when compression-skin specimens reached the desired moisture contents, so tension-skin specimens were tested at higher moisture levels. Of data points falling below the design stress line in Figure 50, three of four are from tension-skin specimens which had been moisture conditioned.

Three specimens (D1, D2, D3) from the Eagle 14 stabilator were cyclically loaded for 16,000 equivalent flight hours with the fatigue spectrum previously used in the design verification of the F-15 stabilator. The peak compressive strain recorded in the stabilator fatigue test was used to establish equivalent test

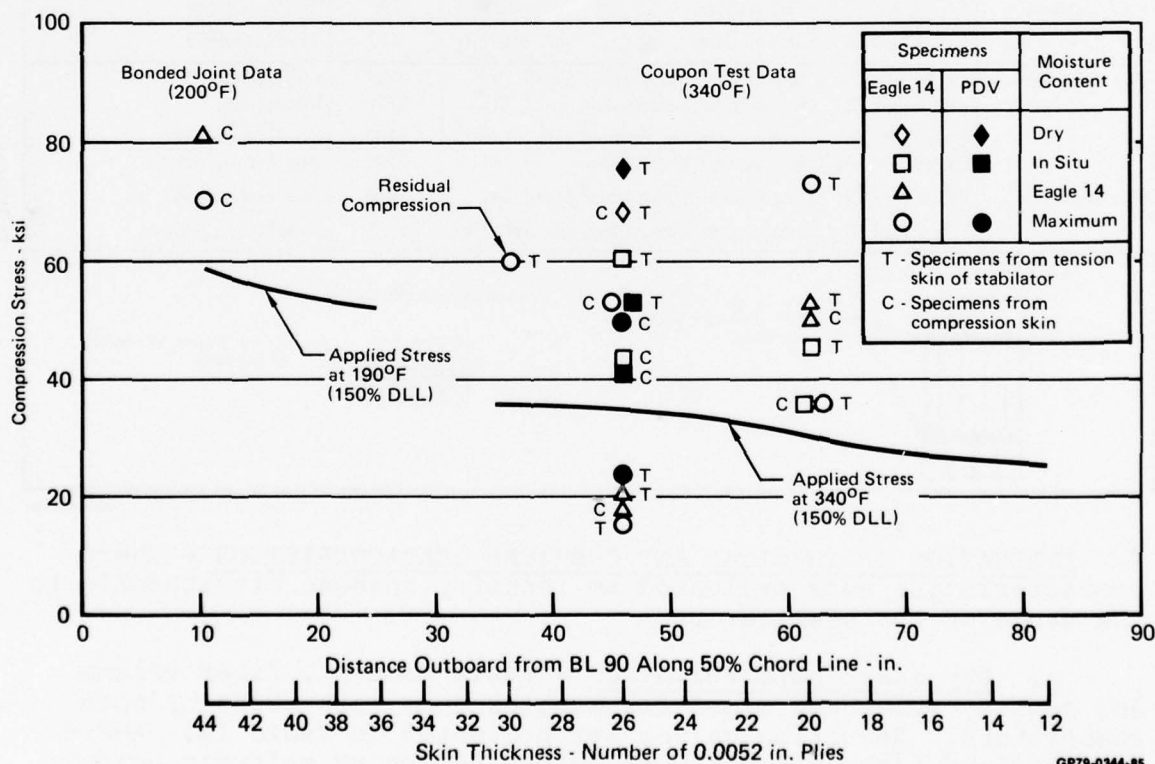


Figure 50. Compressive Strength of Boron/Epoxy Skins

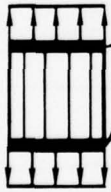
levels for these specimen tests (room temperature). Prior to the fatigue test, these specimens had been conditioned to the maximum expected moisture content. Following the fatigue tests, specimens were used for determining residual compression strengths at 340°F. The average residual strength is shown in Figure 50.

e. Flatwise Tension Specimens - Tests were conducted to assess the skin-to-core bond strength and the interlaminar tension strength of specimens machined from Eagle 14 and PDV stabilators. Average test results are presented in Table 18. The upper and lower skins of the F-15 stabilator are not parallel, and they are slightly curved in the chordwise direction. Consequently, loads applied to specimens machined from these skins were not uniformly distributed by the flat-bottomed load fixture resulting in the scatter of failure stress levels shown in this table. Interlaminar tension strengths are considered representative of values for AVCO 5505. There was no significant effect of moisture content on failure stress.

**TABLE 18. RESULTS OF FLATWISE TENSION TESTS**


Specimen Origin	Specimen ID	Type of Test (R.T.)	Moisture Content	Failure Conditions (R.T.)	
				Stress (psi)	Mode of Failure
Eagle 14 Stabilator	F4, F5, F6	Skin-to-Core	Dry	500	Skin/Core and Skin/Fixture Bonds
	F1, F2, F3	Skin-to-Core	In Situ	860	Skin/Core Bond
PDV Stabilator	F7, F8, F9	Skin-to-Core	Dry	370	Skin/Core Bond
	F10, F11, F12	Skin-to-Core	In Situ	410	Skin/Core Bond
Eagle 14 Stabilator	E3, E4, E7	Interlaminar, Compression Skin	Dry	2240	Interlaminar
	E10, E19, E20	Interlaminar, Tension Skin	Dry	2710	Interlaminar
PDV Stabilator	E1, E2, E5, E6	Interlaminar, Compression Skin	In Situ	2400	Skin/Fixture Bond
	E8, E9, E11, E12	Interlaminar, Tension Skin	In Situ	2200	Skin/Fixture Bond
PDV Stabilator	E13, E14, E15	Interlaminar, Compression Skin	Dry	1880	Skin/Fixture Bond
	E16, E17, E18	Interlaminar, Compression Skin	In Situ	2390	Skin/Fixture Bond

Skin-to-Core Tension (F)



2.0 in. Diameter Section of the Skin

Interlaminar Tension (E)



2.0 in. Diameter Section of the Skin

GP79-0344-80

3. EVALUATION OF PHYSICAL AND CHEMICAL CHARACTERISTICS - These characteristics were evaluated to identify changes attributable to the usage of the stabilators.

a. Physical Characteristics - Resin content, fiber volume and density were determined for samples from both skins of both stabilators. Resulting values are presented in Table 19. Resin contents and fiber volumes were determined using sulfuric acid digestion techniques. Densities were determined by weighing samples in air and in water and calculating the weight per unit of



**TABLE 19. PHYSICAL PROPERTIES**

Skin Location		Resin Content (% by Weight)	Fiber Volume (% by Volume)	Density (lb/in. <sup>3</sup> )
Typical Values from In-House Tests		28 to 30	56 to 54	0.072 to 0.075
Eagle 14	14-Ply Tension Skin	30.0	54.8	0.073
	20-Ply Tension Skin	28.3	55.9	0.073
	28-Ply Tension Skin	28.8	55.1	0.072
	36-Ply Tension Skin	28.3	55.8	0.072
	14-Ply Compression Skin	28.2	56.9	0.074
	20-Ply Compression Skin	26.9	57.9	0.074
	36-Ply Compression Skin	28.1	56.7	0.073
	42-Ply Compression Skin*	30.9	53.9	0.072
PDV	26-Ply Tension Skin	29.4	54.4	0.072
	14-Ply Compression Skin	28.5	56.3	0.073
	26-Ply Compression Skin	30.4	54.0	0.072
	36-Ply Compression Skin	31.2	52.9	0.072

\*Average of 2 measurements for this location. Average of 4 measurements is shown for all other locations.

GP79-0344-73

volume displaced. Most values agree with the cured resin contents, fiber volumes and densities typically measured in production boron/epoxy components.

During moisture conditioning, differences were noticed between the moisture contents of structural specimens from tension and compression skins. Specimens from tension skins exhibited higher moisture contents. It was postulated that this was due to the presence of microcracks in the resin which occurred during the stabilator tests. To examine for surface cracks, the paint was first removed from selected Eagle 14 skin samples, and the surfaces of samples from both stabilators were then examined at magnifications up to 2000X. Numerous microcrack and microvoid indications were found on all samples; however, these may be attributed to the removal of the peel ply prior to stabilator painting.

Metallographic examinations of skin cross sections were also conducted in which the outer three plies were inspected for microcracks using magnifications to 600X. Crack indications were found in all sections examined; however, some of these may be scratches left from the specimen polishing operation. Crack indications did not traverse one ply but extended from a fiber to either surface of that ply. The highest density of these indications occurred in the surface ply of the Eagle 14 tension skin.

b. Chemical Characteristics - Chemical analyses were based on techniques sensitive to resin chemistry yet not requiring dissolution of the epoxy in a solvent. The AVCO 5505 system, like most epoxies, has limited solubility due to the high degree of crosslinking. For these tests samples from the Eagle 14 and PDV stabilators were evaluated in conjunction with baseline samples from a panel fabricated from AVCO 5505.

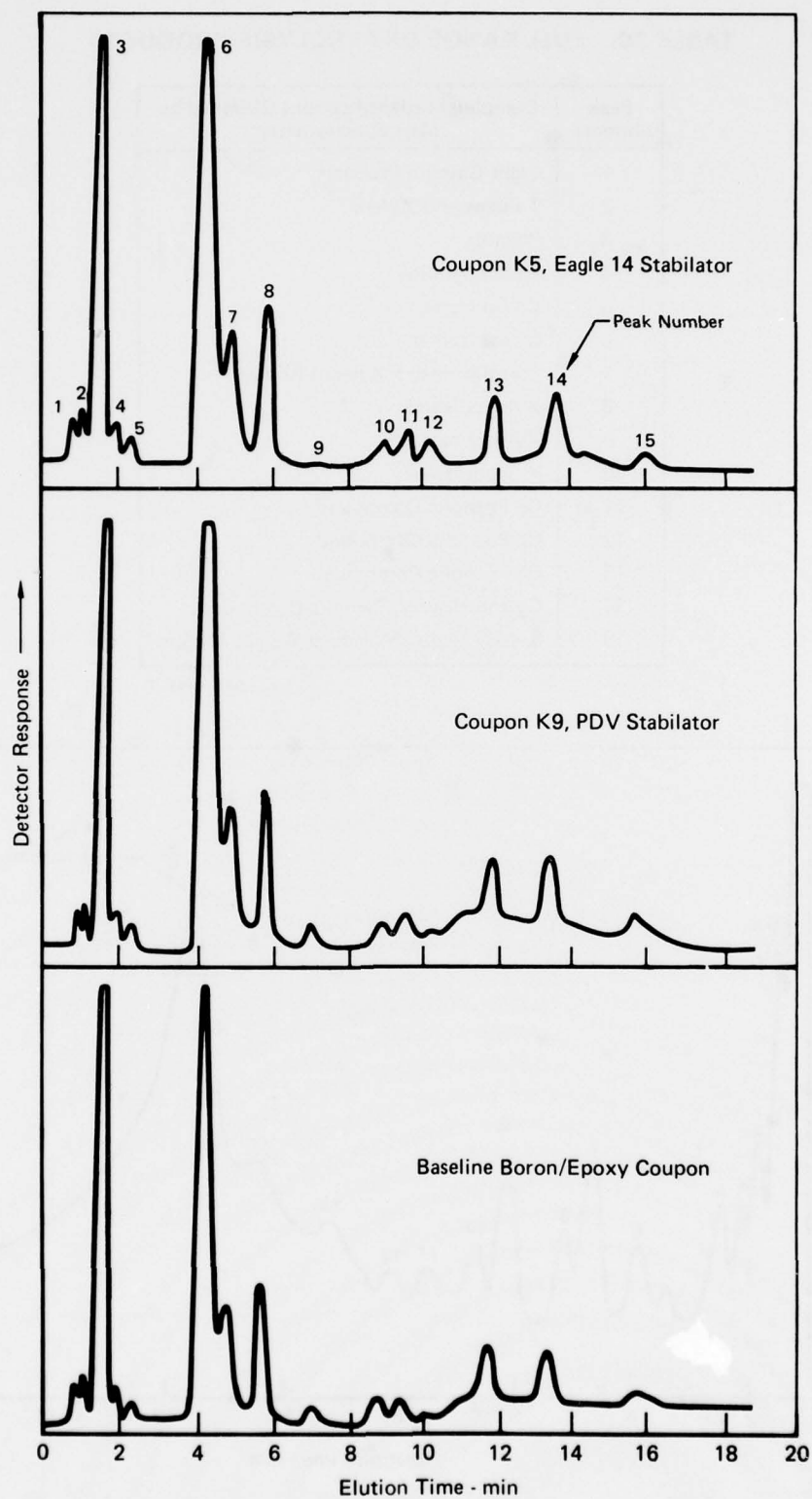
Glass transition temperatures ( $T_g$ ) were measured by differential scanning calorimetry. This transition temperature measures the point at which the epoxy changes from a glass-like to a rubbery material; however, this change in boron/epoxy does not occur at a well-defined temperature but rather within the 200°-225°C range (dry specimens). All samples exhibited  $T_g$ 's within this range.

A well-defined temperature for epoxies is the peak exotherm temperature, which occurs at maximum energy release during thermal degradation. This temperature was measured in samples heated at 5°C/minute, 10°C/minute and 20°C/minute in a nitrogen atmosphere to a maximum temperature of 500°C. The peak exotherm temperature occurred in baseline samples at 346°C, 356°C, and 375°C. All samples from Eagle 14 and PDV stabilators exhibited temperatures within  $\pm 4^\circ\text{C}$  of these values.

Thermogravimetric analyses were used to compare weight losses during thermal degradation. Samples were heated at 10°C/ minute to 600°C in a nitrogen atmosphere. Weight loss was determined as a percent of the initial sample weight. The measured weight losses are: baseline, 22.5%; Eagle 14, 21.4%; and PDV, 21.8%. Only differences exceeding 5% are significant.

Pyrolysis is a controlled high-temperature thermal shock that fragments polymeric materials into characteristic products. These fragments, as identified by gas chromatography (GC) and mass spectroscopy (MS), are related to the chemical composition of the polymer. The pyrolysis GC/MS analyses of Eagle 14, PDV, and baseline samples were performed at 620°C. The resulting pyrolysis products were first separated on a GC column that allowed detection of the full-range of products. Next, samples were again pyrolyzed, and the products were separated on a second GC column that allowed identification of the light (gaseous) pyrolysis products.

The full range of pyrolysis products along with the light gaseous products were characterized by mass spectroscopy as each component eluted from the gas chromatography column. The pyrograms of the full range of products are shown in Figure 51. All pyrolysis fingerprints were identical. Pyrolysis products associated with these fingerprints are shown in Table 20. Light gaseous products (Peak #1 of Figure 51) were separated by the second GC column (Figure 52) and are identified in Table 21.



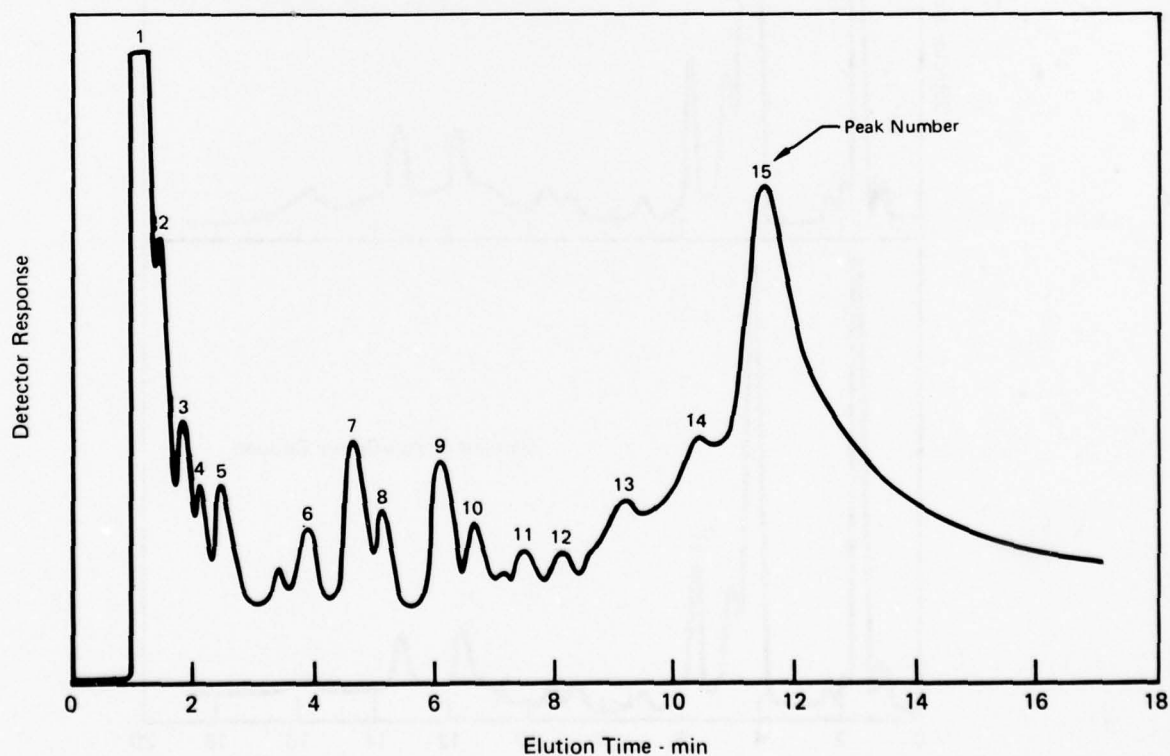
GP79-0344-74

Figure 51. Pyrograms Identifying Full Range of Pyrolysis Products

**TABLE 20. FULL RANGE OF PYROLYSIS PRODUCTS**

Peak Number	Component Identifications Obtained by Mass Spectrometry
1	Light Gaseous Products
2	Toluene and Xylene
3	Phenol
4	Methyl Aniline
5	Cresol Isomer
6	Cresol Isomer
7	Cresol Isomer + Xylenol Isomer
8	Xylenol Isomer
9	Xylenol Isomer
10	Xylenol Isomer
11	Cg Phenolic Compound
12	Cg Phenolic Compound
13	Cg Phenolic Compound
14	Cg and Heavier Phenolic Compounds
15	Several Higher Molecular Weight Phenols

GP79-0344-72



GP79-0344-75

**Figure 52. Pyrogram Identifying Light Gaseous Products**



**TABLE 21. LIGHT GASEOUS PYROLYSIS PRODUCTS**

Peak Number	Component Identification Obtained by Mass Spectrometry
1	Carbon Monoxide
2	Methane
3	Carbon Dioxide
4	Ethylene
5	Ethane
6	Water
7	Propylene
8	Methyl Chloride
9	Methanol
10	2-Butyne
11	Ethyl Chloride
12	Ethanol
13	Acetone
14	2-Propanol
15	Propanol

GP79-0344-71

## SECTION VII

### CONCLUSIONS

1. No defects occurred in boron/epoxy skins or skin splices of the Eagle 14 stabilator as a result of environmental exposure.
2. The strength capability of boron/epoxy skins and skin splices had not degraded as a result of exposures to environmental extremes or service life loadings. In static tests, strains were achieved in boron/epoxy skins which exceeded strain levels demonstrated in previous design verification testing of the F-15 stabilator.
3. The analytic methodology exists for accurately predicting moisture contents. Predictions were made by evaluating the environmental histories of the test articles and were corroborated by moisture contents measured in test article skins at the conclusion of static tests.
4. The strength capabilities of boron/epoxy skins and skin splices on the F-15 stabilator are adequate for static loads occurring under the most severe combinations of realistic skin temperatures and skin moisture contents.
5. No changes occurred in physical or chemical characteristics of the epoxy resin.

## APPENDIX A

### EAGLE 14 ENVIRONMENTAL HISTORY

Data in this appendix comprise the environmental history of the Eagle 14 stabilator from the completion of torque box fabrication to the dissection of boron/epoxy skins following the Eagle 14 static test. These data consist of latitude and longitude of bases associated with the deployment of Ship 14 and surface weather data recorded at these bases during the deployment period. Weather data included are: site factor, ambient temperature (TA), ambient relative humidity (HA), mean cloud cover (MCC), wind speed (VW), frequency of precipitation (P), and duration of these weather data. Indoor exposure periods are denoted by "-99" in the cloud cover column and temperatures and humidities for these periods have been adjusted from outside ambient conditions.

Edwards AFB, California (1 July 1974 - 13 July 1974)

El Centro NAS, California (13 July 1974 - 22 July 1974)

Edwards AFB, California (22 July 1974 - 27 July 1974)

El Centro NAS, California (27 July 1974 - 2 August 1974)

Edwards AFB, California (2 August 1974 - 5 August 1974)



Eglin AFB, Florida (30 September 1974 - 29 November 1974)

	0	1	2	3	4	5	6	7	8	9	10	11	12	13	14	15	16	17	18	19	20	21	22	23	24	25	26	27	28	29	30	31	32	33	34	35	36	37	38	39	40	41	42	43	44	45	46	47	48	49	50	51	52	53	54	55	56	57	58	59	60	61	62	63	64	65	66	67	68	69	70	71	72	73	74	75	76	77	78	79	80	81	82	83	84	85	86	87	88	89	90	91	92	93	94	95	96	97	98	99	100	101	102	103	104	105	106	107	108	109	110	111	112	113	114	115	116	117	118	119	120	121	122	123	124	125	126	127	128	129	130	131	132	133	134	135	136	137	138	139	140	141	142	143	144	145	146	147	148	149	150	151	152	153	154	155	156	157	158	159	160	161	162	163	164	165	166	167	168	169	170	171	172	173	174	175	176	177	178	179	180	181	182	183	184	185	186	187	188	189	190	191	192	193	194	195	196	197	198	199	200	201	202	203	204	205	206	207	208	209	210	211	212	213	214	215	216	217	218	219	220	221	222	223	224	225	226	227	228	229	230	231	232	233	234	235	236	237	238	239	240	241	242	243	244	245	246	247	248	249	250	251	252	253	254	255	256	257	258	259	260	261	262	263	264	265	266	267	268	269	270	271	272	273	274	275	276	277	278	279	280	281	282	283	284	285	286	287	288	289	290	291	292	293	294	295	296	297	298	299	300	301	302	303	304	305	306	307	308	309	310	311	312	313	314	315	316	317	318	319	320	321	322	323	324	325	326	327	328	329	330	331	332	333	334	335	336	337	338	339	340	341	342	343	344	345	346	347	348	349	350	351	352	353	354	355	356	357	358	359	360	361	362	363	364	365	366	367	368	369	370	371	372	373	374	375	376	377	378	379	380	381	382	383	384	385	386	387	388	389	390	391	392	393	394	395	396	397	398	399	400	401	402	403	404	405	406	407	408	409	410	411	412	413	414	415	416	417	418	419	420	421	422	423	424	425	426	427	428	429	430	431	432	433	434	435	436	437	438	439	440	441	442	443	444	445	446	447	448	449	450	451	452	453	454	455	456	457	458	459	460	461	462	463	464	465	466	467	468	469	470	471	472	473	474	475	476	477	478	479	480	481	482	483	484	485	486	487	488	489	490	491	492	493	494	495	496	497	498	499	500	501	502	503	504	505	506	507	508	509	510	511	512	513	514	515	516	517	518	519	520	521	522	523</
--	---	---	---	---	---	---	---	---	---	---	----	----	----	----	----	----	----	----	----	----	----	----	----	----	----	----	----	----	----	----	----	----	----	----	----	----	----	----	----	----	----	----	----	----	----	----	----	----	----	----	----	----	----	----	----	----	----	----	----	----	----	----	----	----	----	----	----	----	----	----	----	----	----	----	----	----	----	----	----	----	----	----	----	----	----	----	----	----	----	----	----	----	----	----	----	----	----	----	----	----	-----	-----	-----	-----	-----	-----	-----	-----	-----	-----	-----	-----	-----	-----	-----	-----	-----	-----	-----	-----	-----	-----	-----	-----	-----	-----	-----	-----	-----	-----	-----	-----	-----	-----	-----	-----	-----	-----	-----	-----	-----	-----	-----	-----	-----	-----	-----	-----	-----	-----	-----	-----	-----	-----	-----	-----	-----	-----	-----	-----	-----	-----	-----	-----	-----	-----	-----	-----	-----	-----	-----	-----	-----	-----	-----	-----	-----	-----	-----	-----	-----	-----	-----	-----	-----	-----	-----	-----	-----	-----	-----	-----	-----	-----	-----	-----	-----	-----	-----	-----	-----	-----	-----	-----	-----	-----	-----	-----	-----	-----	-----	-----	-----	-----	-----	-----	-----	-----	-----	-----	-----	-----	-----	-----	-----	-----	-----	-----	-----	-----	-----	-----	-----	-----	-----	-----	-----	-----	-----	-----	-----	-----	-----	-----	-----	-----	-----	-----	-----	-----	-----	-----	-----	-----	-----	-----	-----	-----	-----	-----	-----	-----	-----	-----	-----	-----	-----	-----	-----	-----	-----	-----	-----	-----	-----	-----	-----	-----	-----	-----	-----	-----	-----	-----	-----	-----	-----	-----	-----	-----	-----	-----	-----	-----	-----	-----	-----	-----	-----	-----	-----	-----	-----	-----	-----	-----	-----	-----	-----	-----	-----	-----	-----	-----	-----	-----	-----	-----	-----	-----	-----	-----	-----	-----	-----	-----	-----	-----	-----	-----	-----	-----	-----	-----	-----	-----	-----	-----	-----	-----	-----	-----	-----	-----	-----	-----	-----	-----	-----	-----	-----	-----	-----	-----	-----	-----	-----	-----	-----	-----	-----	-----	-----	-----	-----	-----	-----	-----	-----	-----	-----	-----	-----	-----	-----	-----	-----	-----	-----	-----	-----	-----	-----	-----	-----	-----	-----	-----	-----	-----	-----	-----	-----	-----	-----	-----	-----	-----	-----	-----	-----	-----	-----	-----	-----	-----	-----	-----	-----	-----	-----	-----	-----	-----	-----	-----	-----	-----	-----	-----	-----	-----	-----	-----	-----	-----	-----	-----	-----	-----	-----	-----	-----	-----	-----	-----	-----	-----	-----	-----	-----	-----	-----	-----	-----	-----	-----	-----	-----	-----	-----	-----	-----	-----	-----	-----	-----	-----	-----	-----	-----	-----	-----	-----	-----	-----	-----	-----	-----	-----	-----	-----	-----	-----	-----	-----	-----	-----	-----	-----	-----	-----	-----	-----	-----	-----	-----	-----	-----	-----	-----	-----	-----	-----	-----	-----	-----	-----	-----	-----	-----	-----	-----	-----	-----	-----	-----	-----	-----	-----	-----	-----	-----	-----	-----	-----	-----	-----	-----	-----	-----	-----	-----	-------



Edwards AFB, California (1 September 1975 - 13 February 1976)

**Is AFB, California (13 June 1975 - 1 September 1975)**



[illegible]



St. Louis, Missouri (1 January 1978 - 21 February 1978)

LAT.	LONG.	SITE	TIME	TA	AMBIENT WEATHER DATA	P	DURATION
°	°		MUN.	(°C)	(°C)	(°C)	(HRS)
38.75	90.33	00	0000	00.0	00.0	0.00	00
38.75	90.33	00	0100	00.0	00.0	0.00	00
38.75	90.33	00	0200	00.0	00.0	0.00	00
38.75	90.33	00	0300	00.0	00.0	0.00	00
38.75	90.33	00	0400	00.0	00.0	0.00	00
38.75	90.33	00	0500	00.0	00.0	0.00	00
38.75	90.33	00	0600	00.0	00.0	0.00	00
38.75	90.33	00	0700	00.0	00.0	0.00	00
38.75	90.33	00	0800	00.0	00.0	0.00	00
38.75	90.33	00	0900	00.0	00.0	0.00	00
38.75	90.33	00	1000	00.0	00.0	0.00	00
38.75	90.33	00	1100	00.0	00.0	0.00	00
38.75	90.33	00	1200	00.0	00.0	0.00	00
38.75	90.33	00	1300	00.0	00.0	0.00	00
38.75	90.33	00	1400	00.0	00.0	0.00	00
38.75	90.33	00	1500	00.0	00.0	0.00	00
38.75	90.33	00	1600	00.0	00.0	0.00	00
38.75	90.33	00	1700	00.0	00.0	0.00	00
38.75	90.33	00	1800	00.0	00.0	0.00	00
38.75	90.33	00	1900	00.0	00.0	0.00	00
38.75	90.33	00	2000	00.0	00.0	0.00	00
38.75	90.33	00	2100	00.0	00.0	0.00	00

## APPENDIX B

### PDV ENVIRONMENTAL HISTORY

Data in this appendix comprise the environmental history of the PDV stabilator from completion of torque box fabrication to the dissection of the boron/epoxy skins following the PDV static test. These data consist of the latitude and longitude for St. Louis, Missouri, and surface weather data recorded in St. Louis over the period of the environmental history. Weather data are: site factor, ambient temperature (TA), ambient relative humidity (HA), mean cloud cover (MCC), wind speed (VW), frequency of precipitation (P), and duration of these weather data. Indoor exposure periods are denoted by "-99" in the cloud cover column and temperatures and humidities for these periods have been adjusted from outside ambient conditions.

St. Louis, Missouri  
(Indoor Exposures, 1 January 1972 - 1 January 1973)

(Indoor Exposures, 20 May 1971 - 1 January 1972)

[illegible][illegible]

(Indoor Exposures, 1 January 1973 - 1 January 1974)

(Indoor Exposures, 1 January 1974 - 1 January 1975)

[illegible]



St. Louis, Missouri

(Indoor Exposures, 1 January 1975 - 1 January 1976)

[illegible]

St. Louis, Missouri

(Indoor Exposures, 1 January 1976 - 1 January 1977)

[illegible]

St. Louis, Missouri  
(Indoor Exposures, 1 January 1978 - 30 March 1978)

[illegible]

St. Louis, Missouri  
(Indoor Exposures, 1 January 1977 ~ 1 January 1978)

[illegible]

## APPENDIX C

### BASE WEATHER DATA FOR PROJECTED F-15 DEPLOYMENTS

Data in this appendix consist of geographic locations of bases included in F-15 deployment projections and averages of surface weather data recorded at these bases. Bases are listed alphabetically by country then by city or base name. Weather data consist of site factor, ambient temperature (TA), ambient relative humidity (HA), mean cloud cover (MCC), wind speed (VW), and frequency of precipitation (P). Duration of these data is taken as the length of the month under which they are listed.

Soesterburg AB, Netherlands

Kadena AB, Okinawa (Japan)

[illegible]



## Kunsan AB, South Korea

0 1 2 3 4 5 6 7 8 9 10 11 12 13 14 15 16 17 18 19 20 21 22 23 24 25 26 27 28 29 30 31 32 33 34 35 36 37 38 39 40 41 42 43 44 45 46 47 48 49 50 51 52 53 54 55 56 57 58 59 60 61 62 63 64 65 66 67 68 69 70 71 72 73 74 75 76 77 78 79 80 81 82 83 84 85 86 87 88 89 90 91 92 93 94 95 96 97 98 99 100 101 102 103 104 105 106 107 108 109 110 111 112 113 114 115 116 117 118 119 120 121 122 123 124 125 126 127 128 129 130 131 132 133 134 135 136 137 138 139 140 141 142 143 144 145 146 147 148 149 150 151 152 153 154 155 156 157 158 159 160 161 162 163 164 165 166 167 168 169 170 171 172 173 174 175 176 177 178 179 180 181 182 183 184 185 186 187 188 189 190 191 192 193 194 195 196 197 198 199 200 201 202 203 204 205 206 207 208 209 210 211 212 213 214 215 216 217 218 219 220 221 222 223 224 225 226 227 228 229 230 231 232 233 234 235 236 237 238 239 240 241 242 243 244 245 246 247 248 249 250 251 252 253 254 255 256 257 258 259 260 261 262 263 264 265 266 267 268 269 270 271 272 273 274 275 276 277 278 279 280 281 282 283 284 285 286 287 288 289 290 291 292 293 294 295 296 297 298 299 300 301 302 303 304 305 306 307 308 309 310 311 312 313 314 315 316 317 318 319 320 321 322 323 324 325 326 327 328 329 330 331 332 333 334 335 336 337 338 339 340 341 342 343 344 345 346 347 348 349 350 351 352 353 354 355 356 357 358 359 360 361 362 363 364 365 366 367 368 369 370 371 372 373 374 375 376 377 378 379 380 381 382 383 384 385 386 387 388 389 390 391 392 393 394 395 396 397 398 399 400 401 402 403 404 405 406 407 408 409 410 411 412 413 414 415 416 417 418 419 420 421 422 423 424 425 426 427 428 429 430 431 432 433 434 435 436 437 438 439 440 441 442 443 444 445 446 447 448 449 450 451 452 453 454 455 456 457 458 459 460 461 462 463 464 465 466 467 468 469 470 471 472 473 474 475 476 477 478 479 480 481 482 483 484 485 486 487 488 489 490 491 492 493 494 495 496 497 498 499 500 501 502 503 504 505 506 507 508 509 510 511 512 513 514 515 516 517 518 519 520 521 522 523 524 525 526 527 528 529 530 531 532 533 534 535 536 537 538 539 540 541 542 543 544 545 546 547 548 549 550 551 552 553 554 555 556 557 558 559 560 561 562 563 564 565 566 567 568 569 570 571 572 573 574 575 576 577 578 579 580 581 582 583 584 585 586 587 588 589 590 591 592 593 594 595 596 597 598 599 600 601 602 603 604 605 606 607 608 609 610 611 612 613 614 615 616 617 618 619 620 621 622 623 624 625 626 627 628 629 630 631 632 633 634 635 636 637 638 639 640 641 642 643 644 645 646 647 648 649 650 651 652 653 654 655 656 657 658 659 660 661 662 663 664 665 666 667 668 669 670 671 672 673 674 675 676 677 678 679 680 681 682 683 684 685 686 687 688 689 690 691 692 693 694 695 696 697 698 699 700 701 702 703 704 705 706 707 708 709 710 711 712 713 714 715 716 717 718 719 720 721 722 723 724 725 726 727 728 729 730 731 732 733 734 735 736 737 738 739 740 741 742 743 744 745 746 747 748 749 750 751 752 753 754 755 756 757 758 759 760 761 762 763 764 765 766 767 768 769 770 771 772 773 774 775 776 777 778 779 780 781 782 783 784 785 786 787 788 789 790 791 792 793 794 795 796 797 798 799 800 801 802 803 804 805 806 807 808 809 810 811 812 813 814 815 816 817 818 819 820 821 822 823 824 825 826 827 828 829 830 831 832 833 834 835 836 837 838 839 840 841 842 843 844 845 846 847 848 849 850 851 852 853 854 855 856 857 858 859 860 861 862 863 864 865 866 867 868 869 870 871 872 873 874 875 876 877 878 879 880 881 882 883 884 885 886 887 888 889 890 891 892 893 894 895 896 897 898 899 900 901 902 903 904 905 906 907 908 909 910 911 912 913 914 915 916 917 918 919 920 921 922 923 924 925 926 927 928 929 930 931 932 933 934 935 936 937 938 939 940 941 942 943 944 945 946 947 948 949 950 951 952 953 954 955 956 957 958 959 960 961 962 963 964 965 966 967 968 969 970 971 972 973 974 975 976 977 978 979 980 981 982 983 984 985 986 987 988 989 990 991 992 993 994 995 996 997 998 999 1000 1001 1002 1003 1004 1005 1006 1007 1008 1009 1010 1011 1012 1013 1014 1015 1016 1017 1018 1019 1020 1021 1022 1023 1024 1025 1026 1027 1028 1029 1030 1031 1032 1033 1034 1035 1036 1037 1038 1039 1

## Clark AB, Philippines

[illegible]

## Torrejon AB, Spain

OP	1	2	3	4	5	6	7	8	9	10	11	12	13	14	15	16	17	18	19	20	21	22	23	24	25	26	27	28	29	30	31	32	33	34	35	36	37	38	39	40	41	42	43	44	45	46	47	48	49	50	51	52	53	54	55	56	57	58	59	60	61	62	63	64	65	66	67	68	69	70	71	72	73	74	75	76	77	78	79	80	81	82	83	84	85	86	87	88	89	90	91	92	93	94	95	96	97	98	99	100	101	102	103	104	105	106	107	108	109	110	111	112	113	114	115	116	117	118	119	120	121	122	123	124	125	126	127	128	129	130	131	132	133	134	135	136	137	138	139	140	141	142	143	144	145	146	147	148	149	150	151	152	153	154	155	156	157	158	159	160	161	162	163	164	165	166	167	168	169	170	171	172	173	174	175	176	177	178	179	180	181	182	183	184	185	186	187	188	189	190	191	192	193	194	195	196	197	198	199	200	201	202	203	204	205	206	207	208	209	210	211	212	213	214	215	216	217	218	219	220	221	222	223	224	225	226	227	228	229	230	231	232	233	234	235	236	237	238	239	240	241	242	243	244	245	246	247	248	249	250	251	252	253	254	255	256	257	258	259	260	261	262	263	264	265	266	267	268	269	270	271	272	273	274	275	276	277	278	279	280	281	282	283	284	285	286	287	288	289	290	291	292	293	294	295	296	297	298	299	300	301	302	303	304	305	306	307	308	309	310	311	312	313	314	315	316	317	318	319	320	321	322	323	324	325	326	327	328	329	330	331	332	333	334	335	336	337	338	339	340	341	342	343	344	345	346	347	348	349	350	351	352	353	354	355	356	357	358	359	360	361	362	363	364	365	366	367	368	369	370	371	372	373	374	375	376	377	378	379	380	381	382	383	384	385	386	387	388	389	390	391	392	393	394	395	396	397	398	399	400	401	402	403	404	405	406	407	408	409	410	411	412	413	414	415	416	417	418	419	420	421	422	423	424	425	426	427	428	429	430	431	432	433	434	435	436	437	438	439	440	441	442	443	444	445	446	447	448	449	450	451	452	453	454	455	456	457	458	459	460	461	462	463	464	465	466	467	468	469	470	471	472	473	474	475	476	477	478	479	480	481	482	483	484	485	486	487	488	489	490	491	492	493	494	495	496	497	498	499	500	501	502	503	504	505	506	507	508	509	510	511	512	513	514	515	516	517	518	519	520	521	522	523	524
----	---	---	---	---	---	---	---	---	---	----	----	----	----	----	----	----	----	----	----	----	----	----	----	----	----	----	----	----	----	----	----	----	----	----	----	----	----	----	----	----	----	----	----	----	----	----	----	----	----	----	----	----	----	----	----	----	----	----	----	----	----	----	----	----	----	----	----	----	----	----	----	----	----	----	----	----	----	----	----	----	----	----	----	----	----	----	----	----	----	----	----	----	----	----	----	----	----	----	----	-----	-----	-----	-----	-----	-----	-----	-----	-----	-----	-----	-----	-----	-----	-----	-----	-----	-----	-----	-----	-----	-----	-----	-----	-----	-----	-----	-----	-----	-----	-----	-----	-----	-----	-----	-----	-----	-----	-----	-----	-----	-----	-----	-----	-----	-----	-----	-----	-----	-----	-----	-----	-----	-----	-----	-----	-----	-----	-----	-----	-----	-----	-----	-----	-----	-----	-----	-----	-----	-----	-----	-----	-----	-----	-----	-----	-----	-----	-----	-----	-----	-----	-----	-----	-----	-----	-----	-----	-----	-----	-----	-----	-----	-----	-----	-----	-----	-----	-----	-----	-----	-----	-----	-----	-----	-----	-----	-----	-----	-----	-----	-----	-----	-----	-----	-----	-----	-----	-----	-----	-----	-----	-----	-----	-----	-----	-----	-----	-----	-----	-----	-----	-----	-----	-----	-----	-----	-----	-----	-----	-----	-----	-----	-----	-----	-----	-----	-----	-----	-----	-----	-----	-----	-----	-----	-----	-----	-----	-----	-----	-----	-----	-----	-----	-----	-----	-----	-----	-----	-----	-----	-----	-----	-----	-----	-----	-----	-----	-----	-----	-----	-----	-----	-----	-----	-----	-----	-----	-----	-----	-----	-----	-----	-----	-----	-----	-----	-----	-----	-----	-----	-----	-----	-----	-----	-----	-----	-----	-----	-----	-----	-----	-----	-----	-----	-----	-----	-----	-----	-----	-----	-----	-----	-----	-----	-----	-----	-----	-----	-----	-----	-----	-----	-----	-----	-----	-----	-----	-----	-----	-----	-----	-----	-----	-----	-----	-----	-----	-----	-----	-----	-----	-----	-----	-----	-----	-----	-----	-----	-----	-----	-----	-----	-----	-----	-----	-----	-----	-----	-----	-----	-----	-----	-----	-----	-----	-----	-----	-----	-----	-----	-----	-----	-----	-----	-----	-----	-----	-----	-----	-----	-----	-----	-----	-----	-----	-----	-----	-----	-----	-----	-----	-----	-----	-----	-----	-----	-----	-----	-----	-----	-----	-----	-----	-----	-----	-----	-----	-----	-----	-----	-----	-----	-----	-----	-----	-----	-----	-----	-----	-----	-----	-----	-----	-----	-----	-----	-----	-----	-----	-----	-----	-----	-----	-----	-----	-----	-----	-----	-----	-----	-----	-----	-----	-----	-----	-----	-----	-----	-----	-----	-----	-----	-----	-----	-----	-----	-----	-----	-----	-----	-----	-----	-----	-----	-----	-----	-----	-----	-----	-----	-----	-----	-----	-----	-----	-----	-----	-----	-----	-----	-----	-----	-----	-----	-----	-----	-----	-----	-----	-----	-----	-----	-----	-----	-----	-----	-----	-----	-----	-----	-----	-----	-----	-----	-----	-----	-----	-----	-----	-----	-----	-----	-----	-----

## Osan AB, South Korea

[illegible]

## ACTIVE DUTY BASES

Hahn AB, West Germany

[illegible]

Bitburg AB, West Germany

[illegible]



## Zweibruchen AB, West Germany

[illegible]

Ramstein AB, West Germany

TIME	1000	1100	1200	1300	1400	1500	1600	1700	1800	1900	2000	2100	2200	2300	2400	2500	2600	2700	2800	2900	3000	3100	3200	3300	3400	3500	3600	3700	3800	3900	4000	4100	4200	4300	4400	4500	4600	4700	4800	4900	5000	5100	5200	5300	5400	5500	5600	5700	5800	5900	6000	6100	6200	6300	6400	6500	6600	6700	6800	6900	7000	7100	7200	7300	7400	7500	7600	7700	7800	7900	8000	8100	8200	8300	8400	8500	8600	8700	8800	8900	9000	9100	9200	9300	9400	9500	9600	9700	9800	9900	10000
DATE	1000	1100	1200	1300	1400	1500	1600	1700	1800	1900	2000	2100	2200	2300	2400	2500	2600	2700	2800	2900	3000	3100	3200	3300	3400	3500	3600	3700	3800	3900	4000	4100	4200	4300	4400	4500	4600	4700	4800	4900	5000	5100	5200	5300	5400	5500	5600	5700	5800	5900	6000	6100	6200	6300	6400	6500	6600	6700	6800	6900	7000	7100	7200	7300	7400	7500	7600	7700	7800	7900	8000	8100	8200	8300	8400	8500	8600	8700	8800	8900	9000	9100	9200	9300	9400	9500	9600	9700	9800	9900	10000
WEATHER	1000	1100	1200	1300	1400	1500	1600	1700	1800	1900	2000	2100	2200	2300	2400	2500	2600	2700	2800	2900	3000	3100	3200	3300	3400	3500	3600	3700	3800	3900	4000	4100	4200	4300	4400	4500	4600	4700	4800	4900	5000	5100	5200	5300	5400	5500	5600	5700	5800	5900	6000	6100	6200	6300	6400	6500	6600	6700	6800	6900	7000	7100	7200	7300	7400	7500	7600	7700	7800	7900	8000	8100	8200	8300	8400	8500	8600	8700	8800	8900	9000	9100	9200	9300	9400	9500	9600	9700	9800	9900	10000
AMOUNT	1000	1100	1200	1300	1400	1500	1600	1700	1800	1900	2000	2100	2200	2300	2400	2500	2600	2700	2800	2900	3000	3100	3200	3300	3400	3500	3600	3700	3800	3900	4000	4100	4200	4300	4400	4500	4600	4700	4800	4900	5000	5100	5200	5300	5400	5500	5600	5700	5800	5900	6000	6100	6200	6300	6400	6500	6600	6700	6800	6900	7000	7100	7200	7300	7400	7500	7600	7700	7800	7900	8000	8100	8200	8300	8400	8500	8600	8700	8800	8900	9000	9100	9200	9300	9400	9500	9600	9700	9800	9900	10000
TA	1000	1100	1200	1300	1400	1500	1600	1700	1800	1900	2000	2100	2200	2300	2400	2500	2600	2700	2800	2900	3000	3100	3200	3300	3400	3500	3600	3700	3800	3900	4000	4100	4200	4300	4400	4500	4600	4700																																																					



Elmendorf AFB, Alaska

Eglin AFB, Florida

## HOLLoman AFB, New Mexico

Homestead AFB, Florida

[illegible]

ACTIVE DUTY BASES

Langley AFB, Virginia

Luke AFB, Arizona

DATA  
WEATHER  
TIME  
SITE

113



MacDill AFB, Florida

Moody AFB, Georgia

[illegible]



St. Louis, Missouri

115

# ACTIVE DUTY BASES

## Warner-Robins AFB, Georgia

SITE	FCU	TIME	AMHINT	MEAL	DATA
1	1	1000	1	1	1
2	2	1000	2	2	2
3	3	1000	3	3	3
4	4	1000	4	4	4
5	5	1000	5	5	5
6	6	1000	6	6	6
7	7	1000	7	7	7
8	8	1000	8	8	8
9	9	1000	9	9	9
10	10	1000	10	10	10
11	11	1000	11	11	11
12	12	1000	12	12	12
13	13	1000	13	13	13
14	14	1000	14	14	14
15	15	1000	15	15	15
16	16	1000	16	16	16
17	17	1000	17	17	17
18	18	1000	18	18	18
19	19	1000	19	19	19
20	20	1000	20	20	20
21	21	1000	21	21	21
22	22	1000	22	22	22
23	23	1000	23	23	23
24	24	1000	24	24	24
25	25	1000	25	25	25
26	26	1000	26	26	26
27	27	1000	27	27	27
28	28	1000	28	28	28
29	29	1000	29	29	29
30	30	1000	30	30	30
31	31	1000	31	31	31
32	32	1000	32	32	32
33	33	1000	33	33	33
34	34	1000	34	34	34
35	35	1000	35	35	35
36	36	1000	36	36	36
37	37	1000	37	37	37
38	38	1000	38	38	38
39	39	1000	39	39	39
40	40	1000	40	40	40
41	41	1000	41	41	41
42	42	1000	42	42	42
43	43	1000	43	43	43
44	44	1000	44	44	44
45	45	1000	45	45	45
46	46	1000	46	46	46
47	47	1000	47	47	47
48	48	1000	48	48	48
49	49	1000	49	49	49
50	50	1000	50	50	50
51	51	1000	51	51	51
52	52	1000	52	52	52
53	53	1000	53	53	53
54	54	1000	54	54	54
55	55	1000	55	55	55
56	56	1000	56	56	56
57	57	1000	57	57	57
58	58	1000	58	58	58
59	59	1000	59	59	59
60	60	1000	60	60	60
61	61	1000	61	61	61
62	62	1000	62	62	62
63	63	1000	63	63	63
64	64	1000	64	64	64
65	65	1000	65	65	65
66	66	1000	66	66	66
67	67	1000	67	67	67
68	68	1000	68	68	68
69	69	1000	69	69	69
70	70	1000	70	70	70
71	71	1000	71	71	71
72	72	1000	72	72	72
73	73	1000	73	73	73
74	74	1000	74	74	74
75	75	1000	75	75	75
76	76	1000	76	76	76
77	77	1000	77	77	77
78	78	1000	78	78	78
79	79	1000	79	79	79
80	80	1000	80	80	80
81	81	1000	81	81	81
82	82	1000	82	82	82
83	83	1000	83	83	83
84	84	1000	84	84	84
85	85	1000	85	85	85
86	86	1000	86	86	86
87	87	1000	87	87	87
88	88	1000	88	88	88
89	89	1000	89	89	89
90	90	1000	90	90	90
91	91	1000	91	91	91
92	92	1000	92	92	92
93	93	1000	93	93	93
94	94	1000	94	94	94
95	95	1000	95	95	95
96	96	1000	96	96	96
97	97	1000	97	97	97
98	98	1000	98	98	98
99	99	1000	99	99	99
100	100	1000	100	100	100





Hickam AFB, Hawaii

Kelly AFB, Texas

[illegible]



# RESERVE DUTY BASES

## New Orleans, Louisiana

## Selfridge, Michigan

TIME	DATE	AMOUNT	WEATHER	DATA
0000	01/01/77	1000	0000	0000
0100	01/01/77	1000	0000	0000
0200	01/01/77	1000	0000	0000
0300	01/01/77	1000	0000	0000
0400	01/01/77	1000	0000	0000
0500	01/01/77	1000	0000	0000
0600	01/01/77	1000	0000	0000
0700	01/01/77	1000	0000	0000
0800	01/01/77	1000	0000	0000
0900	01/01/77	1000	0000	0000
1000	01/01/77	1000	0000	0000
1100	01/01/77	1000	0000	0000
1200	01/01/77	1000	0000	0000
1300	01/01/77	1000	0000	0000
1400	01/01/77	1000	0000	0000
1500	01/01/77	1000	0000	0000
1600	01/01/77	1000	0000	0000
1700	01/01/77	1000	0000	0000
1800	01/01/77	1000	0000	0000
1900	01/01/77	1000	0000	0000
2000	01/01/77	1000	0000	0000
2100	01/01/77	1000	0000	0000
2200	01/01/77	1000	0000	0000
2300	01/01/77	1000	0000	0000
2400	01/01/77	1000	0000	0000
0000	01/02/77	1000	0000	0000
0100	01/02/77	1000	0000	0000
0200	01/02/77	1000	0000	0000
0300	01/02/77	1000	0000	0000
0400	01/02/77	1000	0000	0000
0500	01/02/77	1000	0000	0000
0600	01/02/77	1000	0000	0000
0700	01/02/77	1000	0000	0000
0800	01/02/77	1000	0000	0000
0900	01/02/77	1000	0000	0000
1000	01/02/77	1000	0000	0000
1100	01/02/77	1000	0000	0000
1200	01/02/77	1000	0000	0000
1300	01/02/77	1000	0000	0000
1400	01/02/77	1000	0000	0000
1500	01/02/77	1000	0000	0000
1600	01/02/77	1000	0000	0000
1700	01/02/77	1000	0000	0000
1800	01/02/77	1000	0000	0000
1900	01/02/77	1000	0000	0000
2000	01/02/77	1000	0000	0000
2100	01/02/77	1000	0000	0000
2200	01/02/77	1000	0000	0000
2300	01/02/77	1000	0000	0000
2400	01/02/77	1000	0000	0000
0000	01/03/77	1000	0000	0000
0100	01/03/77	1000	0000	0000
0200	01/03/77	1000	0000	0000
0300	01/03/77	1000	0000	0000
0400	01/03/77	1000	0000	0000
0500	01/03/77	1000	0000	0000
0600	01/03/77	1000	0000	0000
0700	01/03/77	1000	0000	0000
0800	01/03/77	1000	0000	0000
0900	01/03/77	1000	0000	0000
1000	01/03/77	1000	0000	0000
1100	01/03/77	1000	0000	0000
1200	01/03/77	1000	0000	0000
1300	01/03/77	1000	0000	0000
1400	01/03/77	1000	0000	0000
1500	01/03/77	1000	0000	0000
1600	01/03/77	1000	0000	0000
1700	01/03/77	1000	0000	0000
1800	01/03/77	1000	0000	0000
1900	01/03/77	1000	0000	0000
2000	01/03/77	1000	0000	0000
2100	01/03/77	1000	0000	0000
2200	01/03/77	1000	0000	0000
2300	01/03/77	1000	0000	0000
2400	01/03/77	1000	0000	0000

RESERVE DUTY BASES  
Springfield, Illinois

[illegible]

## APPENDIX D

### RESULTS OF STRUCTURAL ELEMENT TESTS

The test results presented in this appendix represent conditions at failure. Specimens are identified by numbers consistent with those shown in Figures 43 through 46. Duplicate entries of strain and modulus indicate that back-to-back strain gages were used. Specimens were conditioned to one-of-four moisture contents prior to testing.

- o dry - specimens were dried at 250° until successive weight readings indicated no further loss in weight.
- o in situ - specimens were tested upon dissection from stabilator skins with the original moisture content
- o Eagle 14 - specimens were dried then conditioned to moisture contents predicted to exist at the time of the Eagle 14 test.
- o maximum - specimens were dried then conditioned to maximum moisture contents expected for F-15 deployments.

Bonded Joint Specimen	Type of Test	Temperature (°F)	Moisture Content	Stress at Failure (ksi)	Strains at Failure (μin/in)	Primary Modulus (msi)
<u>Eagle 14 Stabilator</u>						
G1	tension	200	in situ	73.0	5450/5430	14.8/14.5
G2	tension	200	in situ	68.8	5050/5230	15.0/14.2
G3	tension	200	Eagle 14	71.7	5190/5410	14.4/13.8
G4	tension	200	Eagle 14	71.2	5480/5310	14.0/13.7
G5	tension	200	Eagle 14	73.0	5560/5320	14.5/14.2
G6	tension	200	Eagle 14	74.7	5610/5410	14.6/14.1
<u>PDV Stabilator</u>						
G10	tension	200	maximum	73.0	6160/5610	14.0/14.6
G11	tension	200	maximum	specimen broke during installation		
G12	tension	200	maximum	58.1	4660/4470	13.5/14.0
G13	tension	200	maximum	76.7	6170/6540	13.7/13.7
G14	tension	200	maximum	74.3	5880/6120	14.0/13.2
G15	tension	200	maximum	73.9	6270/5910	13.0/14.0
<u>New Specimens</u>						
N1	tension	RT	Eagle 14	83.9	6500/6770	14.9/13.2
N2	tension	RT	Eagle 14	86.1	6470/7130	14.9/12.7
N3	tension	RT	Eagle 14	83.9	6400/6830	14.9/13.2
N4	tension	200	Eagle 14	75.4	5430/6210	17.4/12.7
N5	tension	200	Eagle 14	84.5	6400/6890	16.1/13.2

<u>Bonded Joint Specimen</u>	<u>Type of Test</u>	<u>Temperature (°F)</u>	<u>Moisture Content</u>	<u>Stress at Failure (ksi)</u>	<u>Strains at Failure (μin/in)</u>	<u>Primary Modulus (msi)</u>
N6	tension	200	Eagle 14	80.5	5980/6660	16.1/12.7
N7	comp.	200	Eagle 14	88.7	5680/-	13.9/13.1
N8	comp.	200	Eagle 14	90.0	5740/8745	14.6/13.4
N9	comp.	200	Eagle 14	64.3	3200/7590	13.9/12.4
N10	tension	200	maximum	76.9	5830/6490	14.8/12.2
N11	comp.	200	maximum	69.9	3980/7260	14.2/13.4
N12	tension	200	maximum	82.2	6270/6870	15.3/12.9
N13	tension	200	maximum	81.7	6270/6730	15.3/12.8
N14	tension	317	maximum	50.7	4430/4370	13.5/11.3
N15	tension	317	maximum	51.8	4570/4190	14.5/11.4
N16	tension	317	maximum	49.4	4180/3920	13.6/11.6
N17	tension	200	dry	85.3	6310/6920	15.7/13.1
N18	tension	200	dry	89.2	6710/7280	14.9/12.9

<u>Test Data at 340°F</u>					
<u>Tension Specimens</u>	<u>Location in Eagle 14</u>	<u>Moisture Content</u>	<u>Stress at Failure (ksi)</u>	<u>Strain at Failure (μin/in)</u>	<u>Primary Modulus (msi)</u>
B1	30-ply	maximum	78.9	6920	19.4
B2	tension	maximum	77.7	>4200	14.2
B3	skin	maximum	72.8	>5400	12.2

<u>Shear Specimens</u>	<u>Location in Eagle 14</u>	<u>Moisture Contents</u>	<u>Rail Primary Modulus at 340°F (msi)</u>
C1	16-ply compression skin	in situ	4.1
C2	16-ply compression skin	in situ	3.9
C3	16-ply compression skin	in situ	3.9
C4	18-ply compression skin	maximum	1.9
C5	18-ply compression skin	maximum	2.5
C6	18-ply compression skin	maximum	2.7
C7	16-ply tension skin	in situ	4.2
C8	16-ply tension skin	in situ	4.3
C9	16-ply tension skin	in situ	4.3
C10	18-ply tension skin	maximum	2.4
C11	18-ply tension skin	maximum	3.1
C12	18-ply tension skin	maximum	3.2



<u>Flatwise Tension Specimen</u>	<u>Location</u>	<u>Moisture Content</u>	<u>Stress at Failure (RT) (psi)</u>
<u>Skin-to-Core</u>	<u>Eagle 14 Stabilator</u>		
F1	36-ply skin	in situ	690
F2	24-ply skin	in situ	910
F3	24-ply skin	in situ	980
F4	24-ply skin	dry	650
F5	24-ply skin	dry	540
F6	40-ply skin	dry	300
<u>Skin-to-Core</u>	<u>PDV Stabilator</u>		
F7	36-ply skin	dry	390
F8	36-ply skin	dry	340
F9	36-ply skin	dry	380
F10	36-ply skin	in situ	280
F11	36-ply skin	in situ	490
F12	36-ply skin	in situ	470
<u>Interlaminar</u>	<u>Eagle 14 Stabilator</u>		
E1	36-ply comp. skin	in situ	1950
E2	36-ply comp. skin	in situ	2630
E3	36-ply comp. skin	dry	2390
E4	36-ply comp. skin	dry	3180
E5	24-ply comp. skin	in situ	2350
E6	24-ply comp. skin	in situ	2650
E7	36-ply comp. skin	dry	1140
E8	36-ply tension skin	in situ	1920
E9	36-ply tension skin	in situ	1840
E10	36-ply tension skin	dry	2260
E11	24-ply tension skin	in situ	2260
E12	24-ply tension skin	in situ	2790
E19	36-ply tension skin	dry	2900
E20	36-ply tension skin	dry	2950
<u>Interlaminar</u>	<u>PDV Stabilator</u>		
E13	24-ply comp. skin	dry	2250
E14	24-ply comp. skin	dry	1810
E15	24-ply comp. skin	dry	1580
E16	24-ply comp. skin	in situ	2120
E17	24-ply comp. skin	in situ	2600
E18	24-ply comp. skin	in situ	2450

Compres- sion Specimen	Location	Temper- ature (°F)	Moisture Content	Stress at Failure (ksi)	Strains at Failure (µin/in)	Primary Modulus (msi)
<u>Eagle 14 Stabilator</u>						
A1	20-ply compression skin	340	maximum	49.2	2760/3000	17.8/17.3
A2		340	maximum	24.0	-/2440	-/23.6
A3		340	maximum	33.3	1530/1650	24.0/24.0
A4		340	Eagle 14	30.4	1700/1820	21.6/21.6
A5		340	Eagle 14	51.8	2700/3900	24.0/15.9
A6		340	Eagle 14	72.1	4670/4700	18.3/17.3
A7		340	in situ	40.3	4650/1860	11.0/16.2
A8		340	in situ	29.6	2520/1800	12.6/14.6
A9		340	in situ	38.6	2890/2850	13.5/13.1
A10	26-ply compression skin	340	maximum	17.8	3780/500	15.1/-
A11		340	maximum	83.0	5330/6150	15.5/14.8
A12		340	maximum	57.8	3730/3860	19.6/16.6
A13		340	dry	71.7	5250/5700	13.5/13.5
A14		340	dry	64.0	5430/4500	13.6/14.1
A15		340	dry	67.8	5220/5430	13.6/13.7
A16		340	Eagle 14	18.5	1820/1650	19.6/5.3
A17		340	Eagle 14	15.6	1880/1090	20.3/6.6
A18		340	in situ	39.7	4760/2420	12.0/14.0
A19		340	in situ	42.3	3480/3200	12.7/13.6
A20		340	in situ	47.5	3170/5300	13.6/12.3
A21	20-ply tension skin	340	maximum	91.5	6150/6640	16.0/16.0
A22		340	maximum	86.5	5390/5910	23.6/20.2
A23		340	maximum	41.3	2050/2230	20.8/19.2
A24		340	Eagle 14	64.4	4230/4560	21.0/17.8
A25		340	Eagle 14	64.2	4360/5050	18.8/14.4
A26		340	Eagle 14	29.0	360/3670	21.1/21.1
A27		340	in situ	48.8	3250/4100	13.7/13.5
A28		340	in situ	43.4	2620	15.4/11.8
A29		340	in situ	43.8	2640	16.6/11.0
A30		340	dry	68.3	5160/5490	13.6/13.1
A31	26-ply tension skin	340	dry	67.7	5910/4560	13.8/13.9
A32		340	dry	66.2	5580/4600	13.4/14.1
A33		340	maximum	10.6	2070/770	10.8/-
A34		340	maximum	22.4	2730/-	15.8/-
A35		340	maximum	14.8	835/572	15.4/19.0
A36		340	Eagle 14	24.1	1100/4260	22.0/7.4
A37		340	Eagle 14	15.6	1230/1400	17.0/7.2
A38		340	in situ	64.4	>4480	13.2/12.4
A39		340	in situ	64.9	>6000	13.1/12.8
A40		340	in situ	49.2	4000/3840	14.7/11.6
<u>PDV Stabilator</u>						
A62	26-ply	340	maximum	21.6	-	-
A41	compression	340	maximum	13.7	-	-
A42	skin	RT	maximum	88.3	6860/7280	14.9/13.9

Compres- sion Specimen	Location	Temper- ature (°F)	Moisture Content	Stress at Failure (ksi)	Strains at Failure ( $\mu$ in/in)	Primary Modulus (msi)
A43	26-ply compression skin	340	maximum	116.3	7530/8750	19.0/17.8
A44		RT	dry	98.4	6800/7100	14.0/14.5
A45		RT	dry	101.3	7160/7050	14.3/14.5
A46		RT	dry	102.6	7830/6780	13.7/14.7
A47		340	in situ	34.9	2000/3920	12.9/12.6
A48		340	in situ	37.4	2290/3560	12.7/13.1
A49		340	in situ	48.4	5000/3270	12.5/13.3
A50		340	in situ	47.2	6000/2660	13.1/13.3
A51	26-ply tension skin	340	dry	78.8	5940/6040	13.5/13.8
A52		340	dry	76.9	5835/5970	13.7/13.8
A53		340	dry	75.8	5880/5880	14.0/13.8
A54		340	dry	70.2	5640/5100	13.7/13.8
A55		340	maximum	12.0	570/780	16.3/16.7
A56		340	maximum	36.4	2000/2580	17.4/14.1
A57		340	maximum	20.7	650/2350	18.5/12.9
A58		340	in situ	52.8	4740/3840	14.0/12.6
A59		340	in situ	50.6	3350/4710	13.3/12.7
A60		340	in situ	55.6	4220/4910	13.9/12.1
A61		340	in situ	53.0	5240/3820	11.8/14.0

Eagle 14 Stabilator  
(residual compression)

D1	30-ply	340	maximum	17.3	300/1400	24.8/21.5
D2	tension	340	maximum	58.8	3800/4900	16.0/14.7
D3	skin	340	maximum	104.4	6650/7650	19.4/17.1

## REFERENCES

1. L. R. Sanders, "Quality Assurance for Advanced Composite Aircraft Structures", AFML-TR-73-162 Volume I, AD-915 591L, July 1973.
2. J. Whiteside, "Environmental Sensitivity of Advanced Composites", Grumman Aerospace Corporation, AFFDL Contract F33615-76-C-5324.
3. J. A. Ford, et al, "F-15 AFDT&E High Temperature Desert Test and Climatic Laboratory Evaluation", AFFTC-TR-75-19, AD-B011 345L, October 1975.
4. G. C. Cardea, et al, "F-15 AFDT&E Arctic Evaluation", AFFTC-TR-75-39, AD-B014 557L, November 1975.
5. J. A. Ford, et al, "F-15 AFDT&E Tropic Evaluation", AFFTC-TR-75-44, AD-B014 562L, December 1975.
6. R. Dogniaux, "Geographic and Climatic Variations of Exposure of Solar Energy on Horizontal and Vertical Receiving Surfaces", NASA-TT-F-16912, N76-20053, March 1976.
7. F. Kreith, Principles of Heat Transfer, International Textbook Co., September 1959.
8. W. Rohsenow and H. Choi, Heat, Mass and Momentum, Prentice Hall, 1961.
9. R. DeIasi and J. B. Whiteside, "Effect of Moisture on Epoxy Resins and Composites", Advanced Composite Materials - Environmental Effects, ASTM STP 658, 1978.
10. Chi-Hung Shen and G. S. Springer, "Moisture Absorption and Desorption of Composite Materials", Journal of Composite Materials, Volume 10, January 1976.
11. J. M. Whitney, "Moisture Diffusion in Fiber Reinforced Composites", AFML-TR-78-42, AD-A056 557, April 1978.
12. E. L. McKague, "Life Assurance of Composite Structures - Volume I: Moisture Effects", AFML-TR-75-51, AD-B006 906, May 1975.
13. C. D. Shirrell, "Diffusion of Water Vapor in Graphite/Epoxy Composites", Advanced Composite Materials - Environmental Effects, ASTM STP 658, 1978.
14. J. M. Augl and A. E. Berger, "The Effect of Moisture on Carbon Fiber Reinforced Composites: Part III, Prediction of Moisture Sorption in a Real Outdoor Environment", NSWC/WOL TR-77-13, AD-A046 294, 14 June 1977.



**DAT**  
**ILM**